

***AN INRUSH CURRENT MODEL
FOR
CORE TYPE TRANSFORMERS***

by

Iraj Farzadfar

A Thesis

submitted to the Faculty of Graduate Studies

in partial fulfillment of the requirements for the Degree of

Masters of Science

Department of Electrical and Computer Engineering

University of Manitoba

Winnipeg, Manitoba, CANADA.

July, 1997



**National Library
of Canada**

**Acquisitions and
Bibliographic Services**

395 Wellington Street
Ottawa ON K1A 0N4
Canada

**Bibliothèque nationale
du Canada**

**Acquisitions et
services bibliographiques**

395, rue Wellington
Ottawa ON K1A 0N4
Canada

Your file Votre référence

Our file Notre référence

The author has granted a non-exclusive licence allowing the National Library of Canada to reproduce, loan, distribute or sell copies of this thesis in microform, paper or electronic formats.

The author retains ownership of the copyright in this thesis. Neither the thesis nor substantial extracts from it may be printed or otherwise reproduced without the author's permission.

L'auteur a accordé une licence non exclusive permettant à la Bibliothèque nationale du Canada de reproduire, prêter, distribuer ou vendre des copies de cette thèse sous la forme de microfiche/film, de reproduction sur papier ou sur format électronique.

L'auteur conserve la propriété du droit d'auteur qui protège cette thèse. Ni la thèse ni des extraits substantiels de celle-ci ne doivent être imprimés ou autrement reproduits sans son autorisation.

0-612-23298-0

**THE UNIVERSITY OF MANITOBA
FACULTY OF GRADUATE STUDIES
COPYRIGHT PERMISSION**

AN INRUSH CURRENT MODEL FOR CORE TYPE TRANSFORMERS

BY

IRAJ FARZADFAR

**A Thesis submitted to the Faculty of Graduate Studies of the University of Manitoba
in partial fulfillment of the requirements of the degree of**

MASTER OF SCIENCE

Iraj Farzadfar © 1997

Permission has been granted to the LIBRARY OF THE UNIVERSITY OF MANITOBA to lend or sell copies of this thesis, to the NATIONAL LIBRARY OF CANADA to microfilm this thesis and to lend or sell copies of the film, and to UNIVERSITY MICROFILMS to publish an abstract of this thesis.

This reproduction or copy of this thesis has been made available by authority of the copyright owner solely for the purpose of private study and research, and may only be reproduced and copied as permitted by copyright laws or with express written authorization from the copyright owner.

Acknowledgments

The author gratefully acknowledges his indebtedness to Professor G. W. Swift for his guidance, encouragement, support, and patience throughout the course of this study at the University of Manitoba.

The author also would like to thank Erwin Dirks, the Power Technician who was always ready to help with the supplies.

The author is also grateful to the University of Manitoba for providing the facilities to complete this project. Also a thanks to all friends for their encouragement and valuable advice.

Finally, the author is thankful to his daughters, Rahin and Saba for their patience and support during the whole program.

Abstract

A detailed mathematical model based on circuit approach has been developed for simulating inrush current for core type transformers. The model is capable of computing inrush current for various phase connection schemes under different initial conditions. A three phase thyristor controlled switch has been designed and constructed to be used in consistent recording of inrush current at zero-crossing and positive going voltage. Also a method for determining the zero-sequence permeance of the transformer was introduced.

The model can be applied to power transformers for inrush current investigations which are necessary for designing system protection relays.

Table of Contents

Acknowledgments	i
Abstract	ii
List of Figures	vi
Chapter 1	
Introduction	1
1.1 Literature Review	2
1.2 The Present Study.....	3
1.3 Thesis Structure	3
Chapter 2	
Single Phase Transformer	6
2.1 Magnetic Flux.....	7
2.2 Equivalent Circuits	7
2.3 Analysis of the Electric Equivalent Circuit.....	8
2.4 Analysis of the Magnetic Circuit.....	9
2.5 Core Characteristics.....	11
2.5.1 Saturation Effect	11
2.5.2 Hysteresis Effect	13
2.5.3 Eddy-Current Effect	15
2.6 Modeling the Core Characteristics	16
2.7 Complete Solution for a Single-Phase Transformer.....	19
2.8 Remanent Flux.....	21
Chapter 3	
Three Phase Transformer	22
3.1 Electric Equivalent Circuit for 4-wire Star/Delta Transformer.....	23
3.2 Magnetizing Flux as a Function of Total Mmfs.....	26

3.3	Geometry of the Three Phase Transformer's Core.....	29
3.4	Magnetic Equivalent Circuit of the Three Phase Transformer.....	32
3.5	Determination of the P-Matrix	37
3.5.1	Bank of Three Single Phase Transformers	38
3.6	The Diagram of Solution Procedures	38

Chapter 4

	Electric and Magnetic Parameters Measurement	40
4.1	Electrical Parameters of the Three Phase Transformer	40
4.1.1	Source Impedance	41
4.2	Measurement of the Core Characteristic	42
4.3	Core Characteristics of a Three Phase Transformer.....	42
4.4	Measurement Procedures.....	47
4.5	60-Hz. AC Hysteresis Loop	51
4.6	Curve Fitting.....	52
4.7	Zero-Sequence Permeance Measurement.....	54
4.7.1	Experimental Setup	54
4.7.2	Computation Part	58

Chapter 5

	Comparison of the Actual and Computed Inrush Currents	61
5.1	4-Wire Star/Star (Without Secondaries Loading.)	64
5.2	4-Wire Star/Closed Delta (Without Secondaries Loading.).....	66
5.3	Star/Star (Without Secondaries Loading.)	68
5.4	Star/Closed Delta (Without Secondaries Loading.)	70
5.5	4-Wire Star/Star (Steady-State, Without Secondaries Loading.).....	72

Chapter 6

	Summary & Conclusions	74
6.1	Summary.....	75
6.2	Conclusions	77
	List of References	79

Appendix-A

Determination of P-Matrix 82

Appendix-B

Star/Delta Electric Equivalent Circuit 94

Appendix-C

Delta/Delta Electric Equivalent Circuit 98

Appendix-D

Schematic Diagram of the 3-Phase Thyristor Switch 100

D.1 List of components: 102

Appendix-E

MatLab files 103

E.1 Null Grounded Star/Delta Connection Functions 104

E.1.1 Main Routine 104

E.1.2 Electric Circuit and Parameters 109

E.1.3 Supply Voltage Vector 111

E.1.4 Coefficient Matrices 112

E.2 Magnetic Circuit Solver Routine 113

E.3 Star/Delta Connection Functions 115

E.3.1 Main Routine 115

E.3.2 Electric Circuit and Parameters 120

E.3.3 Supply Voltage Vector 122

E.3.4 Coefficient Matrices 123

E.4 P-matrix..... 124

E.5 Plot Routine..... 125

E.6 Core Characteristics 127

E.6.1 Core Characteristics for Limb "a" 127

E.6.2 Core Characteristics for Limb "b" 128

E.6.3 Core Characteristics for Limb "c" 129

E.7 Integrator 130

List of Figures

Fig.2.1:	Core type single-phase transformer.....	6
Fig.2.2:	Electric equivalent circuit of a single-phase transformer.....	8
Fig.2.3:	Analogy between Electric circuit and Magnetic circuit.....	10
Fig.2.4:	Duality between electric and magnetic circuit.....	11
Fig.2.5:	A typical saturation curve.....	12
Fig.2.6:	Viewing the iron core as a system.....	13
Fig.2.7:	A steady-state hysteresis loop for a 10 KVA commercial transformer.....	14
Fig.2.8:	Subtrajectories of a core characteristics under transient condition [14], p.2209.....	15
Fig.2.9:	60-hertz hysteresis loop of a 5-KVA transformer.....	16
Fig.2.10:	Pure hysteresis loop for a 500-MVA power autotransformer [17], p1918.....	18
Fig.2.11:	One computational step in finding the current.....	20
Fig. 3.1:	Core type three-phase transformer.....	23
Fig. 3.2:	Star/delta connected transformer.....	24
Fig. 3.3:	Geometry of the three-phase core type transformer.....	30
Fig. 3.4:	Comparison between a magnetic element (iron core) and an electric element (resistor).....	32
Fig. 3.5:	Input and output of the magnetic circuit.....	33
Fig. 3.6:	the equivalent magnetic circuit of the three-phase core type transformer.....	34
Fig. 3.7:	One computation step towards solving the three-phase transformer.....	39

Fig. 4.1:	Electrical parameters of the tested transformer.....	41
Fig. 4.2:	flux path for an excited iron segment.....	44
Fig. 4.3:	Eliminating the effect of center limb.....	45
Fig. 4.4:	Analysis of the induced current in the center limb when it is short circuited	46
Fig. 4.5:	Experimental setup for obtaining the core characteristics of the three-phase transformer	48
Fig. 4.6:	Sampled current and search coil voltage for setup in Fig. 4.5	49
Fig. 4.7:	Flux measurement for setup in Fig. 4.5.....	50
Fig. 4.8:	Flux-mmf plot for each outer limbs in Fig. 4.5 setup	50
Fig. 4.9:	60-Hertz steady-state hysteresis loop for outer limbs	51
Fig. 4.10:	plot of fitted curve superimposed on the plot of actual magnetic data for limb "a"	53
Fig. 4.11:	Setup for determining the zero-sequence permeance.....	55
Fig. 4.12:	Plot of magnetic data recorded in the setup of Fig. 4.11.....	56
Fig. 4.13:	Plot of applied mmf vs. the center limb's flux.....	57
Fig. 4.14:	Magnetic circuit of the core-type three-phase transformer	58
Fig. 5.1:	The instant of switching on the voltage cycle.....	62
Fig. 5.2:	Setup for sampling the inrush currents for the case of 4-wire star/star.....	64
Fig. 5.3:	Comparison of the actual and computed inrush currents for 4-wire star/star.....	65
Fig. 5.4:	Setup for sampling the inrush currents for the case of 4-wire star/closed delta	66

Fig. 5.5:	Comparison of actual and computed inrush currents for 4-wire star/closed delta	67
Fig. 5.6:	Setup for sampling the inrush currents for the case of star/star	68
Fig. 5.7:	Comparison of actual and computed inrush current for star/star	69
Fig. 5.8:	Setup for sampling the inrush currents for the case of star/closed delta	70
Fig. 5.9:	Comparison of actual and computed inrush currents for star/closed delta	71
Fig. 5.10:	Setup for sampling the magnetizing currents for the case of 4-wire star/star	72
Fig. 5.11:	Comparison of actual and computed magnetizing currents for star/star	73
Fig. B.1:	Electric equivalent circuit of star/delta connection	94
Fig. C.1	Delta/Delta connected transformer	98
Fig. C.2	The Star/Delta equivalent circuit, after delta to star transform	99
Fig. D.1:	Schematic diagram of the three-phase thyristor-controlled switch	101

Chapter 1

Introduction

During the initial energization of a transformer a transient current known as *magnetizing inrush current* flows into the primary winding due to overfluxing the transformer magnetic core temporarily. This current continues to flow until the dc-component of the magnetic flux dies out completely. The start-up of the transformer is not the only cause of inrush currents, after fault clearance fast voltage recovery can also initiate inrush current in any transformer connected to the system[1] [2],[3].

The magnitude of the inrush current depends on two major parameters: the switch-in angle on the voltage cycle, and the total resistance in the primary circuit.

For many years power transmission engineers have been concerned with this phenomenon, not because this excessive current has the potential to damage the system apparatus, but because it may confuse the protection relays by unneces-

sary tripping. It may also cause enough voltage drop to impair the function of other equipments connected to the same system.

1.1 Literature Review

This phenomenon was first observed in 1892 [4], but according to Blum et al [5] up to 1944 no information regarding which parameters may affect the inrush current or how the inrush current can be affected by the design had been found in the literature. The production of cold-rolled steel for transformer core resulted in higher inrush currents as well as higher efficiency. This lead to more severe problems regarding the false tripping of protection relays, this stimulated interests in this phenomenon [6][7][8]. Early efforts mostly involved the calculation for the first peak of inrush current of a single phase transformer [9][10][11]. A bibliographical review and historical background of this subject is presented by Hudson [12].

Due to the complex behavior of the core, difficulty to record the inrush current for power transformers, and unavailability of digital computers the problem of inrush could not have been solved properly. Later however, digital computers facilitated solving the problem.

1.2 The Present Study

The purpose of this study is to develop a *mathematical model* for a *three-phase core type transformer*. This model should be capable of simulating the magnetizing inrush current for various initial conditions and winding connection schemes. A 120V/600V, 10KVA three-phase core type transformer was provided by the Electrical Engineering department of University of Manitoba to perform the necessary tests. In order to record the inrush currents consistently, a three-phase thyristor-controlled switch was constructed capable of switching in the transformer at zero-crossing and positive going voltage. The developed model was implemented in MatLab and as of M-files.

1.3 Thesis Structure

The thesis is subdivided into 6 chapters and 4 appendices. In Chapter 2. the problem of a single-phase transformer is discussed. The discussion includes the analysis of magnetic core behavior, magnetic circuit as well as the electric circuit. Also the basic elements of core behavior including the non-linearity, saturation and hysteresis are taken into considerations. It is shown, when computing the inrush current, core losses are not major factors (especially for modern power transformers). Therefore, the core is characterized only by its saturation behavior, which greatly simplifies the core modeling. At the end of the chapter a complete

solution for a single-phase transformer is presented.

Chapter 3 discusses the three-phase transformer. As an example to start with, a null grounded star/delta core type transformer is discussed thoroughly. The magnetic and electric circuits of a three-phase transformer is far more complicated than those of a single phase transformer. Due to the core interconnections, in this particular case the current in each phase depends on all magnetizing fluxes. The difficulty arises when an attempt is made to express the current vector in terms of the flux vector. The idea of P-matrix is used to deal with this problem. P-matrix relates the derivatives of currents to those of the fluxes. Within the computation steps, it is necessary to find system fluxes for specified system currents. This is done by numerically solving the system of non-linear equations which characterizes the magnetic circuit. The solution to the three-phase transformer is provided at the end of the chapter.

Chapter 4 discusses the experimental setup for determining the core characteristics and the zero-sequence permeance of the transformer under test.

Chapter 5 compares the predicted inrush current by the model for different winding connections and different initial condition against the actual recorded current. The results indicate a reasonable agreement between the model prediction and the actual values based on the approximations made in the model.

Chapter 6 summarizes the work done and discusses the limits of validity of the model and the source(s) of discrepancies.

Determination of P-matrix with complete steps can be found in Appendix-A.

The solution to star/delta phase connection is presented in Appendix-B.

The diagram of the three-phase thyristor switch can be found in Appendix-C.

And finally, the Appendix-D contains all the necessary codes to run the program in MatLab.

Chapter 2

Single Phase Transformer

In order to get an insight into the three phase transformer, it is beneficial to pause and analyze the single-phase transformer. The basic principles apply to both single-phase and three-phase transformers. Single-phase *transformers* lie in the category of magnetically *coupled circuits*. In most cases it consists of two coils known as secondary and primary windings, which are closely wound around a closed end iron core as shown in the following

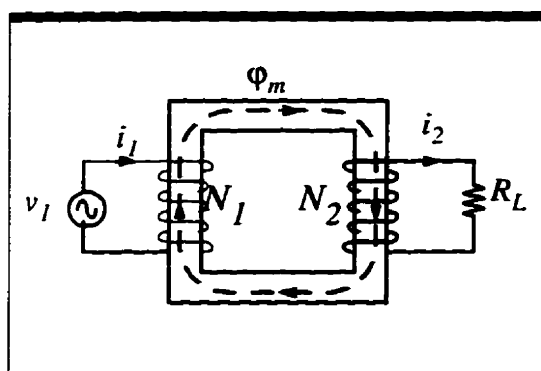


Fig.2.1: Core type single-phase transformer

2.1 Magnetic Flux

By connecting the primary winding to a sinusoidal voltage source, a time-varying magnetic flux is developed in the windings. This flux is composed of two components. One is called a *leakage flux* and the other is known as *linkage flux* or *magnetizing flux*.

The path of the leakage flux is mostly in the air. In contrast, the path of the linkage flux lies entirely in the magnetic core and links both primary and secondary windings. Due to the constant permeability of the air the effect of *leakage flux* can be modeled as a *constant inductance*.

2.2 Equivalent Circuits

When dealing with transformers two different circuits should be considered. One is the *electric equivalent circuit* the other being the *magnetic equivalent circuit*. Magnetic circuit usually consists of a *magnetomotive force* and some iron segments in series or in parallel or both. These iron segments are characterized by their magnetic *reluctance* which is the counterpart of electric *resistance* in an electric circuit. The electric circuit provides magnetomotive force to the magnetic circuit which in turn drives the magnetic flux in the iron core. When modeling a transformer a major difficulty is the solution of the magnetic circuits due to the non-linearity of core characteristics.

2.3 Analysis of the Electric Equivalent Circuit

To simplify matters, let us consider the single-phase transformer shown in Fig. 2.2 with open secondary.

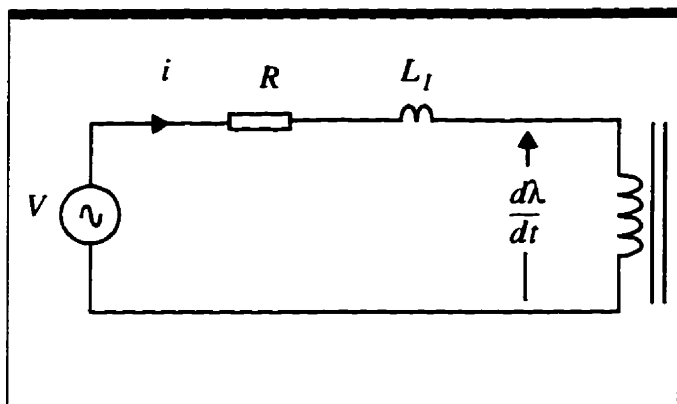


Fig.2.2: Electric equivalent circuit of a single-phase transformer

The primary winding is connected to a sinusoidal voltage source. Applying KVL to the primary circuit yields:

$$V = R \cdot i + L_l \cdot \frac{di}{dt} + N \cdot \frac{d\phi_m}{dt} \quad (2.1)$$

where:

R = resistance of the primary winding (the voltage source is assumed ideal.).

L_l = leakage inductance of primary winding.

i = primary current.

N = number of turns of primary.

ϕ_m = magnetizing flux.

$N \cdot \phi_m$ is called the primary *linkage flux* and is denoted as λ . The Eqn. 2.1 can be written as:

$$V = R \cdot i + L_l \cdot \frac{di}{dt} + \frac{d\lambda}{dt} \quad (2.2)$$

λ is a nonlinear function of the *applied mmf* and in general is expressed as:

$$\lambda = h(F) \quad (2.3)$$

Where F is the total *mmf* applied to the core.

2.4 Analysis of the Magnetic Circuit

When current i flows into the primary winding, it produces an mmf equal to $F = N \cdot i$. This is the *magnetomotive force* which drives the *magnetizing flux* in the iron core, the amount of this *flux* depends on two quantities, the *applied mmf* and the *magnetic reluctance* of the core. Using the *Ampere's Law*, it is straight forward to show that the *magnetizing flux* can be expressed as:

$$\phi_m = \frac{F}{\mathfrak{R}} \quad , \quad \phi_m = p \cdot F \quad (2.4)$$

Where \mathfrak{R} and p are magnetic *reluctance* and *permanence* of the iron core respec-

tively and have the following expressions.

$$\mathfrak{R} = \frac{L}{\mu \cdot A} \quad , \quad \rho = \frac{\mu \cdot A}{L} \quad (2.5)$$

Where L , A and μ are the *length*, *cross section* and *permeability* of the iron core.

Eqn. 2.4 is analogous to the Ohm's Law. The following table illustrates the analogy between electric and magnetic quantities.

Electric Quantity	Magnetic Quantity
Electromotive force	Magnetomotive force
Current	Flux
Resistance	Reluctance
Conductance	Permeance
$i = \frac{v}{R}$	$\phi_m = \frac{F}{\mathfrak{R}}$

Fig.2.3: Analogy between Electric circuit and Magnetic circuit

Fig. 2.4 illustrates the duality between these two circuits based on the above analogy.

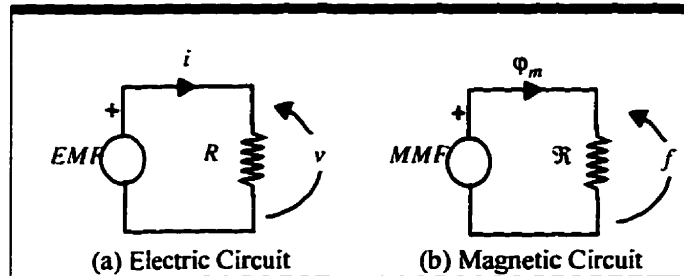


Fig.2.4: Duality between electric and magnetic circuit

The *magnetic reluctance* of the iron is not constant because iron is a non-linear magnetic material, therefore it's reluctance varies with the *applied mmf* or the *flux* in the core. In other words the flux being produced in the core by the *applied mmf* is a nonlinear function as expressed in Eqn. 2.3

2.5 Core Characteristics

The relation between the *magnetizing flux* and the applied *mmf* in an iron core is a nonlinear relationship due to *saturation* and *hysteresis*.

2.5.1 Saturation Effect

Suppose that the iron core of a single-phase transformer is initially demagnetized and the primary winding is connected to a dc source. By slowly increasing the current from zero to a finite value, the flux in the iron core builds up. For lower values of the exciting current, the iron core exhibits *small reluctance*. result-

ing a large amount of flux in the iron core. At higher values of current the ferromagnetic medium exhibits very *high reluctance*, which results in a small increase in the flux. This phenomenon is called *magnetic saturation* and as mentioned earlier, it is a significant aspect of the core characteristics. The plot of $(\lambda - f)$ is called either the *Anhysteric curve* or *saturation curve*. The saturation curve is a *single-value* and *monotonic* curve and mathematically is expressed by Equation:

$$\lambda = h(f) \quad . \quad (2.6)$$

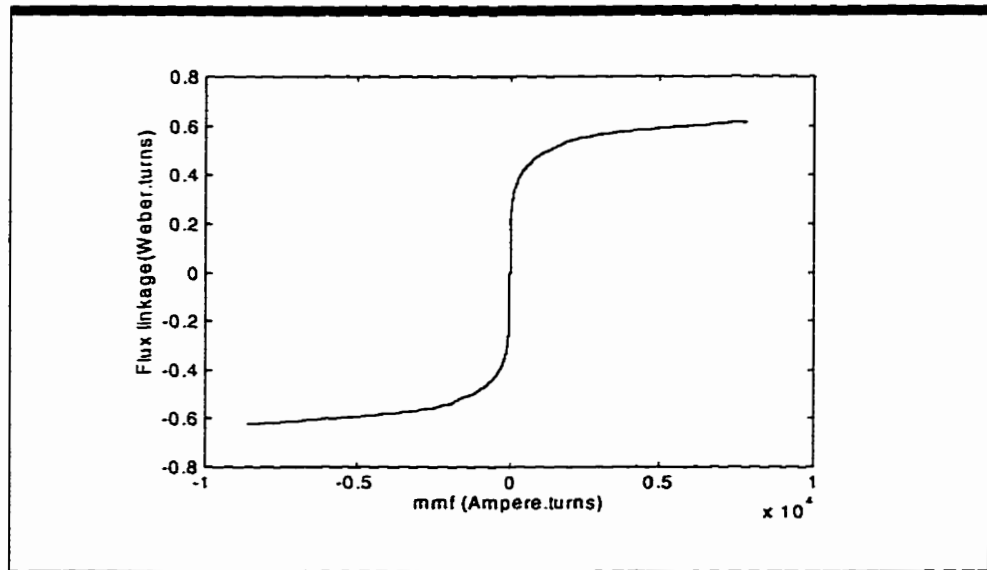


Fig.2.5: A typical saturation curve

The *slope* of this curve is equal to the *incremental inductance* of the primary winding. On the other hand this *slope* is also proportional to the *incremental permeance* of the iron core [13]. This curve can be divided into two regions, the

linear region and the *saturation region*. In the linear region, the iron core exhibits the highest permeance, whereas in the saturation region, the iron core shows the lowest permeance. The iron core can be thought as a *system* which takes the *mmf* as its input, and outputs the *flux* as shown in Fig. 2.6.

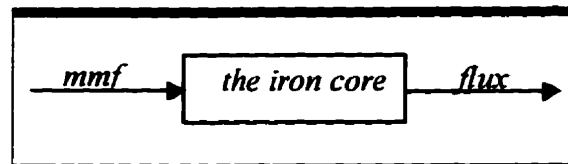


Fig.2.6: Viewing the iron core as a system

This system is nonlinear since its *gain* depends on its input.

2.5.2 Hysteresis Effect

When the flux in the iron core is reversed, the operating point in the $(\lambda - f)$ plane follows a different *trajectory*. In other words, at any instant the operating point in the $(\lambda - f)$ plane, depends not only on the magnitude of the *flux* or *mmf* but also depends on the *immediate past history of the flux variation*. This phenomenon is called *hysteresis*. As a result of hysteresis the plot of λ versus F is no longer single-valued as depicted in Fig. 2.7. When an unloaded transformer is at the steady-state operation, the $(\lambda - f)$ plot is a symmetric loop and consists of two trajectories known as rising and falling trajectories

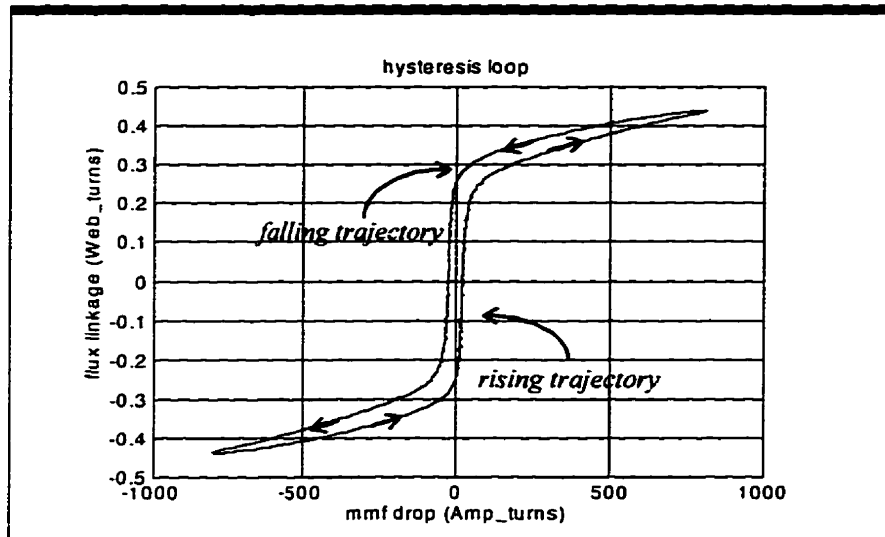


Fig.2.7: A steady-state hysteresis loop for a 10 KVA commercial transformer

The area of the loop is proportional to the energy loss per cycle and this energy is dissipated in the core as heat. When the transformer is operating under the transient-state, the rising and falling trajectories are no longer symmetrical and the $(\lambda - f)$ plane can get much more complicated.

Fig. 2.8 is an oscilloscope trace of *flux* versus *current* for a 10-KVA distribution transformer core. It clearly shows that at each point of flux reversal a new rising trajectory is assumed.

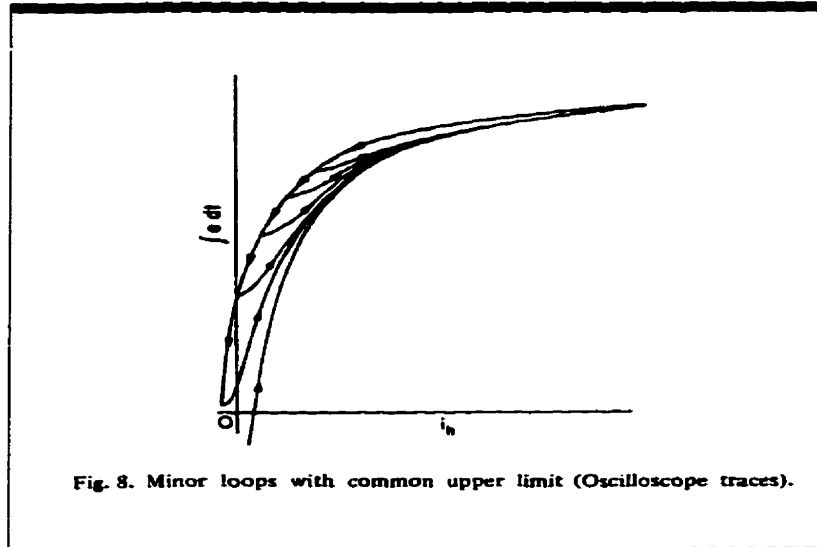


Fig.2.8: Subtrajectories of a core characteristics under transient condition [14], p.2209

2.5.3 Eddy-Current Effect

Another source of loss in the iron core is the eddy-current. This loss is due to the fact that circulating currents are induced in the iron core due to the time-varying flux and these currents produce an $|i|^2 R$ loss in the iron called *eddy-current loss*. Previous studies have revealed that eddy-currents are an almost linear phenomenon and can be modeled as an equivalent current flowing into a linear resistance in parallel with the primary or the secondary winding [14][11][15]. The eddy-current effect broadens the steady-state hysteresis loop (increases the area of the loop). Fig. 2.9 illustrates this effect for a 5-KVA distribu-

tion single-phase transformer

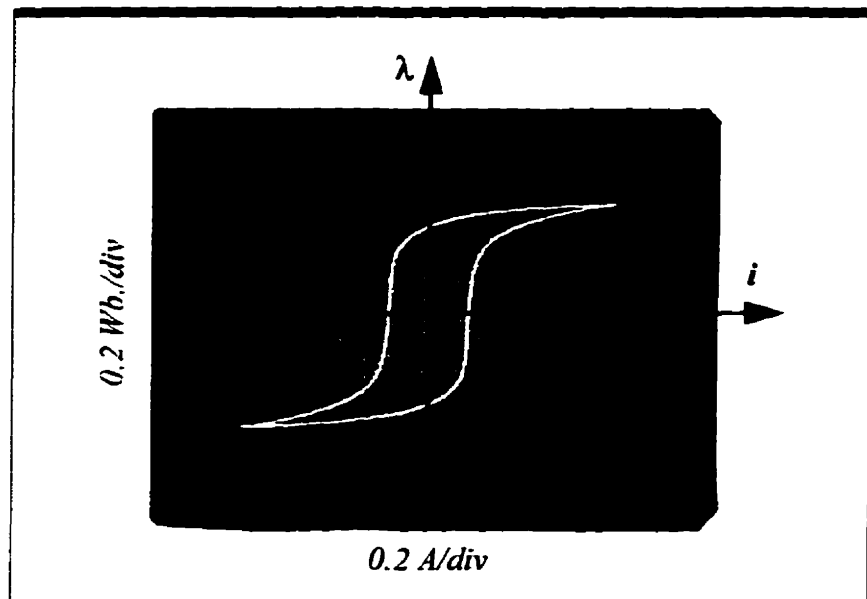


Fig.2.9: 60-hertz hysteresis loop of a 5-KVA transformer

2.6 Modeling the Core Characteristics

In modeling the core characteristics, three effects should be considered:

- i The saturation effect
- ii The hysteresis effect
- iii The eddy- current effect

Among these quantities the saturation effect is the most important one. It is also easy to model due to being a single-valued function. The criteria for dealing

with the other two remaining effects depend on the purpose of modeling the *core characteristic*. In the previous chapter it was said that the purpose of this thesis is to develop a computer program. This program should be capable of predicting the *magnetizing inrush current* for a three-legged, three-phase, and a core type *power transformer* for various winding connection schemes.

Even though modeling the hysteresis effect is the most difficult and challenging its effect is less significant for modern transformers with *grain-oriented silicon iron core*. For these transformers, the eddy-current and hysteresis loss are comparable in size[14].

Fig. 2.10 depicts the pure hysteresis loop for a modern power autotransformer and it is interesting evidence for the fact that hysteresis loss is negligible for modern power transformers.

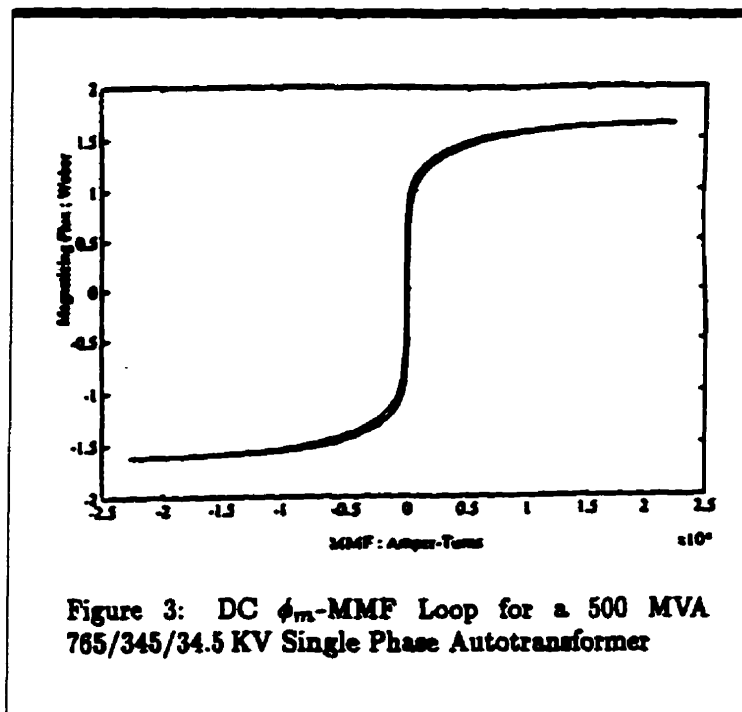


Fig.2.10: Pure hysteresis loop for a 500-MVA power autotransformer [16], p1918.

For the purpose of investigation of the *magnetizing inrush current* in *power transformers*, the core characteristics can be adequately represented by the saturation effect. In other words when dealing with magnetizing inrush current in *power transformers*, the core characteristics can be represented by *saturation curve*, similar to that shown in Fig. 2.5. When studying phenomena such as *ferroresonance* or *subharmonic oscillations*, it would not be a valid assumption to consider only the saturation aspect of the core characteristics.

2.7 Complete Solution for a Single-Phase Transformer

The electrical description of the single-phase transformer is formulated in terms of Eqn. 2.2. The magnetic description is formulated in Eqn. 2.3 (saturation curve). The term $\frac{d\lambda}{dt}$ in Eqn. 2.3 can be expressed in terms of the primary current.

Taking the derivative of both sides of Eqn. 2.3 with respect to time yields:

$$\frac{d\lambda}{dt} = \frac{d\lambda}{dF} \cdot \frac{dF}{dt} \quad \frac{d\lambda}{dt} = p \cdot \frac{dF}{dt} \quad (2.7)$$

where

$$p = \frac{d\lambda}{dF} \quad (2.8)$$

is proportional to the permeance of the iron core. This permeance is equal to the slope of the saturation curve and can be found either analytically or numerically at any operating point by making use of Eqn. 2.3. Substituting Eqn. 2.6 back to the Eqn. 2.2 yields:

$$V = R \cdot i + L_l \cdot \frac{di}{dt} + p \cdot \frac{dF}{dt} \quad (2.9)$$

Considering the fact that the total applied mmf is $F = N \cdot i$, Eqn. 2.7 will be:

$$V = R \cdot i + L_l \cdot \frac{di}{dt} + p \cdot N \cdot \frac{di}{dt} \quad (2.10)$$

Solving this equation for $\frac{di}{dt}$ yields:

$$\frac{di}{dt} = \left(\frac{I}{L_l + N \cdot p} \right) \cdot (V - R \cdot i) \quad (2.11)$$

This equation is in standard form for numerical integration. At each computation step using the initial value of current and permeance (recalling that permeance is a function of current) the next value of current is obtained. Then based on the computed current at the previous stage, the new value for permeance and accordingly the next value of current would be found and so on. Fig. 2.11 shows this procedure. The time step must be sufficiently small.

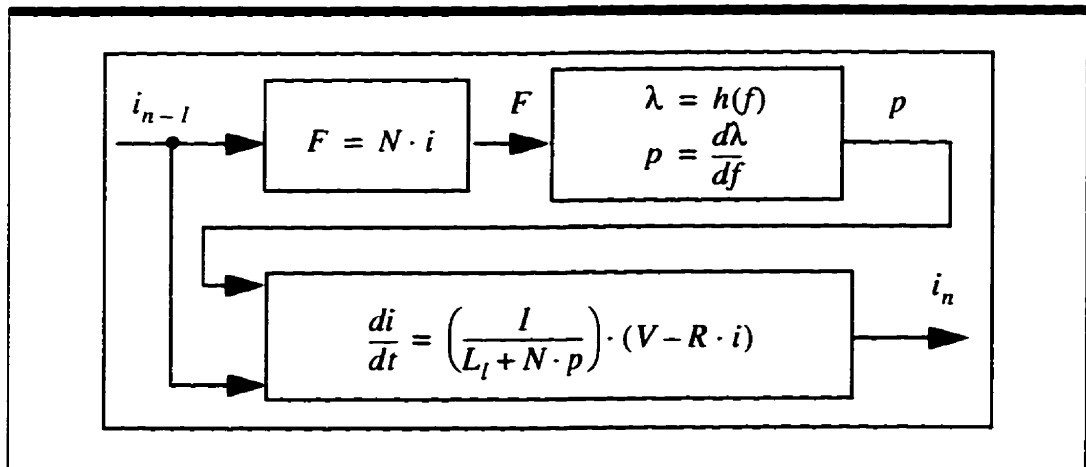


Fig.2.11: One computational step in finding the current

2.8 Remanent Flux

One of the initial conditions that affects the magnetizing inrush current is the *remanent flux* in the iron core, the other one being the *source phase angle* at the instant of energizing the transformer. Therefore any transformer model should take the remanent flux into account as the initial condition of the magnetic state. This is not straight -forward if the core characteristic model does not include hysteresis. This problem can be circumvented by considering an additional temporary *dc mmf* which produces the *initial remanent flux*.

Suppose that the remanent flux is φ_0 and we would want to know how much dc-current can produce this flux. Using the saturation curve:

$$\lambda_0 = h(F_0) \quad \text{where } F_0 = N \cdot i_0$$

The above equation can be rearranged as:

$$\lambda_0 - h(N \cdot i_0) = 0 \quad (2.12)$$

The above is a nonlinear equation which can be easily solved for the current i_0 i.e:

$$i_0 = \left(\frac{I}{N}\right) \cdot h^{-1}(\lambda_0) \quad (2.13)$$

This much imposed initial current would produce the prescribed remanent flux.

After one computational time-step, the saturation curve reverts to a symmetrical characteristic.

Chapter 3

Three Phase Transformer

In this chapter the *three-phase core type transformer* will be analyzed.

Since the purpose of the present study is computing the *magnetizing inrush current*, it is assumed that the secondaries are unloaded and delta connected. Although the basic principles apply to both a *bank of three single-phase transformers* and a *three-phase transformer*, treating the three-phase transformer is much more complicated. In the case of the bank of three transformers, the flux in each transformer is solely a function of current of that transformer, while in the three-phase transformer, the flux in each core is a function of all currents in all windings due to the interconnection of cores of different phases. The following figure shows a three-phase core type transformer with two windings.

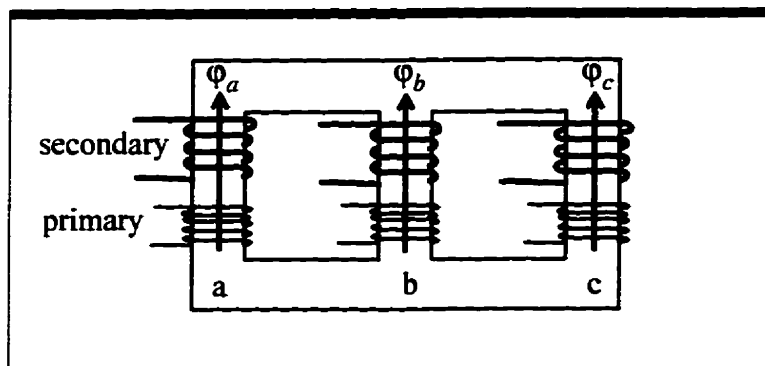


Fig. 3.1: Core type three-phase transformer

In the following, the electrical and magnetic equivalent circuit of the unloaded, core type three-phase, 4-wire star / delta transformer will be discussed. The complete solution for the above transformer will be presented by the end of this chapter.

3.1 Electric Equivalent Circuit for 4-wire Star/Delta Transformer

In Fig. 3.2, the transformer is connected to a three-phase supply via four wires. The secondary is connected in delta. The resistances r_a , r_b and r_c in series with the ideal voltage source represent the connection cable, the primary winding, and the source resistance. The inductances L_a , L_b and L_c are the source, connection cable and primary leakage inductances. L_s is the secondary leakage inductance of each winding and r_s accounts for secondary resistances.

Finally r_e and L_e represent the neutral return resistance and inductance.

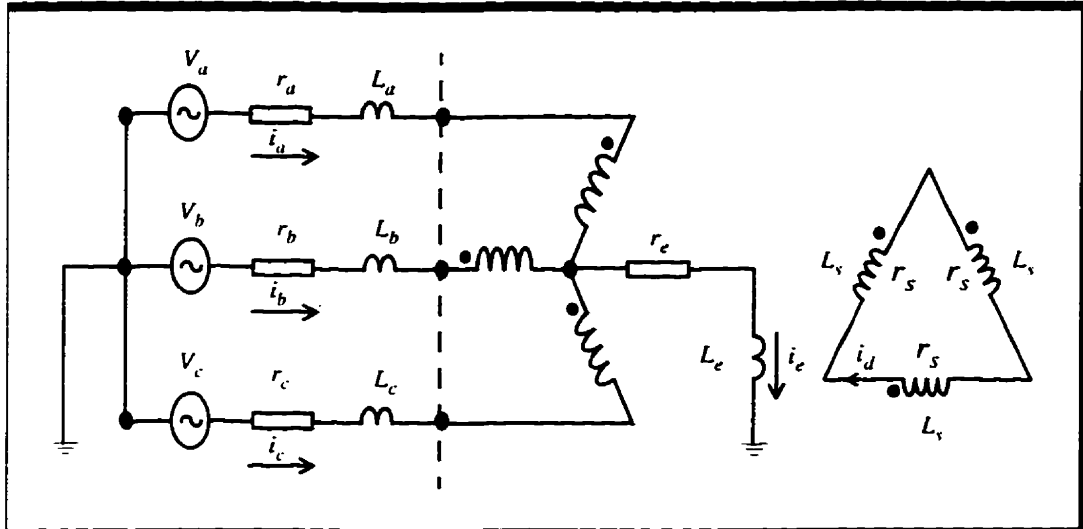


Fig. 3.2: Star/delta connected transformer

Applying *KVL* to the above circuit yields four differential equations.

$$\begin{aligned}
 V_a &= r_a \cdot i_a + r_e \cdot (i_a + i_b + i_c) + L_a \cdot \frac{di_a}{dt} + L_e \cdot \frac{d}{dt}(i_a + i_b + i_c) + \frac{d\lambda_a}{dt} \\
 V_b &= r_b \cdot i_b + r_e \cdot (i_a + i_b + i_c) + L_b \cdot \frac{di_b}{dt} + L_e \cdot \frac{d}{dt}(i_a + i_b + i_c) + \frac{d\lambda_b}{dt} \\
 V_c &= r_c \cdot i_c + r_e \cdot (i_a + i_b + i_c) + L_c \cdot \frac{di_c}{dt} + L_e \cdot \frac{d}{dt}(i_a + i_b + i_c) + \frac{d\lambda_c}{dt} \\
 0 &= 3 \cdot r_s \cdot i_d + 3 \cdot L_s \cdot \frac{di_d}{dt} + n \cdot \left(\frac{d\lambda_a}{dt} + \frac{d\lambda_b}{dt} + \frac{d\lambda_c}{dt} \right)
 \end{aligned} \tag{3.1}$$

Eqn. 3.1 can be written in matrix form.

$$V = R \cdot i + L \cdot \frac{di}{dt} + C \cdot \frac{d\lambda}{dt} \quad (3.2)$$

Where:

$$V = \begin{bmatrix} V_a \\ V_b \\ V_c \\ 0 \end{bmatrix} \quad R = \begin{bmatrix} (r_a + r_e) & r_e & r_e & 0 \\ r_e & (r_b + r_e) & r_e & 0 \\ r_e & r_e & (r_c + r_e) & 0 \\ 0 & 0 & 0 & (3 \cdot r_s) \end{bmatrix} \quad C = \begin{bmatrix} 1 & 0 & 0 \\ 0 & 1 & 0 \\ 0 & 0 & 1 \\ n & n & n \end{bmatrix}$$

$$\lambda = \begin{bmatrix} \lambda_a \\ \lambda_b \\ \lambda_c \end{bmatrix} \quad L = \begin{bmatrix} (L_a + L_e) & L_e & L_e & 0 \\ L_e & (L_b + L_e) & L_e & 0 \\ L_e & L_e & (L_c + L_e) & 0 \\ 0 & 0 & 0 & (3 \cdot L_s) \end{bmatrix} \quad i = \begin{bmatrix} i_a \\ i_b \\ i_c \\ i_d \end{bmatrix}$$

C is the coefficient matrix and n is the turn ratio of the windings, where

$n = \frac{N_2}{N_1}$. In Eqn. 3.2, the current vector i and the magnetic flux vector λ , are the

two unknowns. Since the flux is a function of the current, only one of the two variables is independent. *This function is a property of the magnetic circuit as well as the core saturation characteristics of the transformer under analysis.*

The following approach presents a method of expressing the flux derivatives in terms of current derivatives, incorporating the concept and a method of determining the “ P matrix”. The approach will lead to solving Eqn. 3.2 for the cur-

rent vector. This approach is based on the earlier works, mostly that of the Nakra and Barton [13].

3.2 Magnetizing Flux as a Function of Total Mmfs

A three-phase transformer consists of three segments of iron namely *limbs a, b and c* which are interconnected in a manner illustrated in Fig. 3.1. Two coils are wound around each limb and constitute a winding set (usually referred to as primary and secondary). Current flow in these coils provides an *mmf* to the core of that winding. Since the three limbs are interconnected, the *applied mmf* to each limb drives the flux in all three limbs. In other words each of the *mmf*'s contribute to the flux in every segment of the core. As a result the flux in each core (expressed in terms of primary linkage flux for convenience) is a function of the three *net mmfs*.

$$\begin{cases} \lambda_a = h_1(F_a, F_b, F_c) \\ \lambda_b = h_2(F_a, F_b, F_c) \\ \lambda_c = h_3(F_a, F_b, F_c) \end{cases} \quad (3.3)$$

$$\begin{cases} F_a = N_1 \cdot i_a - N_2 \cdot i_d \\ F_b = N_1 \cdot i_b - N_2 \cdot i_d \\ F_c = N_1 \cdot i_c - N_2 \cdot i_d \end{cases} \quad (3.4)$$

Where F_a , F_b and F_c are the *net mmfs* applied to limbs a , b and c respectively.

N_1 and N_2 are the primary and secondary *number of turns*. Taking the derivative of both sides of Eqn. 3.3 with regard to time, yields:

$$\begin{aligned}\frac{d\lambda_a}{dt} &= \frac{\partial\lambda_a}{\partial F_a} \cdot \frac{dF_a}{dt} + \frac{\partial\lambda_a}{\partial F_b} \cdot \frac{dF_b}{dt} + \frac{\partial\lambda_a}{\partial F_c} \cdot \frac{dF_c}{dt} \\ \frac{d\lambda_b}{dt} &= \frac{\partial\lambda_b}{\partial F_a} \cdot \frac{dF_a}{dt} + \frac{\partial\lambda_b}{\partial F_b} \cdot \frac{dF_b}{dt} + \frac{\partial\lambda_b}{\partial F_c} \cdot \frac{dF_c}{dt} \\ \frac{d\lambda_c}{dt} &= \frac{\partial\lambda_c}{\partial F_a} \cdot \frac{dF_a}{dt} + \frac{\partial\lambda_c}{\partial F_b} \cdot \frac{dF_b}{dt} + \frac{\partial\lambda_c}{\partial F_c} \cdot \frac{dF_c}{dt}\end{aligned}\quad (3.5)$$

This can also be written in matrix form:

$$\begin{bmatrix} \frac{d\lambda_a}{dt} \\ \frac{d\lambda_b}{dt} \\ \frac{d\lambda_c}{dt} \end{bmatrix} = \begin{bmatrix} \frac{\partial\lambda_a}{\partial F_a} & \frac{\partial\lambda_a}{\partial F_b} & \frac{\partial\lambda_a}{\partial F_c} \\ \frac{\partial\lambda_b}{\partial F_a} & \frac{\partial\lambda_b}{\partial F_b} & \frac{\partial\lambda_b}{\partial F_c} \\ \frac{\partial\lambda_c}{\partial F_a} & \frac{\partial\lambda_c}{\partial F_b} & \frac{\partial\lambda_c}{\partial F_c} \end{bmatrix} \cdot \begin{bmatrix} \frac{dF_a}{dt} \\ \frac{dF_b}{dt} \\ \frac{dF_c}{dt} \end{bmatrix}\quad (3.6)$$

Or in a matrix notation,

$$\frac{d\lambda}{dt} = \mathbf{P} \cdot \frac{d\mathbf{F}}{dt}\quad (3.7)$$

where \mathbf{P} stands for “*P-matrix*” and its elements are partial derivative.

$$P = \begin{bmatrix} \frac{\partial \lambda_a}{\partial F_a} & \frac{\partial \lambda_a}{\partial F_b} & \frac{\partial \lambda_a}{\partial F_c} \\ \frac{\partial \lambda_b}{\partial F_a} & \frac{\partial \lambda_b}{\partial F_b} & \frac{\partial \lambda_b}{\partial F_c} \\ \frac{\partial \lambda_c}{\partial F_a} & \frac{\partial \lambda_c}{\partial F_b} & \frac{\partial \lambda_c}{\partial F_c} \end{bmatrix} \quad (3.8)$$

Eqn. 3.4 can also be arranged as:

$$\begin{bmatrix} F_a \\ F_b \\ F_c \end{bmatrix} = \begin{bmatrix} N_1 & 0 & 0 & -N_2 \\ 0 & N_1 & 0 & -N_2 \\ 0 & 0 & N_1 & -N_2 \end{bmatrix} \cdot \begin{bmatrix} i_a \\ i_b \\ i_c \\ i_d \end{bmatrix} \quad (3.9)$$

$$F = M \cdot i \quad i = \begin{bmatrix} i_a \\ i_b \\ i_c \\ i_d \end{bmatrix} \quad M = \begin{bmatrix} N_1 & 0 & 0 & -N_2 \\ 0 & N_1 & 0 & -N_2 \\ 0 & 0 & N_1 & -N_2 \end{bmatrix}$$

The following is the result of combining Eqn. 3.7 and Eqn. 3.9:

$$\frac{d\lambda}{dt} = P \cdot M \cdot \frac{di}{dt} \quad (3.10)$$

Eqn. 3.10 leads the way to solve the three-phase transformer problem. It relates the flux and current derivatives to each other. This is exactly what we were looking for to solve the Eqn. 3.2. Combining Eqn. 3.2 and Eqn. 3.10 results in:

$$V = R \cdot i + L \cdot \frac{di}{dt} + C \cdot \left(P \cdot M \cdot \frac{di}{dt} \right) \quad (3.11)$$

$$V = R \cdot i + (L + C \cdot P \cdot M) \cdot \frac{di}{dt}$$

The last equation can be rearranged as:

$$\frac{di}{dt} = (L + C \cdot P \cdot M)^{-1} \cdot (V - R \cdot i) \quad (3.12)$$

This matrix equation is in standard form for integration. The fourth order Runge-Kutta method is employed to numerically solve this system of equations. This method is known to be the most accurate one for the solution of differential equations.

3.3 Geometry of the Three Phase Transformer's Core

A core type transformer consists of three cores, each carrying a set of phase windings, these cores are interconnected in a manner shown in Fig. 3.3. It is observed that the center limb is shorter than the outer limbs. Therefore under the same magnetic state (i.e. the same flux density), the center limb exhibits less reluctance than the outer ones. This is implying that the steady-state peak value of the three magnetizing currents will not be the same even if the supply is balanced (which it usually is). Hence, the asymmetry in the core geometry leads to asymme-

try in the magnetizing currents. In fact, the peak value of the center limb's current is smaller than those of the outer limbs. In this regard, there is a difference between the three-phase and the bank of three single-phase transformers.

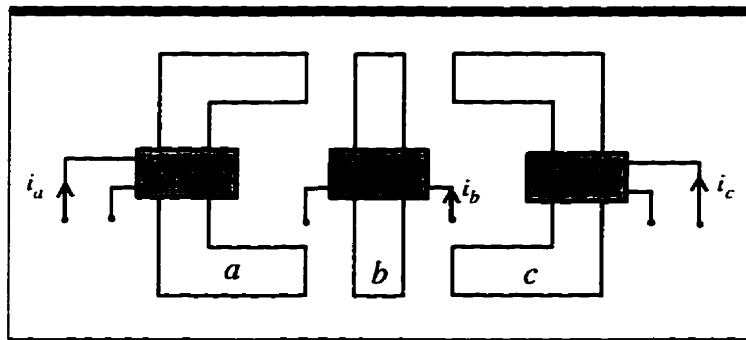


Fig. 3.3: Geometry of the three-phase core type transformer

Before analyzing the magnetic circuit, the followings need to be considered.

- [i] Each core by itself is a magnetic element and like any other circuit element, it is characterized by a functional relation between its input and the output which is usually called the *characteristic curve*. Any characteristic curve is a *physical property* of the element. The characteristic curve for an iron core can be assumed as the $(\lambda - f)$ curve. (discussed in the preceding chapter).

- [ii] Like any other, a magnetic circuit consists of both active and passive elements. The *active elements* are the *net applied mmfs*. (this is the input.)
- [iii] While the characteristic curve describes an individual element, the *KVL* and *KCL* describe the *topology* of the circuit.
- [iv] Once the characteristic, the circuit topology, and the input (inputs) are given, the circuit can be solved.

Fig. 3.4 demonstrates the similarities between a magnetic circuit element and its electric counterpart. “*v*” represents the *voltage drop* across the *resistor*, while “*f*” represents the *mmf drop* across the iron core.

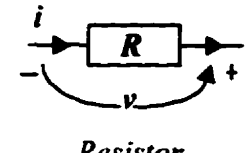
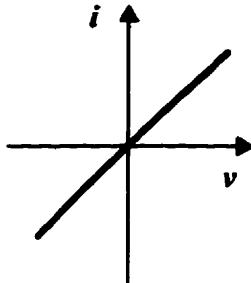
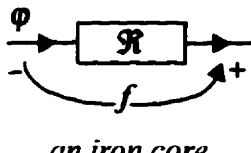
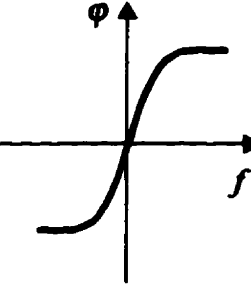
Circuit element	Characteristic curve	Slope of the curve
 <p>Resistor</p>		R^{-1} (Conductance)
 <p>an iron core</p>		\mathfrak{R}^{-1} (Permeance)

Fig. 3.4: Comparison between a magnetic element (iron core) and an electric element (resistor)

3.4 Magnetic Equivalent Circuit of the Three Phase Transformer

As one of the computational steps toward solving the three-phase transformer, it is necessary to find the *magnetizing flux in each limb* for a given set of *mmfs*. This has to be done by solving the magnetic circuit.

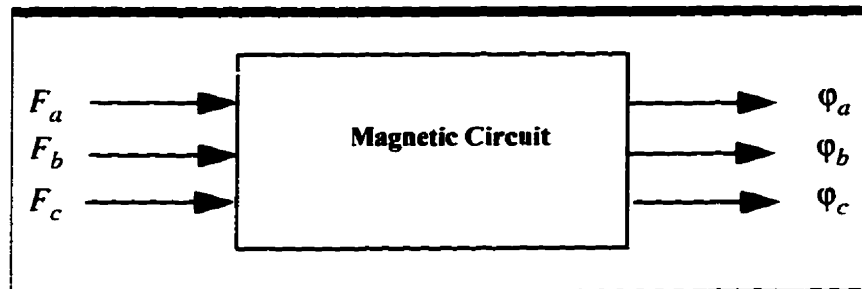


Fig. 3.5: Input and output of the magnetic circuit

The magnetic equivalent circuit of a three-phase transformer is shown below. It consists of three nonlinear elements, one linear magnetic element, and three mmfs. The linear element is the zero-sequence flux path in the air. This *magnetic equivalent circuit is the same* for all possible winding connection schemes.

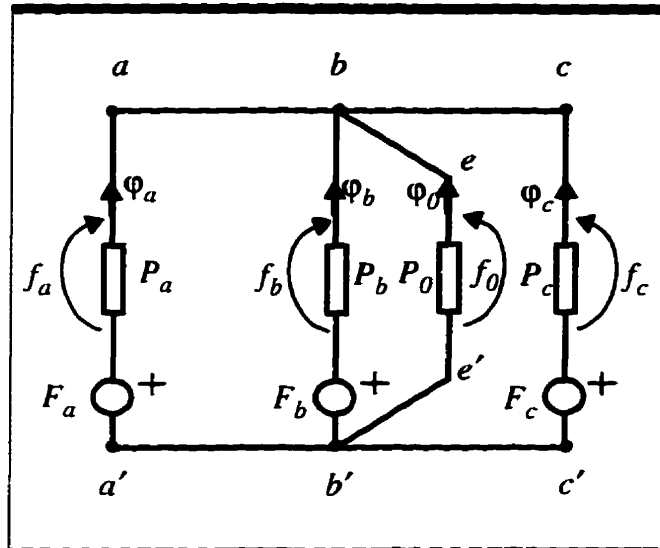


Fig. 3.6: the equivalent magnetic circuit of the three-phase core type transformer

F_a , F_b and F_c are the net or *effective mmf* applied by each winding to the corresponding core, and are given by Eqn. 3.9. f_a , f_b and f_c are the *mmf drop* across each limb is analogous to the voltage drop across the resistor. P_a , P_b and P_c are the *permeances* of the corresponding cores.

Under balanced voltage conditions, the sum of the three magnetizing fluxes (i.e. ϕ_a , ϕ_b and ϕ_c) is zero. However, under unbalanced operations, the sum is no longer zero. The net sum will emerge out of the transformer and flow into the many continuously distributed paths in the air between the upper and lower part of the transformer. To simplify calculations, it is assumed that these

paths are concentrated around the center limb and its permeance is designated as by P_0 . The *zero-sequence permeance* is constant since the permeability of the air is constant.

Applying *KCL* to node “b” of the circuit in Fig. 3.6 the following is obtained:

$$\lambda_a + \lambda_b + \lambda_c + \lambda_0 = 0 \quad (3.13)$$

Applying *KVL* to the three loops $abe - e'b'a'$, $be - e'b'$ and $cbe - e'b'c'$ results in the following:

$$\begin{aligned} F_a &= f_a - f_0 \\ F_b &= f_b - f_0 \\ F_c &= f_c - f_0 \end{aligned} \quad (3.14)$$

The *mmf drop* across the *zero-sequence path* is a linear function of the flux; therefore:

$$f_0 = \frac{\lambda_0}{P_0} \quad (3.15)$$

Combining the above with the two previous equations we get:

$$\begin{aligned}
 F_a &= f_a + \frac{I}{p_0} \cdot (\lambda_a + \lambda_b + \lambda_c) \\
 F_b &= f_b + \frac{I}{p_0} \cdot (\lambda_a + \lambda_b + \lambda_c) \\
 F_c &= f_c + \frac{I}{p_0} \cdot (\lambda_a + \lambda_b + \lambda_c)
 \end{aligned} \tag{3.16}$$

Recall that, $\lambda_a, \lambda_b, \lambda_c$ are characteristics of the corresponding cores which are generally expressed as (nonlinear) functions of the mmf drops.

$$\begin{aligned}
 \lambda_a &= h_1(f_a) \\
 \lambda_b &= h_1(f_b) \\
 \lambda_c &= h_1(f_c)
 \end{aligned} \tag{3.17}$$

Putting Eqn. 3.16 and Eqn. 3.17 together we'll get:

$$\begin{aligned}
 H_1(f_a, f_b, f_c, F_a, p_0) &= f_a + \frac{I}{p_0} \cdot [h_1(f_a) + h_2(f_b) + h_3(f_c)] - F_a = 0 \\
 H_2(f_a, f_b, f_c, F_a, p_0) &= f_b + \frac{I}{p_0} \cdot [h_1(f_a) + h_2(f_b) + h_3(f_c)] - F_b = 0 \\
 H_3(f_a, f_b, f_c, F_a, p_0) &= f_c + \frac{I}{p_0} \cdot [h_1(f_a) + h_2(f_b) + h_3(f_c)] - F_c = 0
 \end{aligned} \tag{3.18}$$

This system of non-linear equation is in standard form for solving numerically for the three unknowns (f_a, f_b and f_c). Back substituting of these *mmf drops* into the Eqn. 3.17 yields the fluxes.

The *Newton-Raphson* method was employed to solve the above set of non-linear equations.

3.5 Determination of the P-Matrix

Recall that the currents are found by numerically integrating the Eqn. 3.12.

In order to do this, at each computational step the *P-Matrix* should be evaluated first. The *P-Matrix* is defined by Eqn. 3.8. The diagonal elements of this matrix are the incremental inductances of the primary windings (*self inductance*), whereas the off diagonal elements represent the incremental *mutual inductances*, between windings. In order to evaluate this matrix, both sides of Eqn. 3.16 have to be differentiated with regard to F_a , F_b and F_c . This would produce nine equations.

After significant algebraic manipulation, the nine unknowns (the nine elements of the *P-matrix*) can be obtained. The detailed derivation of the *P-Matrix* can be found in *Appendix A*. The result is as follows:

$$\mathbf{P} = \frac{\begin{bmatrix} p_a \cdot (p_b + p_c + p_0) & -(p_a \cdot p_b) & -(p_a \cdot p_c) \\ -(p_a \cdot p_b) & p_b \cdot (p_c + p_a + p_0) & -(p_b \cdot p_c) \\ -(p_a \cdot p_c) & -(p_b \cdot p_c) & p_c \cdot (p_a + p_b + p_0) \end{bmatrix}}{(p_a + p_b + p_c + p_0)} \quad (3.19)$$

where p_i is the permeance of the core i , ($i = a, b, c$) and is defined as: $p_i = \frac{\partial \lambda_i}{\partial f_i}$

where it is found directly by differentiating the core characteristics.

3.5.1 Bank of Three Single Phase Transformers

A bank of three single-phase transformers is a special case of the three-phase transformer. Since the magnetic circuits of the three phases are completely separated from one another, the *P-Matrix* consists of only the diagonal elements. In other words, there is no mutual inductances between the primary windings. When solving a bank of three-single-phase transformers, it is only required to replace the permeance of each limb with that of each transformer core, and to set the off-diagonal elements in the *p-Matrix* along with the zero-sequence permeance to zero as shown below.

$$\mathbf{P} = \begin{bmatrix} p_a & 0 & 0 \\ 0 & p_b & 0 \\ 0 & 0 & p_c \end{bmatrix} \quad (3.20)$$

3.6 The Diagram of Solution Procedures

It is useful to review the whole procedure of solving the three-phase transformer in a block diagram. This is shown in block diagram in Fig. 3.7. Details of the MatLab program are given in appendix E. In particular, the 4th and 5th order Runge-Kutta integration routine with an adaptive time-step in the order of micro second is used.

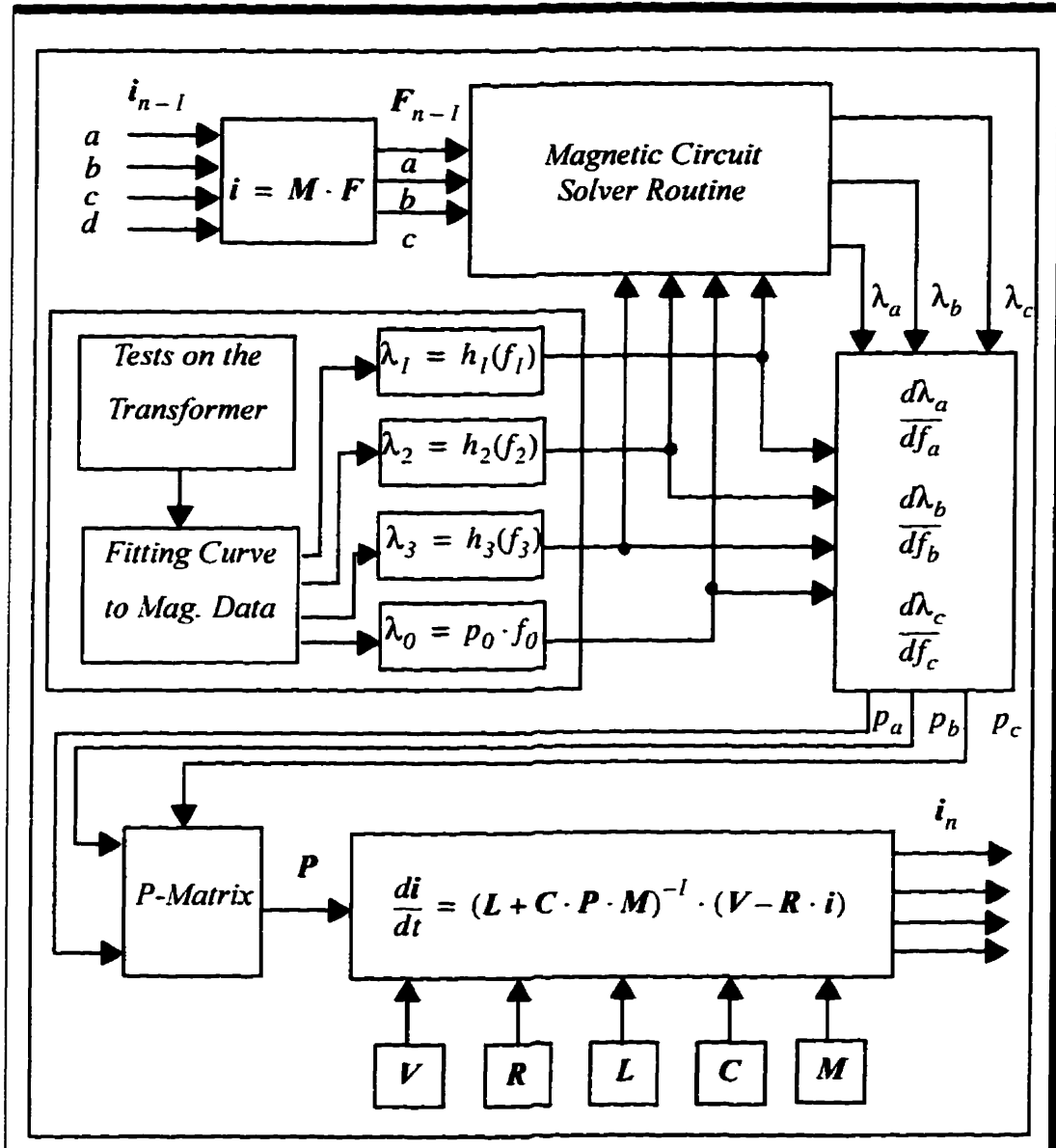


Fig. 3.7: One computation step towards solving the three-phase transformer

Chapter 4

Electric and Magnetic Parameters Measurement

The transformer under test was a *10-KVA, 120 V/600 V three-limb core type* which was provided by the Department of Electrical Engineering at the University of Manitoba. The measurement procedures covered both electrical and magnetic parameters. Electrical parameters include the winding resistances and leakage-inductances. Magnetic parameters are the $(\lambda - f)$ curves for the three limbs and the zero-sequence permeance.

4.1 Electrical Parameters of the Three Phase Transformer

The copper resistance was measured by applying a dc-voltage and recording the current in each coil. Since the values agreed within $\pm 1\%$, they were averaged for the primary winding resistances and for the secondary winding resistances. In measuring the leakage inductances the conventional short circuit

test was carried out by applying a 60-Hz low voltage to the high-voltage side of the transformer. Also it was assumed that the *per-unit leakage inductances of primary and secondary of each winding* were the same. This is a valid assumption for a well designed transformer [17].

4.1.1 Source Impedance

It was assumed that the three-phase source was ideal, since the impedance of the cables connecting the transformer to the source was found to be negligible. Therefore the only impedance that will appear between the ideal source and the transformer will be the impedance of the *thyristor-controlled switch*. Fig. 4.1 shows the measured electrical parameters for this transformer.

	Resistance (Ω)	Leakage inductance H	Number of turns
<i>primary</i>	0.11	3.5×10^{-4}	75
<i>secondary</i>	2.73	8.74×10^{-3}	375
<i>source</i>	0.1	0	-

Fig. 4.1: Electrical parameters of the tested transformer

4.2 Measurement of the Core Characteristic

The magnetic characteristic of each core is the functional relation between the *flux* and the *mmf drop* across it. In Chapter 2 it was concluded that when modeling the transformer for simulating the inrush current it was adequate to represent the core characteristics by the saturation curve. The procedure of obtaining the saturation curve consisted of exciting one of the coils which are wound around the core by a slow-varying dc-current, and then measuring the flux developed in that core. The flux measurement can be done by integrating the induced voltage across a coil (usually called the search coil) which is linked by the magnetic flux, then it is multiplied by the turn ratio in order to get the linkage flux of the primary.

In the test, the secondary winding was chosen as the search coil. Also it was found more reliable to integrate the induced voltage by software rather than hardware. The hardware integration incorporates operational amplifiers which are normally associated with the drift problem.

4.3 Core Characteristics of a Three Phase Transformer

Referring to Fig. 3.3, the core of a three-phase transformer consists of three branches. The outer limbs are identical but the center limb is shorter. It is assumed that these three cores are made of the same magnetic material and have the same uniform cross-sections. In other words, the per-unit characteristic is the same for

all three branches. Suppose that this per-unit characteristic is given as:

$$\lambda = h(f) \quad (4.1)$$

Then the characteristics of each core is found by multiplying this *per-unit mmf drop* by the length of that core in the above equation.

$$\begin{aligned} \lambda_a &= h(f \cdot l_a) \\ \lambda_b &= h(f \cdot l_b) \\ \lambda_c &= h(f \cdot l_c) \end{aligned} \quad (4.2)$$

Where l_a , l_b and l_c are the length of the three cores (mean path values.) Eqn. 4.2 implies that the core characteristic measurement has to be done for only one of the branches, but in doing this two problems emerge:

- i None of these branches is detachable
- ii Even if they were detachable they would not be suitable for the test since the flux path would not be limited to the iron core. Fig. 4.2 illustrates this point.

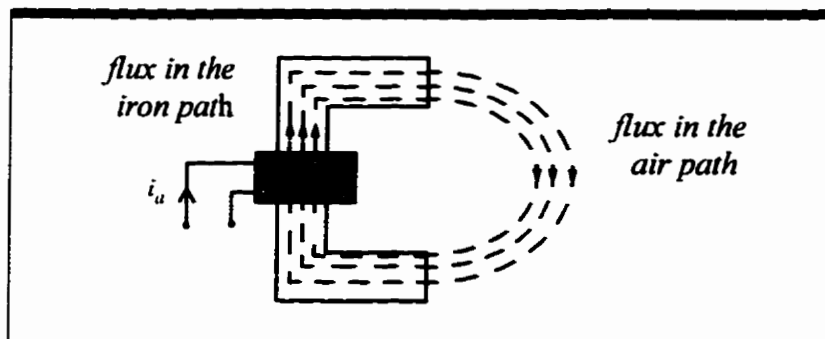


Fig. 4.2: flux path for an excited iron segment

This figure clearly shows that in order to obtain the magnetic characteristic of an iron, the iron must constitute a closed path, otherwise the magnetic characteristic of the air will dominate. Now, let's consider the three-phase transformer shown in Fig. 3.1. Suppose that limb "a" is excited by applying current to its primary winding. The flux in this limb will not follow a single closed path, rather it branches out between the other two limbs. In order to establish a single closed path either the center limb or the right most limb should be eliminated. Since it is impossible to do this physically, one has to force the flux in one of these two limbs to zero. As shown in Fig. 4.3 applying two equal and opposite *mmf*'s to the outer limbs will force the flux in the center limb equal zero.

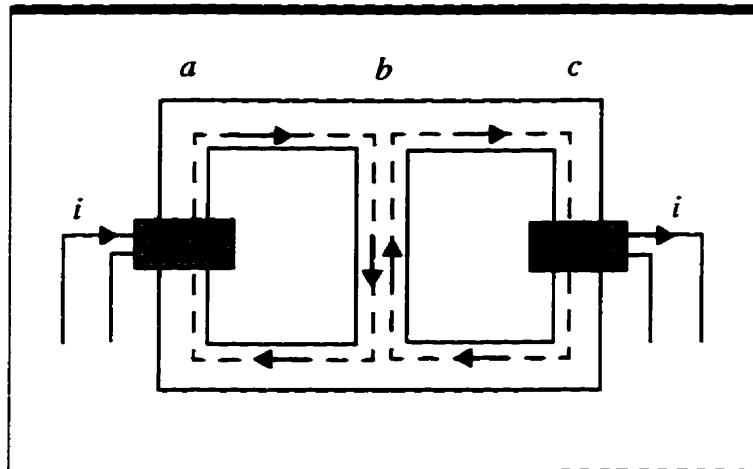


Fig. 4.3: *Eliminating the effect of center limb*

In practice the two outer limbs might not be perfectly identical, and hence the flux in the center limb might be slightly larger than zero. In this case the primary of the center limb can be short circuited. Since the winding resistance is very small, the inductive component of the induced current will dominate and establishes a flux in the center limb that *almost equals and opposite* to the original non-zero one. The following figure illustrates this point.

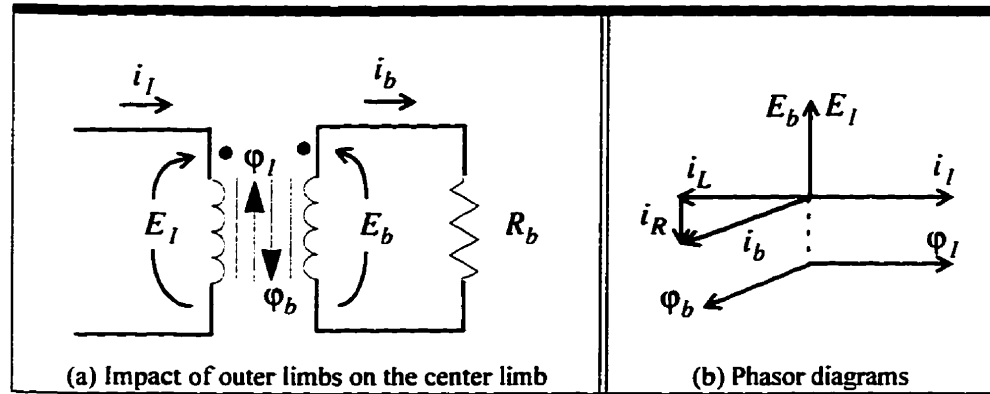


Fig. 4.4: Analysis of the induced current in the center limb when it is short circuited

In part (a) of Fig. 4.4 the left circuit is an equivalent circuit of the outer limbs and the right one is the center limb when its primary is short circuited. When the outer limbs are not perfectly identical then the net flux driven in the center limb (ϕ_L) would be slightly larger than zero. It is hoped that by shorting the primary terminals of the center limb, an opposing flux would be developed in the center limb which would counterbalance the non-zero flux. As shown in the phasor diagram this is true only if the winding resistance of the center limb is zero. The induced current has two components, one is the resistive current and the other the inductive component. If saturation is not encountered (in the center limb) then due to having relatively large inductance, the inductive component of the induced current will dominate and this will establish a counter flux which almost cancels out the original non-zero flux in the center limb. If saturation is encountered then the

inductive component of the current no longer dominates and the developed flux cannot completely oppose the non-zero one.

Once the combined magnetic characteristic is found for the outer limbs, the characteristic for any of the three limbs can be found by using Eqn. 4.2.

4.4 Measurement Procedures

Experimental setup used for measuring the core characteristics of the three-phase transformer is in Fig. 4.4 the primary windings of phase "a" and phase "c" were connected in series so that their corresponding flux in the outer limbs aid and in the center limb cancel each other. A variable dc voltage source used to drive current into the primaries in series. The secondaries of the outer limbs were also connected in series to serve as a search coil. A two-channel digital data acquisition equipment was used to digitize and store the voltage and current data in a file. Later on using software the data of the sampled voltage was appropriately scaled and integrated in order to yield the flux. Since the time interval between two subsequent samples was very small, the trapezoidal rule was used for integration. A sampling resistor of value of $1\ \Omega$ was used to sample the current. This current was multiplied by the number of primary turns to get the mmf drop. By varying the dc source the current was increased from zero to +30 amperes and then decreased back to zero.

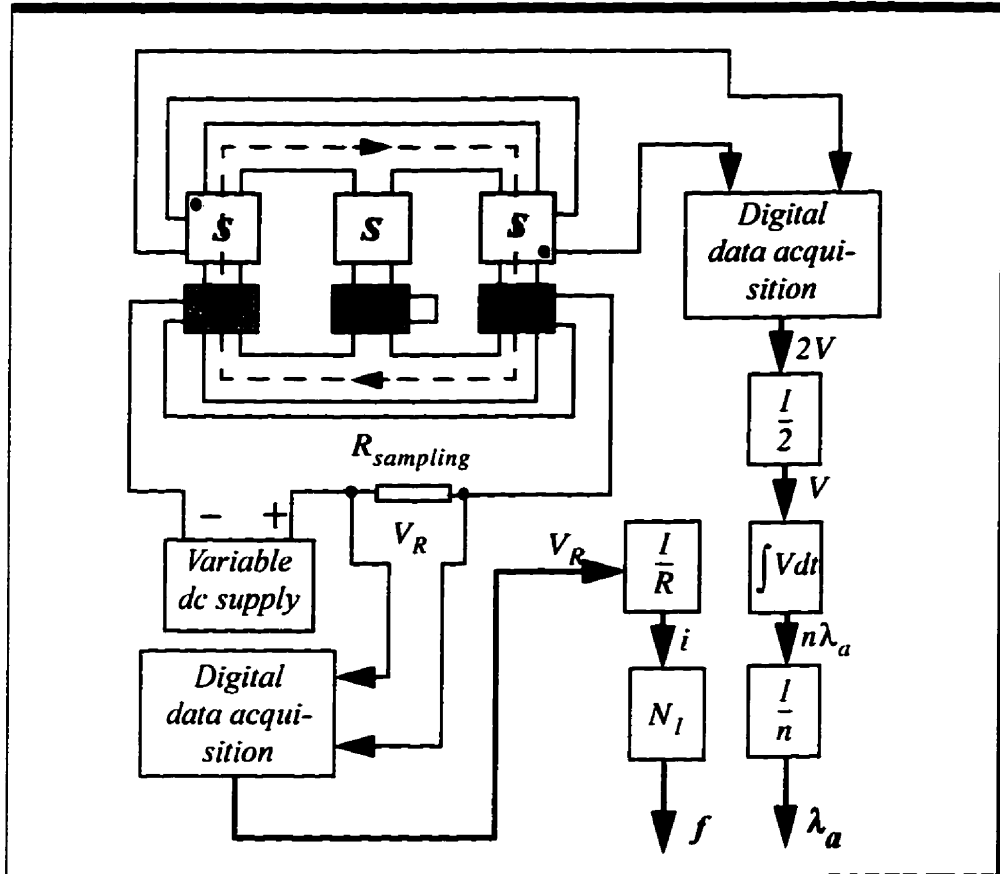


Fig. 4.5: Experimental setup for obtaining the core characteristics of the three-phase transformer

Fig. 4.6 shows the plot of the actual sampled current and induced voltage versus time for the above setup.

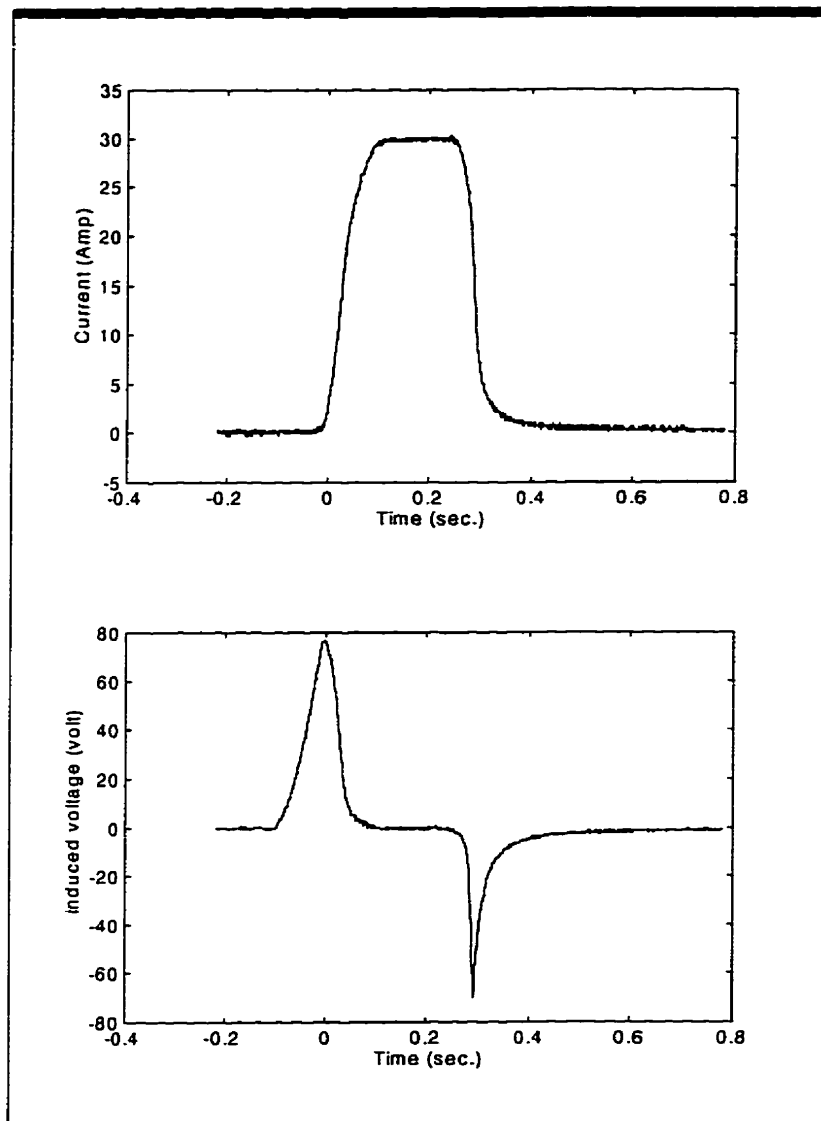


Fig. 4.6: Sampled current and search coil voltage for setup in Fig. 4.5

As mentioned earlier, flux measurement was done by numerically integrating the induced voltage across the secondary windings. This flux (in terms of the

primary linkage flux) is plotted in Fig. 4.7 And finally this flux is plotted as

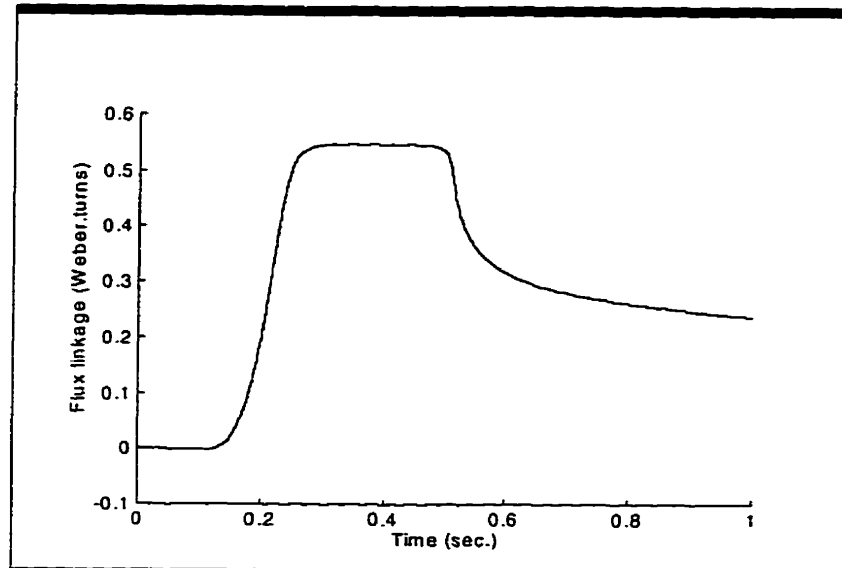


Fig. 4.7: Flux measurement for setup in Fig. 4.5

function of the applied mmf in Fig. 4.8.

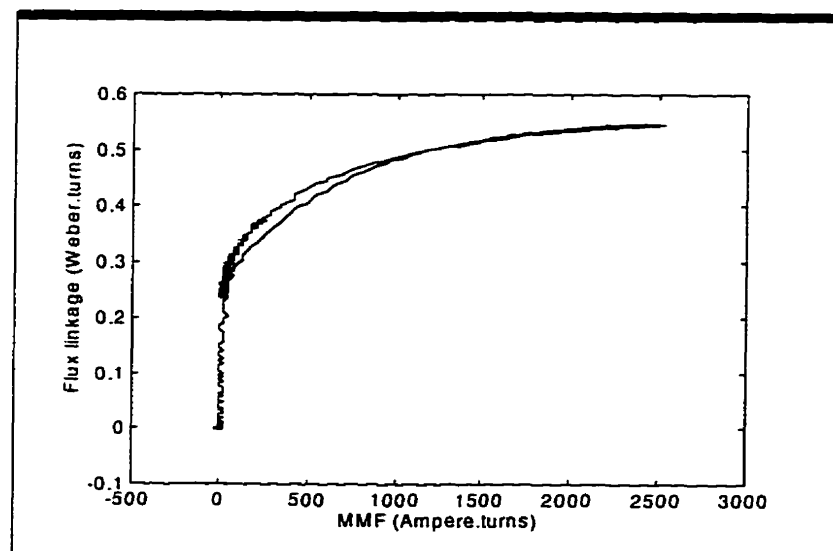


Fig. 4.8: Flux-mmf plot for each outer limbs in Fig. 4.5 setup

This is half of the dc-hysteresis loop for outer limbs. Due to symmetry the other half can be easily found just by changing the sign of both flux and mmf drop.

This plot reveals that the residual flux is $\phi_{res} = \frac{0.25}{75} = 3.33 \times 10^{-3} \text{ Weber}$.

4.5 60-Hz. AC Hysteresis Loop

Using the same setup as illustrated in Fig. 4.5 and applying the winding's *rated ac voltage*, measurement for the steady-state hysteresis loop was carried out. The loop can give some idea about the size of core losses due to hysteresis and eddy currents. Fig. 4.9 shows the steady-state hysteresis loop for limb "a".

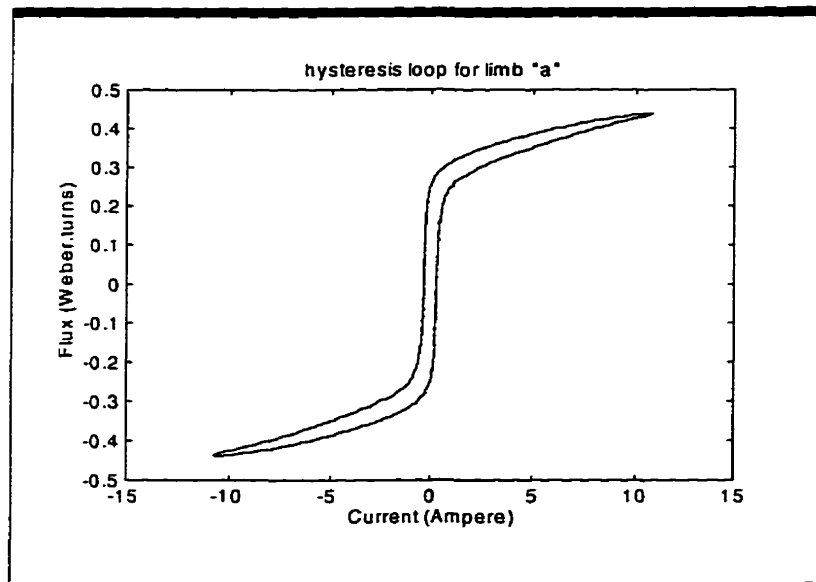


Fig. 4.9: 60-Hertz steady-state hysteresis loop for outer limbs

The area of the loop accounts for the core loss per cycle. This area was

numerically calculated and it was almost $1 \frac{\text{Joule}}{\text{cycle}}$. In other words the total power loss in this core was about 60 *Watts*. Since the voltage of each phase is 120 *V*, this much power accounts for an equivalent current of 1/2 *A*. This current is less than 5 percent of the steady-state magnetizing current and less than 0.5 percent of the first peak of the magnetization inrush current, therefore it is a reasonable approximation to ignore the core losses and represent the core characteristic by only the saturation curve. For modern power transformers, as it was discussed in chapter 2, this approximation is definitely valid since the area of the loop is almost zero.

4.6 Curve Fitting

Fig. 4.8 depicts the core characteristic experimentally obtained for limbs "a" and "c". This curve is almost a single-valued one. An eight-piece curve was experimentally fitted to this magnetic data in order to serve as the expression for the magnetic characteristic. For the center limb the same equation was used the only difference being that the *mmf drop* was multiplied by the ratio of center limb length to outer limb length. The following expression shows the equation for the fitted curve for the outer limbs.

$$f(\lambda) = \begin{cases} 52\lambda & 0.1 \geq \lambda \geq 0.0 \\ 5.2 + 5.2(\lambda - 0.1)e^{10.3(\lambda - 0.1)} & 0.45 \geq \lambda \geq 0.1 \\ 675 + 8808(\lambda - 0.45)e^{6.123(\lambda - 0.45)} & 0.53 \geq \lambda \geq 0.45 \\ 1824.6 + 2141.7(\lambda - 0.53)e^{14(\lambda - 0.53)} & \lambda \geq 0.53 \\ 52\lambda & -0.1 \leq \lambda \leq 0.0 \\ -5.2 + 5.2(\lambda - 0.1)e^{(-10.3)(\lambda + 0.1)} & -0.45 \leq \lambda \leq -0.1 \\ -675 + 8808(\lambda + 0.45)e^{(-6.123)(\lambda + 0.45)} & -0.53 \leq \lambda \leq -0.45 \\ -1824.6 + 2141.7(\lambda + 0.53)e^{(-14)(\lambda + 0.53)} & \lambda \leq -0.53 \end{cases}$$

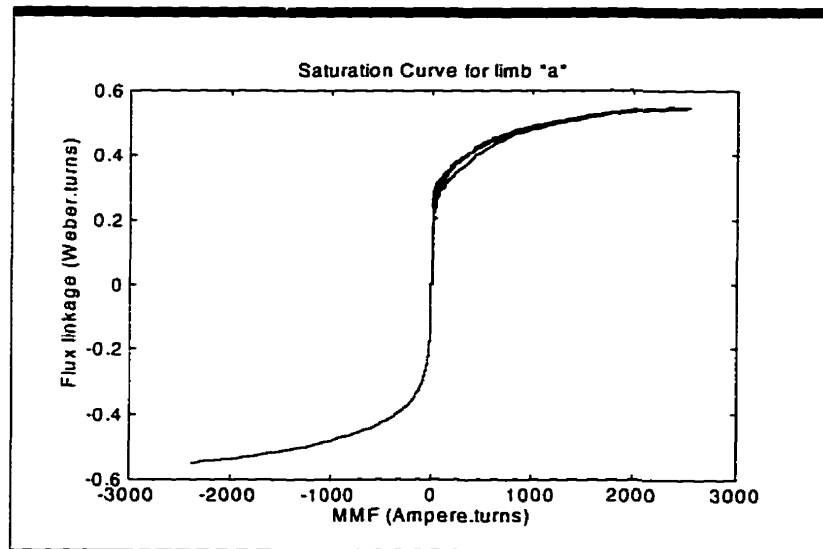


Fig. 4.10: plot of fitted curve superimposed on the plot of actual magnetic data for limb "a"

Fig. 4.10 shows the plot of both the actual data and the plot of the fitted curve superimposed over each other. The agreement between them is good.

4.7 Zero-Sequence Permeance Measurement

Under steady-state operation, the sum of magnetizing fluxes in the three limbs is zero. However in the transient-state, this sum is no longer zero. This non-zero flux which emerges out and flows into the air surrounding the transformer is usually called the *zero-sequence flux*. Although the zero-sequence path is continuously distributed between the upper and lower parts of the transformer, it is assumed that this flux is concentrated around the single path between the upper and lower nodes (b, b'). This assumption will greatly simplify the magnetic circuit and decreases the number of related equations. It might introduce a slight discrepancy between the computed value and the measured value of currents. Since the permeability of air is constant, the *zero-sequence flux* is a linear function of the *applied mmf*.

4.7.1 Experimental Setup

In order to create the zero-sequence flux, the primary windings of the three limbs are connected in series in a manner that the three applied mmfs were of the same polarity and magnitude as shown in Fig. 4.11. This would force the magnetizing flux in the three limbs to have the same direction. At the center node these fluxes add up, emerging out of the transformer and flowing into the surrounding

air. The secondary winding of the center limb was chosen to serve as a search coil. The current in the primary circuit was slowly increased from zero to almost 30 Amperes, then decreased back to zero.

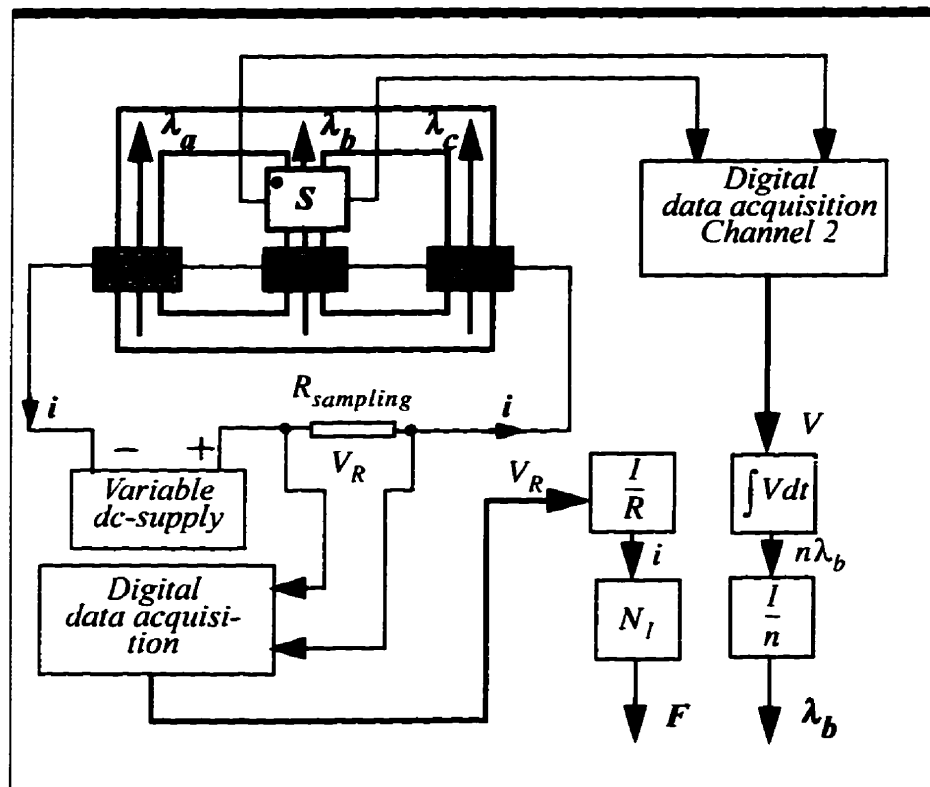


Fig. 4.11: Setup for determining the zero-sequence permeance

The time-varying flux in the center limb develops a voltage across its secondary winding. This voltage and the primary current was digitally recorded.

These data are plotted in Fig. 4.12.

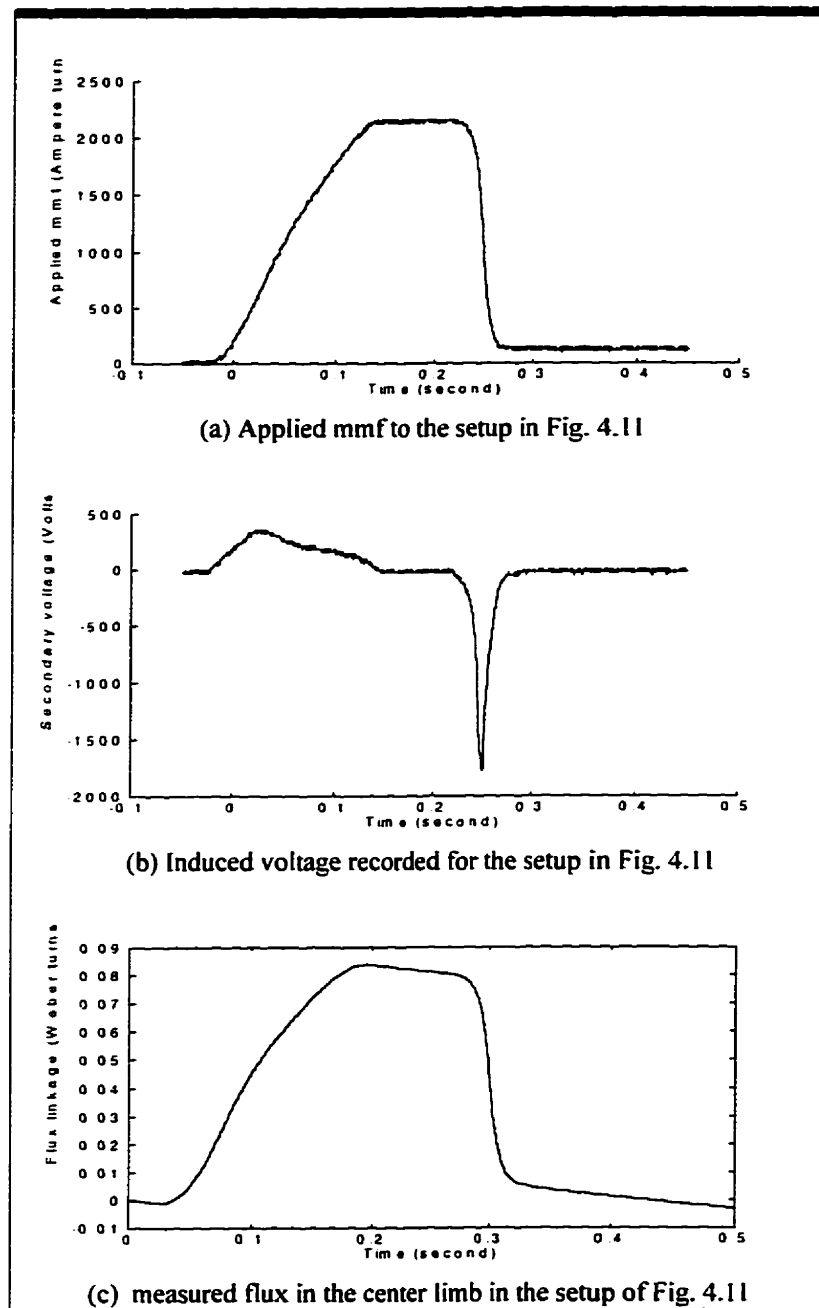


Fig. 4.12: Plot of magnetic data recorded in the setup of Fig. 4.11

According to Fig. 4.12 the *flux* in the center limb is very similar to the *applied mmf*. This implies that the derived flux and the applied mmf are proportional to each other. In other words the center limb and consequently the other limbs operate in the linear region of their characteristics. This is true since the maximum developed flux in the center limb (part (c)) is less than *0.09 weber.turns*. This corresponds to the region of linear operations in the saturation curve (see Fig. 4.8 or Fig. 4.10). The following plot verifies this point.

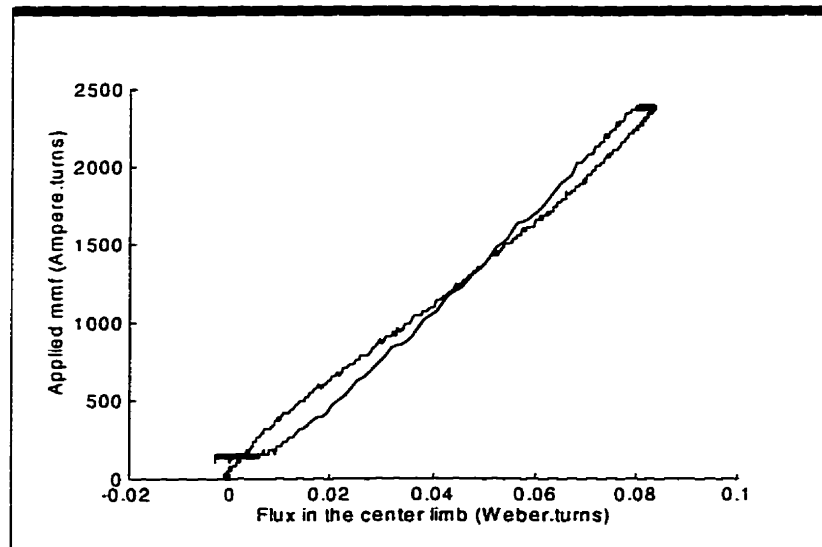


Fig. 4.13: Plot of applied mmf vs. the center limb's flux

The plot is almost identical to a straight line with the following expression:

$$F = 28000 \cdot \lambda_b \quad (4.3)$$

4.7.2 Computation Part

Using the measured linkage flux (λ_b) and the applied mmf (F) in the setup of Fig. 4.11, it is possible to determine the zero-sequence permeance as it follows. The magnetic circuit of the three-phase transformer is redrawn in Fig. 4.14 for convenience. Since the three applied mmfs are identical in magnitude and direction, they behave as a single mmf which drives the flux in the air.

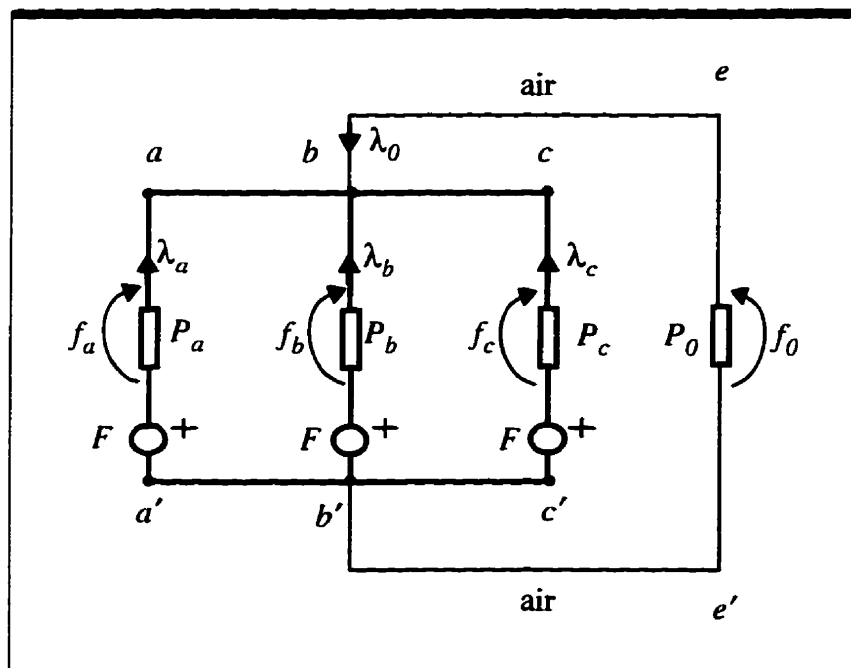


Fig. 4.14: Magnetic circuit of the core-type three-phase transformer

Referring to Fig. 4.14 and considering the fact that the three externally applied mmf's are equal, it is concluded that the three mmf drops must be equal.

Writing *KVL* for loop $be - e'b'$ and *KCL* for node b yields:

$$\begin{aligned} F - f_b &= -f_0 \\ \lambda_0 + \lambda_a + \lambda_b + \lambda_c &= 0 \end{aligned} \quad (4.4)$$

Since the characteristic of the air is linear:

$$f_0 = \frac{\lambda_0}{\rho_0} \quad (4.5)$$

Combining Eqn. 4.4 and Eqn. 4.5:

$$\rho_0 = \frac{(\lambda_a + \lambda_b + \lambda_c)}{F - f_b} \quad (4.6)$$

The *mmf drop* across the center limb (f_b) is much smaller than the *applied mmf*

(F). Therefore Eqn. 4.6 can be written as:

$$\rho_0 = \frac{(\lambda_a + \lambda_b + \lambda_c)}{F} \quad (4.7)$$

F has already been found as a linear function of λ_b , (see Eqn. 4.3) and so the

above equation can be re-written as:

$$\rho_0 = \frac{(\lambda_a + \lambda_b + \lambda_c)}{28000 \cdot \lambda_b} \quad (4.8)$$

All of the three limbs operating in the linear region are made of the same material and carry the same mmf. Therefore, it is concluded that the flux in each limb must be inversely proportional to the length of each limb, so:

$$\frac{\lambda_a}{\lambda_b} = \frac{\lambda_c}{\lambda_b} = \frac{l_b}{l_a} \quad (4.9)$$

But $\frac{l_b}{l_a}$ (the ratio of mean path values) was measured as 0.35

This means that:

$$\lambda_a = \lambda_c = 0.35 \cdot \lambda_b \quad (4.10)$$

Substituting this equation back into Eqn. 4.8 results in:

$$p_0 = \frac{(0.35 \cdot \lambda_b + \lambda_b + 0.35 \cdot \lambda_b)}{28000 \cdot \lambda_b} = 6.07 \times 10^{-5} \cdot \frac{Wb}{A} \quad (4.11)$$

The same result was obtained when the Eqn. 4.6 and the non-linear equation $f_a(\lambda_a) - f_b(\lambda_b) = 0$ were numerically solved.

Chapter 5

Comparison of the Actual and Computed Inrush Currents

The only way to judge the validity of a *model* is to compare the *experimental results* and the *predicted outcomes* of the model under the given conditions. In this chapter the actual inrush current and the computed ones will be compared for different connection schemes and Initial conditions. The initial condition for each case of comparison consists of the *switch-in angle* of the supply voltage and the *remanent flux* in each limb of the transformer. In Chapter 1 it was mentioned that a three-phase thyristor switch was constructed to control the switch-in angle on the voltage cycle. This switch energizes the transformer consistently at the instant of positive-going and zero-crossing of phase “a”. Fig. 5.1 shows the voltage of phase “a” as well as the voltage applied to transformer at the instant of which the switch is turned on.

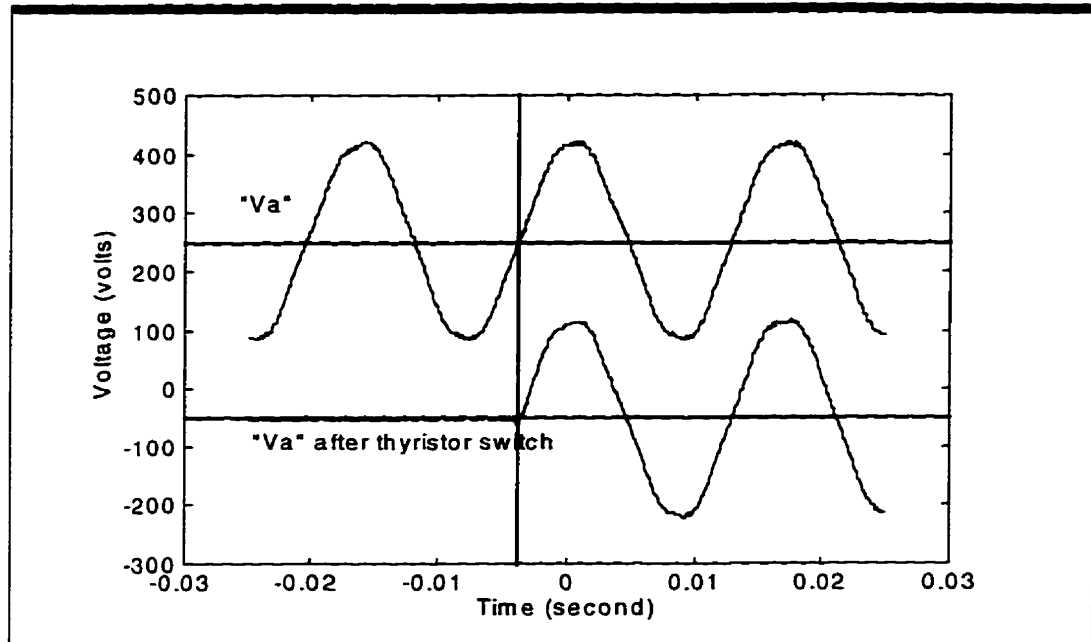


Fig. 5.1: The instant of switching on the voltage cycle

The initial flux for each limb and case was established as listed:

- (iii) A variable three-phase supply was connected to the transformer and set to the rated voltage.
- (iv) The transformer limbs were demagnetized by gradually reducing the voltage down to zero.

- (v) Primaries of the outer limbs were connected in series with regard to appropriate polarity such that when connected to a dc-source, the resulting fluxes were added up in the center limb. The dc-current was raised to 30 Amperes. As a result the center limb was magnetically saturated.

Computations showed that the first peak of inrush current for the transformer under test can reach as high as 500 Amperes. Three 600 amperes (rms) CTs were chosen for measuring the inrush currents. Direct measurements revealed that the CTs are not completely faithful to the current waveforms simply because they are ac-coupling devices. In other words they can't detect the decaying dc-component of the inrush current. It is for this reason that the idea of using CT's was almost disregarded. Three *resistors* with the value of $1\ \Omega$ were connected in series with the primary windings to serve as *current samplers*. Smaller values could not be used because of excessive noise at low currents. The side effect of using the resistors was that they reduce the peak of inrush current down to almost 25 percent of its actual value. In the following, the plot of actual currents and that of the computed currents for different windings connection schemes is depicted. In the following plots all the currents actually start from zero.

5.1 4-Wire Star/Star (Without Secondaries Loading.)

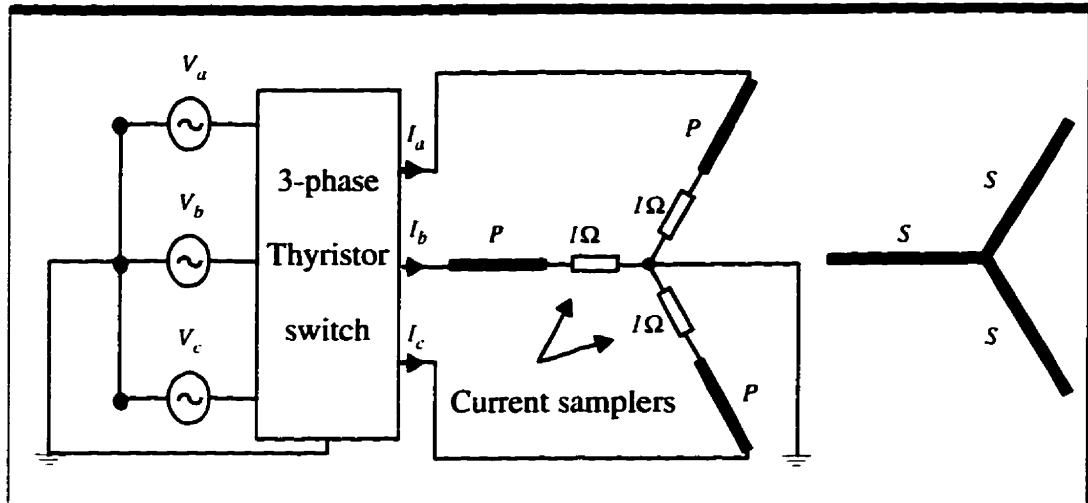


Fig. 5.2: Setup for sampling the inrush currents for the case of 4-wire star/star

Supply voltages:

$$V_a = 120 \cdot \sqrt{2} \cdot \sin(2\pi \cdot 60 \cdot t + \theta_0)$$

$$V_b = 120 \cdot \sqrt{2} \cdot \sin\left(2\pi \cdot 60 \cdot t + \theta_0 - \frac{2 \cdot \pi}{3}\right)$$

$$V_c = 120 \cdot \sqrt{2} \cdot \sin\left(2\pi \cdot 60 \cdot t + \theta_0 - \frac{4 \cdot \pi}{3}\right)$$

Initial Conditions: $\theta_0 = 0$

$$\lambda_{a0} = 0.2 \quad (\text{Wb} \cdot \text{turns})$$

$$\lambda_{b0} = -0.4 \quad (\text{Wb} \cdot \text{turns})$$

$$\lambda_{c0} = 0.2 \quad (\text{Wb} \cdot \text{turns})$$

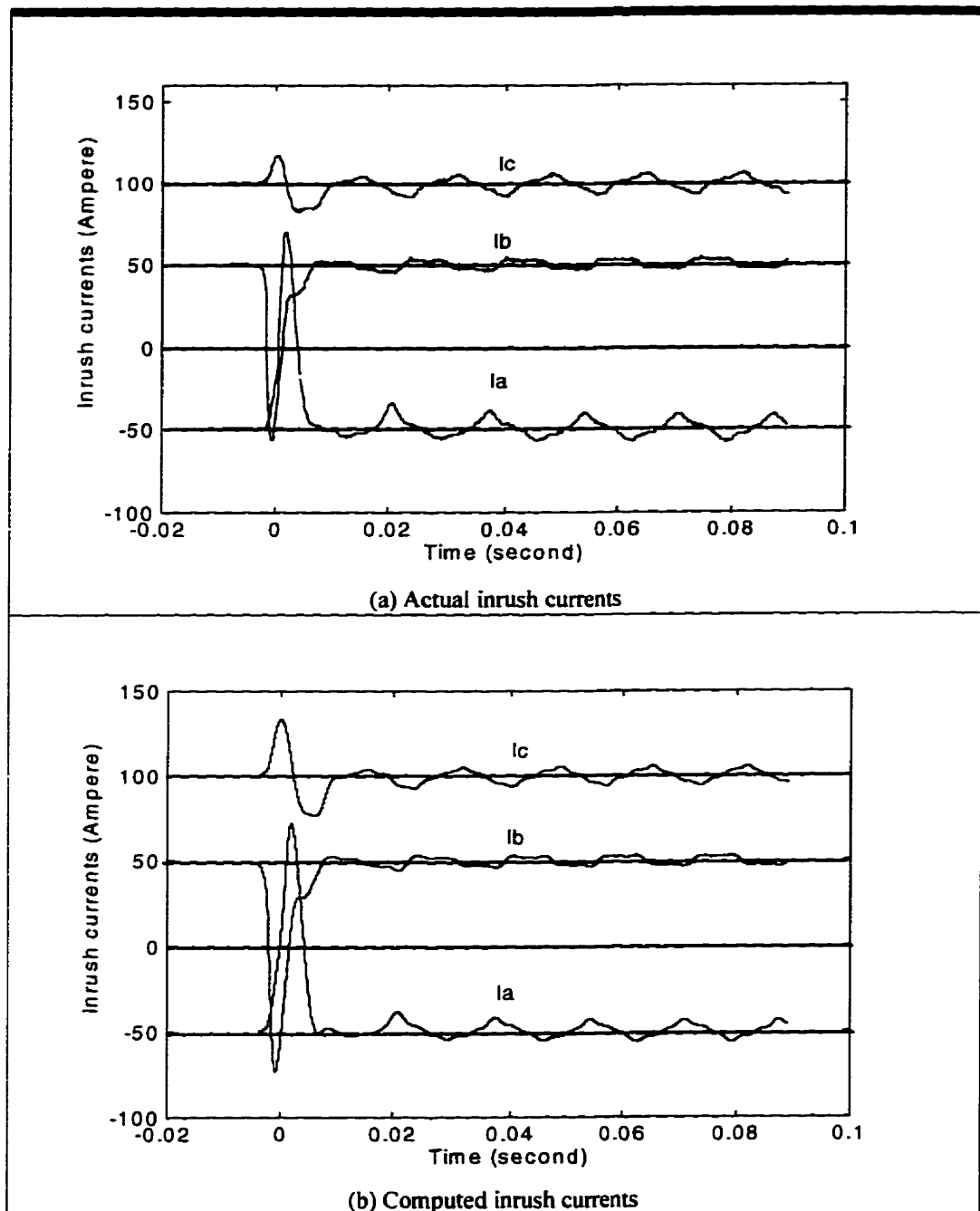


Fig. 5.3: Comparison of the actual and computed inrush currents for 4-wire star/star

NOTE: All currents artificially shifted.

5.2 4-Wire Star/Closed Delta (Without Secondaries Loading.)

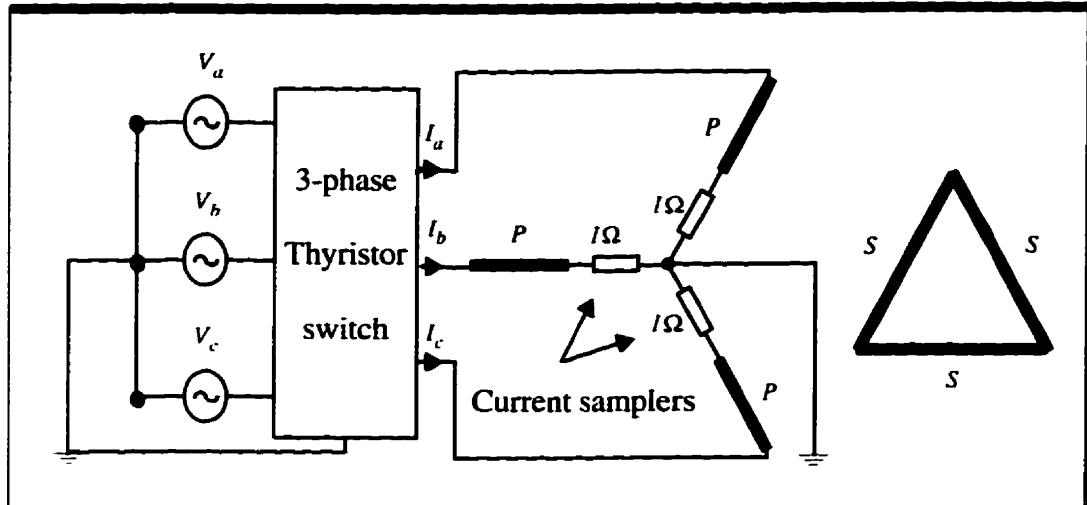


Fig. 5.4: Setup for sampling the inrush currents for the case of 4-wire star/closed delta

Supply Voltages:

$$V_a = 120 \cdot \sqrt{2} \cdot \sin(2\pi \cdot 60 \cdot t + \theta_0)$$

$$V_b = 120 \cdot \sqrt{2} \cdot \sin\left(2\pi \cdot 60 \cdot t + \theta_0 - \frac{2 \cdot \pi}{3}\right)$$

$$V_c = 120 \cdot \sqrt{2} \cdot \sin\left(2\pi \cdot 60 \cdot t + \theta_0 - \frac{4 \cdot \pi}{3}\right)$$

Initial Conditions: $\theta_0 = 0$

$$\lambda_{a0} = 0.2 \quad (\text{Wb} \cdot \text{turns})$$

$$\lambda_{b0} = -0.4 \quad (\text{Wb} \cdot \text{turns})$$

$$\lambda_{c0} = 0.2 \quad (\text{Wb} \cdot \text{turns})$$

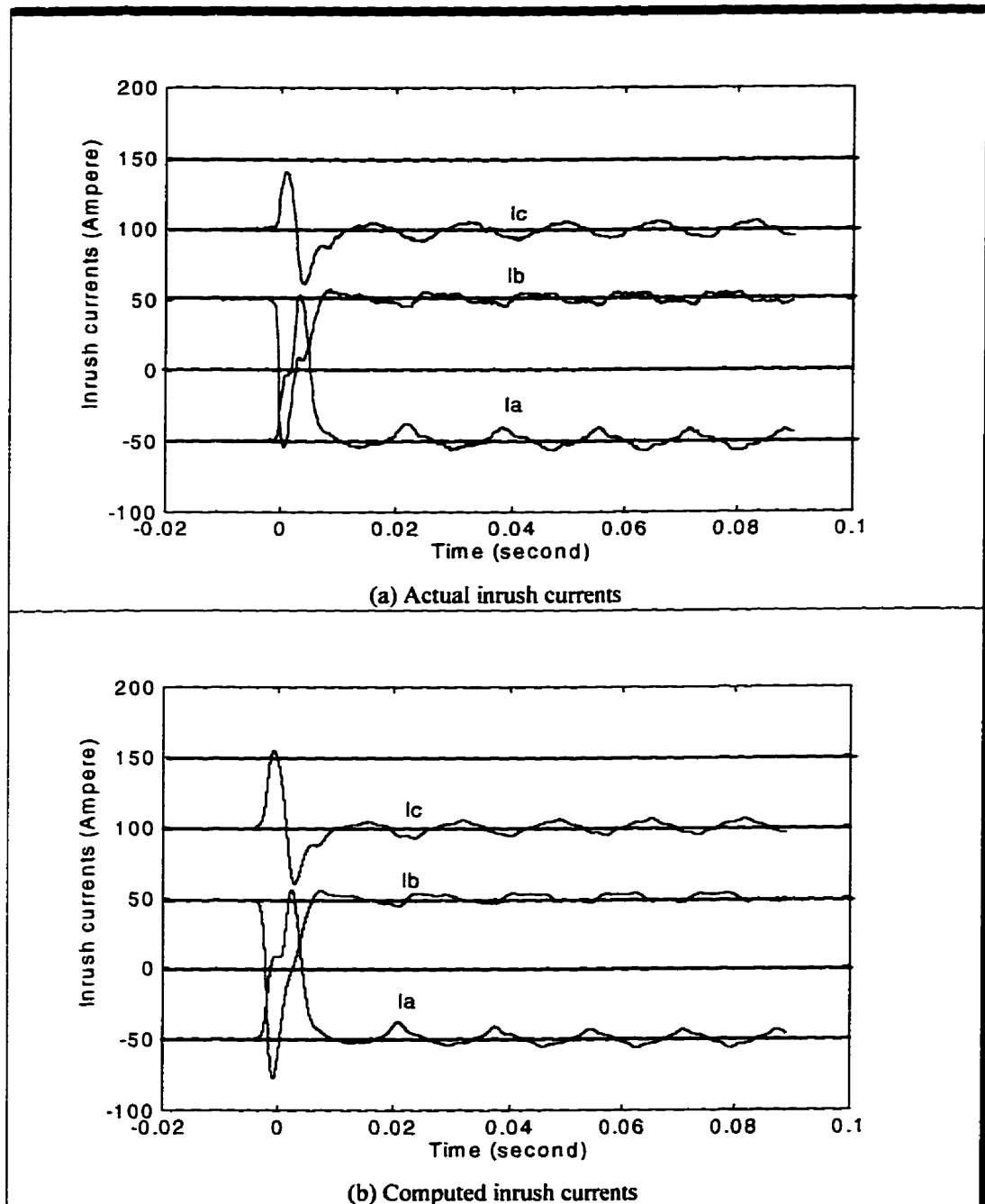


Fig. 5.5: Comparison of actual and computed inrush currents for 4-wire star/closed delta

NOTE: All currents artificially shifted.

5.3 Star/Star (Without Secondaries Loading.)

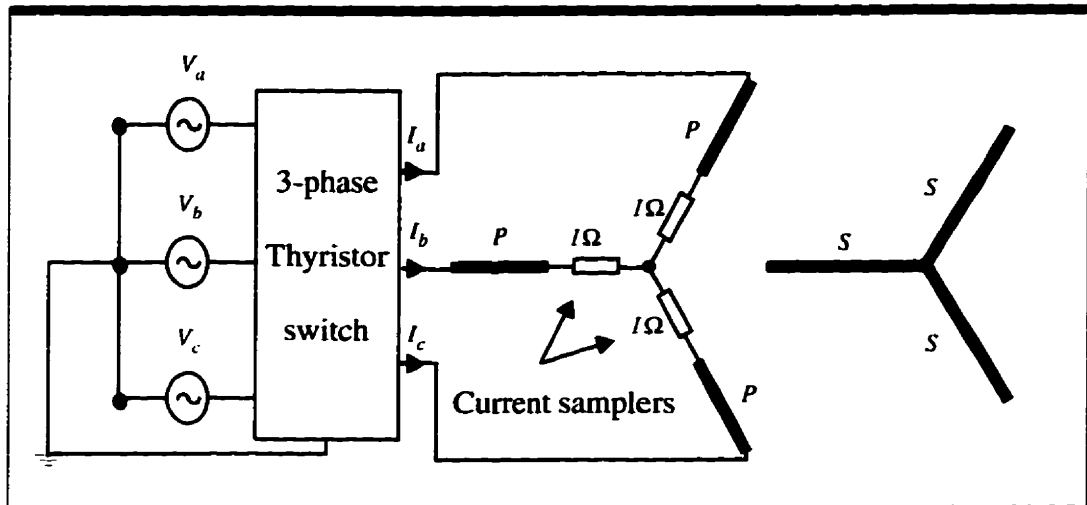


Fig. 5.6: Setup for sampling the inrush currents for the case of star/star

Supply Voltages:

$$V_a = 120 \cdot \sqrt{2} \cdot \sin(2\pi \cdot 60 \cdot t + \theta_0)$$

$$V_b = 120 \cdot \sqrt{2} \cdot \sin\left(2\pi \cdot 60 \cdot t + \theta_0 - \frac{2 \cdot \pi}{3}\right)$$

$$V_c = 120 \cdot \sqrt{2} \cdot \sin\left(2\pi \cdot 60 \cdot t + \theta_0 - \frac{4 \cdot \pi}{3}\right)$$

Initial Conditions: $\theta_0 = 0$

$$\lambda_{a0} = 0.2 \quad (\text{Wb} \cdot \text{turns})$$

$$\lambda_{b0} = -0.4 \quad (\text{Wb} \cdot \text{turns})$$

$$\lambda_{c0} = 0.2 \quad (\text{Wb} \cdot \text{turns})$$

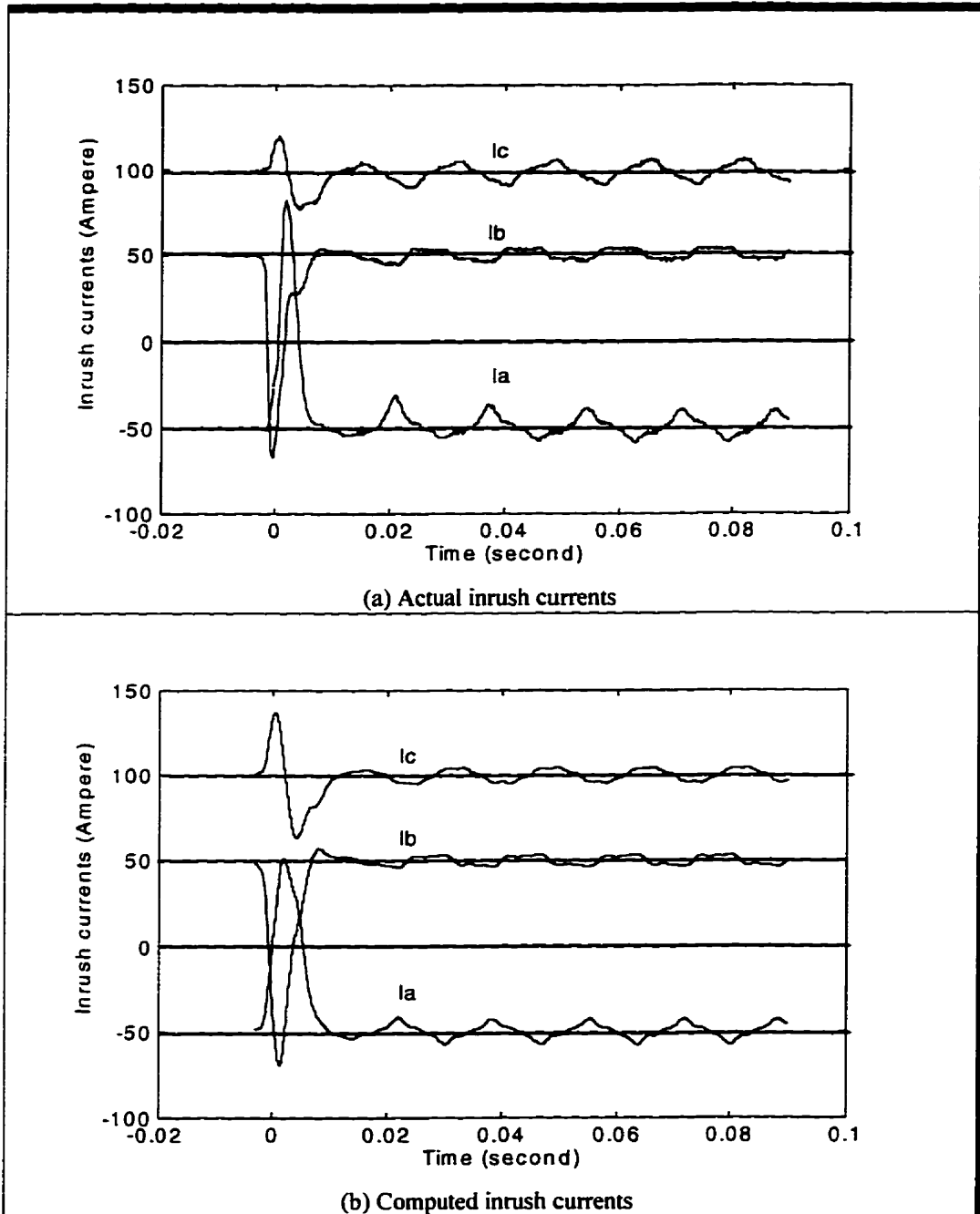


Fig. 5.7: Comparison of actual and computed inrush current for star/star

NOTE: All currents artificially shifted.

5.4 Star/Closed-Delta (Without Secondaries Loading.)

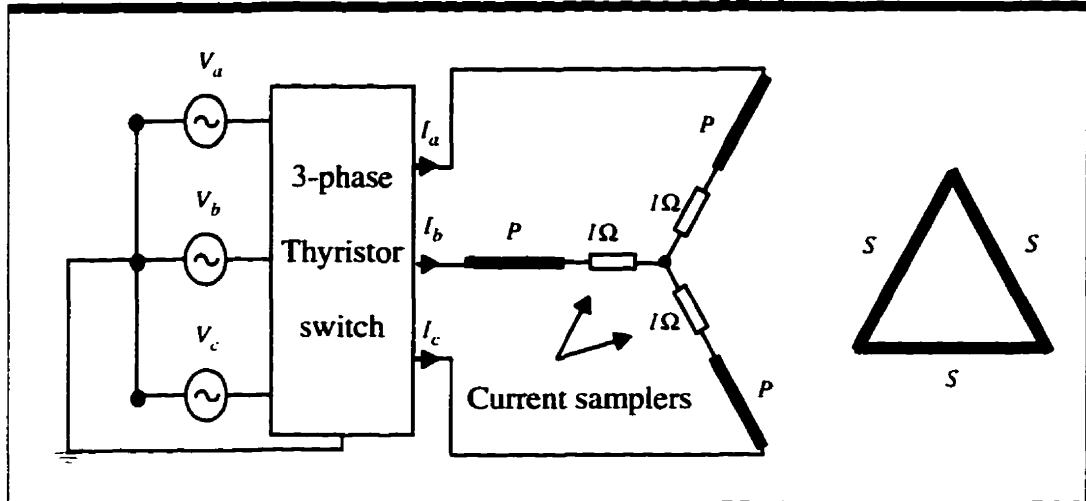


Fig. 5.8: Setup for sampling the inrush currents for the case of star/closed delta

Supply Voltages:

$$V_a = 120 \cdot \sqrt{2} \cdot \sin(2\pi \cdot 60 \cdot t + \theta_0)$$

$$V_b = 120 \cdot \sqrt{2} \cdot \sin\left(2\pi \cdot 60 \cdot t + \theta_0 - \frac{2 \cdot \pi}{3}\right)$$

$$V_c = 120 \cdot \sqrt{2} \cdot \sin\left(2\pi \cdot 60 \cdot t + \theta_0 - \frac{4 \cdot \pi}{3}\right)$$

Initial Conditions: $\theta_0 = 0$

$$\lambda_{a0} = 0.2 \quad (\text{Wb} \cdot \text{turns})$$

$$\lambda_{b0} = 0 \quad (\text{Wb} \cdot \text{turns})$$

$$\lambda_{c0} = -0.2 \quad (\text{Wb} \cdot \text{turns})$$

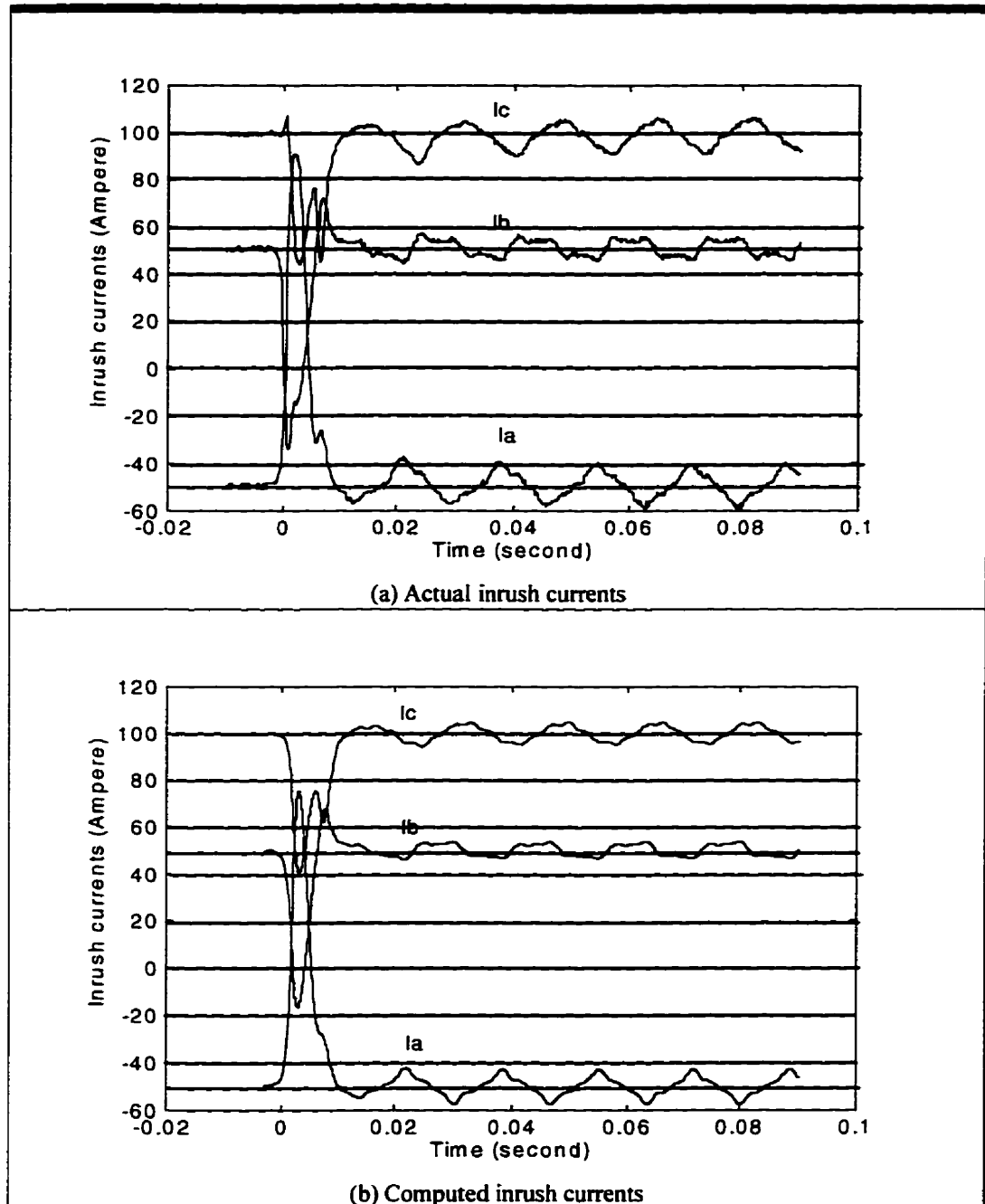


Fig. 5.9: Comparison of actual and computed inrush currents for star/closed delta

NOTE: All currents artificially shifted.

5.5 4-Wire Star/Star (Steady-State, Without Secondaries Loading.)

This case compares the actual *magnetizing current* and the computed one for the *steady-state operation* of the transformer.

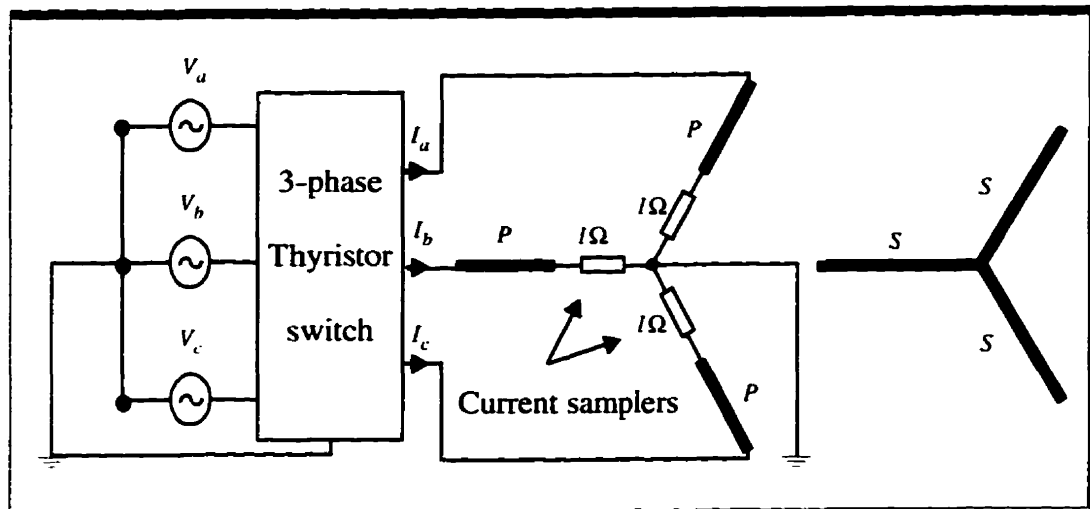


Fig. 5.10: Setup for sampling the magnetizing currents for the case of 4-wire star/star

Supply Voltages:

$$V_a = 120 \cdot \sqrt{2} \cdot \sin(2\pi \cdot 60 \cdot t + \theta_0)$$

$$V_b = 120 \cdot \sqrt{2} \cdot \sin\left(2\pi \cdot 60 \cdot t + \theta_0 - \frac{2 \cdot \pi}{3}\right)$$

$$V_c = 120 \cdot \sqrt{2} \cdot \sin\left(2\pi \cdot 60 \cdot t + \theta_0 - \frac{4 \cdot \pi}{3}\right)$$

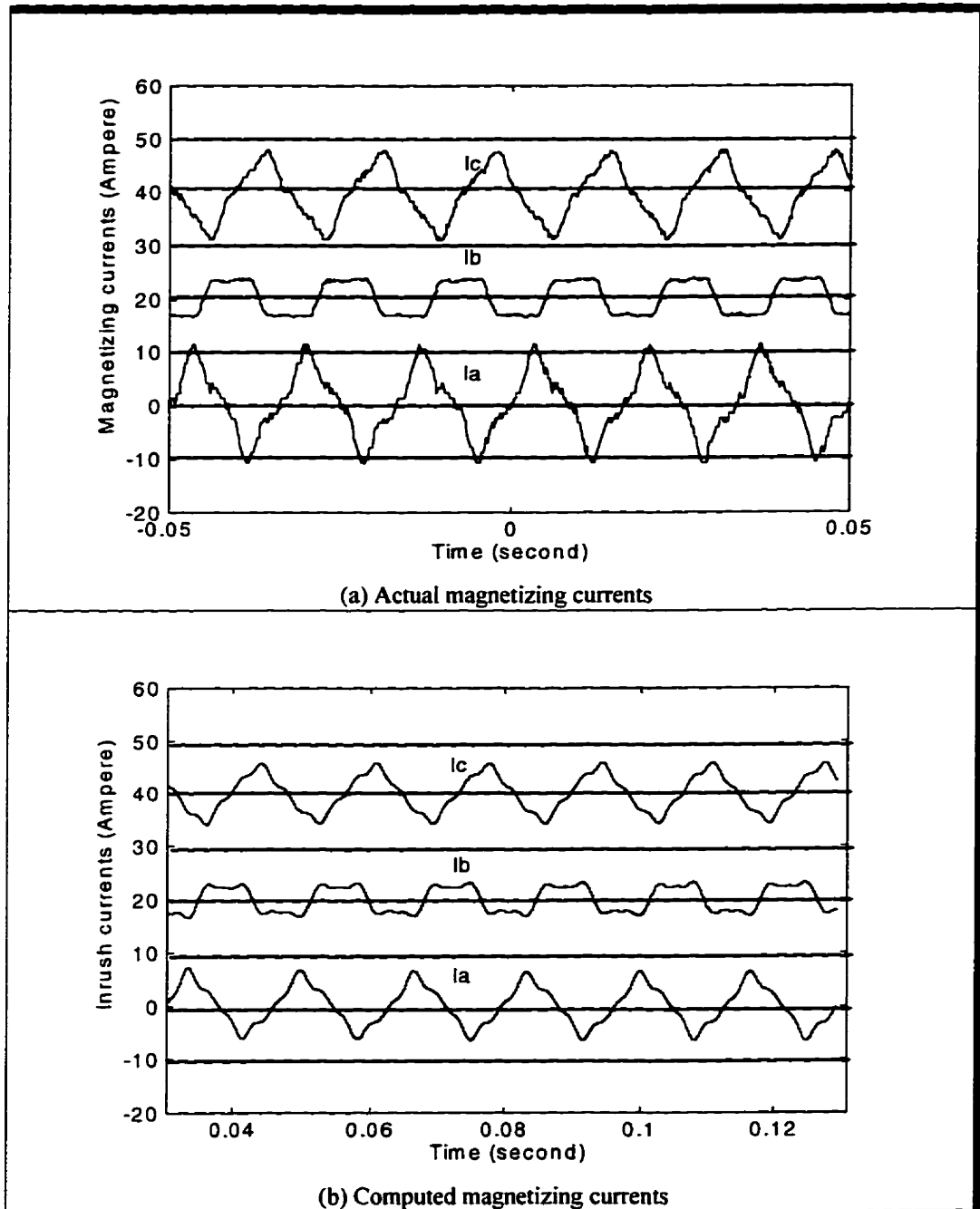


Fig. 5.11: Comparison of actual and computed magnetizing currents for 4-wire star/star

NOTE: All currents artificially shifted.

Chapter 6

Summary & Conclusions

A detailed mathematical model for computing the magnetizing inrush current for a *three-phase core type transformer* has been developed. The model takes the nonlinearity and the saturation aspect of the core characteristic into account. It can be applied to any single-phase or three-phase core type power transformer. Provided that the core characteristics of each limb in terms of the saturation curve and the zero-sequence permeance of the transformer, and the electrical parameters are accurately determined. This model is satisfactorily capable of predicting the inrush current for cases of 4-wire star/delta and star/delta with floating null phase connection schemes for a 10-KVA commercial transformer. The model also considers the initial conditions which would be the initial phase on the voltage cycle and the remanent flux in each limb. The basic idea of how to analyze a single phase transformer was discussed in Chapter 1. The idea was based on dividing the task into the electric equivalent and the magnetic circuit. A complete solution to a

single-phase transformer was presented at the end.

6.1 Summary

The following list summarizes the work presented through the course of this project:

- (i) A detailed treatment of the single-phase transformer including analysis of the magnetic and electric equivalent circuits, as well as discussion on the different aspects of core characteristics and core modeling.
- (ii) A thorough discussion of the three-phase core type transformer with the star/delta phase connections. The discussion included analysis of magnetic circuit. The relatively complicated magnetic circuit was broken down into three non-linear circuit elements. This approach lead the way to relate the derivatives of flux vectors to those of current vectors. The complete solution for the three-phase transformer was presented at the end of chapter 3.
- (iii) A method to determine the permeance of the

zero-sequence path was discussed in detail.

- (iv) Various tests on the 10-KVA core type three-phase transformer were carried out in order to determine:
- The core characteristics for each of the three limbs.
 - The zero-sequence path permeance.
 - Recording the inrush currents for various phase connection schemes and initial remanent flux in order to be compared with the computed ones.
- (v) Design and construction of a three-phase thyristor switch capable of consistently energizing the three-phase transformer at the instant of zero-crossing and positive-going.
- (vi) Implementation of the transformer model by developing a computer program written in MatLab Language in terms of M-files and computing the inrush currents for different situations.

6.2 Conclusions

The comparison between the actual inrush currents and computed currents show that:

- (a) - There is a good agreement between the actual currents and the computed ones in case of a 4-wire star/delta configuration.
- (b) - There is a reasonable agreement between the actual currents and the computed ones in case of the star/delta configuration.
- (c) - The resemblance between the actual and computed current wave forms in the steady-state operations is good but not identical. The peak value of the computed currents is however a bit smaller than that of the actual currents. The discrepancy is due to the total core losses (including the eddy current and hysteresis) which was completely ignored in the model.
- (d) - For the higher values of currents the agreement between the actual currents and the computed currents is not expected to be as good as at lower current levels. This is because not enough magnetizing current was used (30 Amperes) when obtaining the saturation curve. The peak of inrush is much higher than 30 Amperes. The saturation curve was only obtained for maxi-

imum magnetizing current of 30 Amperes. The saturation curve was extrapolated beyond this value. It is a known fact that in a deep saturation a small deviation in the slope results in a large deviation in the current.

- (e) - The assumption of the zero-sequence path concentrated around the center limb is an approximation, so it is not completely accurate. A part of the accuracy was compromised to simplify and reduce the number of equations involved in the magnetic circuit.
- (f) - Direct measurement and computation of inrush current revealed that the *switching angle* on the voltage cycle has a larger effect on the magnitude of the inrush current than the remanent flux.

Given the saturation curve, the electrical parameters of the transformer it is possible to solve the problem of inrush current for a three-phase transformer. It is critical to determine the saturation curve in the region of deep saturation as accurate as possible.

List of References

- [1] Michelson, E.L.: "*Rectifier Relay for Transformer Protection.*" A.I.E.E. Transaction, May, 1945, Vol.64, No.
- [2] Hicks, B.C.: Contribution to Discussion on ref. [1]. A.I.E.E. Transaction. 1947, Vol.66, pp. 915-917.
- [3] Sharp, R.L. and Glassburn, W.E: "*A Transformer Differential Relay with Second Harmonic Restraint.*" A.I.E.E. Transactions, December, 1958, Vol.77, Part III, pp.884-892.
- [4] Flemming, J.A.. "*Experimental Researches on Alternating Current Transformers.*" Jour. IEE. Vol.21 (1892), Sec. VIII, pp. 677-685.
- [5] Blume, L.F, Camilli, G. Farnham, S.B and Peterson, H.A: "*Transformer Magnetizing Inrush Currents and Influence on System Operation.*" A.I.E.E. Transaction. June. 1944. Vol.63, pp.366-375 and pp.423-424.
- [6] Cordary, R.E., "*Preventing False Operation.*" Electrical World, July 1931. pp. 160-161
- [7] Kurtz, E.B., "*Transformer Current and Power Inrushes under Load.*" Electrical Engineering, V. 56 (1937), pp. 989-994.

-
- [8] Hayward, C.D., "*Prolonged Inrush Currents with Parallel Transformers Affect Differential Relaying.*" Trans. A.I.E.E., Vol. 60 (1941) pp. 1096-1101.
- [9] Specht, T.R., "*Transformer Magnetizing Inrush Current.*" Trans. A.I.E.E., Vol. 70 (1951), p. 323.
- [10] Finzi, L. A. and Mutschler, W.H. Jr., "*The inrush Magnetizing Current in single phase Transformers.*" Trans. A.I.E.E., Vol. 70 (1951), pp. 1436-1438.
- [11] Gravett, K.W.E., "*Magnetizing Inrush Currents in Transformers.*" Electrical Times, Vol. 123 (1953), pp.617-622 and pp. 677-681.
- [12] Hudson, A.A., "*Transformer Magnetizing Inrush Current. A Resume of Published Information.*" The Electrical Research Association, Report No. 5152.
- [13] H.L. Nakra and T.H. Barton, "*Three-Phase Transformer Transients.*" IEEE Trans., Vol. PAS-93, July-December 1974, pp. 1810-1819.
- [14] Swift, G.W.: "*Power Transformer core behavior under Transient conditions*". IEEE Trans. PAS, Sept./Oct. 1971, PAS-90, pp.2206-2210.
- [15] Chen, X.S. and Neudorfer, P., "*Digital model for transient studies of a three-phase five-legged transformer.*", IEE Proceedings-C, Vol. 139, No. 4, July 1992.
-

- [16] Vikilian, M. and Degeneff, R.C., "*A Method for Modeling Nonlinear Core Characteristics of Transformers During Transients.*", IEEE Transactions on Power Delivery, Vol. 9, No. 4, October 1994.
- [17] Sen, P.C, "Principles of Electric Machines and Power Electronics.", 1989 p. 56.
- [18] Motorola *Power Device Data*, Motorola Semiconductor Products Inc.

APPENDIX-A***Determination of P-Matrix***

In chapter 3 it was discussed that by taking derivative of both sides of Eqn. 3.16 the elements of P-matrix can be evaluated, for convenience this equation is reproduced here.

$$\begin{aligned}F_a &= f_a + \frac{I}{p_0} \cdot (\lambda_a + \lambda_b + \lambda_c) \\F_b &= f_b + \frac{I}{p_0} \cdot (\lambda_a + \lambda_b + \lambda_c) \\F_c &= f_c + \frac{I}{p_0} \cdot (\lambda_a + \lambda_b + \lambda_c)\end{aligned}\tag{A.1}$$

Taking derivative of both sides three times with respect to F_a , F_b and F_c produces nine equations as follows.

$$\frac{\partial F_a}{\partial F_a} = \frac{\partial f_a}{\partial F_a} + \frac{1}{p_0} \cdot \left[\frac{\partial \lambda_a}{\partial F_a} + \frac{\partial \lambda_b}{\partial F_a} + \frac{\partial \lambda_c}{\partial F_a} \right]$$

$$\frac{\partial F_b}{\partial F_a} = \frac{\partial f_b}{\partial F_a} + \frac{1}{p_0} \cdot \left[\frac{\partial \lambda_a}{\partial F_a} + \frac{\partial \lambda_b}{\partial F_a} + \frac{\partial \lambda_c}{\partial F_a} \right]$$

$$\frac{\partial F_c}{\partial F_a} = \frac{\partial f_c}{\partial F_a} + \frac{1}{p_0} \cdot \left[\frac{\partial \lambda_a}{\partial F_a} + \frac{\partial \lambda_b}{\partial F_a} + \frac{\partial \lambda_c}{\partial F_a} \right]$$

...

$$\frac{\partial F_a}{\partial F_b} = \frac{\partial f_a}{\partial F_b} + \frac{1}{p_0} \cdot \left[\frac{\partial \lambda_a}{\partial F_b} + \frac{\partial \lambda_b}{\partial F_b} + \frac{\partial \lambda_c}{\partial F_b} \right]$$

$$\frac{\partial F_b}{\partial F_b} = \frac{\partial f_b}{\partial F_b} + \frac{1}{p_0} \cdot \left[\frac{\partial \lambda_a}{\partial F_b} + \frac{\partial \lambda_b}{\partial F_b} + \frac{\partial \lambda_c}{\partial F_b} \right]$$

$$\frac{\partial F_c}{\partial F_b} = \frac{\partial f_c}{\partial F_b} + \frac{1}{p_0} \cdot \left[\frac{\partial \lambda_a}{\partial F_b} + \frac{\partial \lambda_b}{\partial F_b} + \frac{\partial \lambda_c}{\partial F_b} \right]$$

...

$$\frac{\partial F_a}{\partial F_c} = \frac{\partial f_a}{\partial F_c} + \frac{1}{p_0} \cdot \left[\frac{\partial \lambda_a}{\partial F_c} + \frac{\partial \lambda_b}{\partial F_c} + \frac{\partial \lambda_c}{\partial F_c} \right]$$

$$\frac{\partial F_b}{\partial F_c} = \frac{\partial f_b}{\partial F_c} + \frac{1}{p_0} \cdot \left[\frac{\partial \lambda_a}{\partial F_c} + \frac{\partial \lambda_b}{\partial F_c} + \frac{\partial \lambda_c}{\partial F_c} \right]$$

$$\frac{\partial F_c}{\partial F_c} = \frac{\partial f_c}{\partial F_c} + \frac{1}{p_0} \cdot \left[\frac{\partial \lambda_a}{\partial F_c} + \frac{\partial \lambda_b}{\partial F_c} + \frac{\partial \lambda_c}{\partial F_c} \right]$$

(A.2)

Using chain rule,

$$\frac{\partial f_m}{\partial F_n} = \frac{\partial f_m}{\partial \lambda_m} \cdot \frac{\partial \lambda_m}{\partial F_n} \quad \text{where } m,n=a,b,c$$

and considering the following identities:

$$\frac{\partial F_i}{\partial F_j} = 1, \quad \text{if } i = j$$

and $\frac{\partial F_i}{\partial F_j} = 0,$ if $i \neq j$

and also $\frac{\partial f_m}{\partial \lambda_m} = \frac{1}{p_m}$ where $m = a, b, c$

then Eqn. A.2 is rearranged as:

$$\begin{aligned}
1 &= \frac{1}{p_a} \cdot \frac{\partial \lambda_a}{\partial F_a} + \frac{1}{p_0} \cdot \left[\frac{\partial \lambda_a}{\partial F_a} + \frac{\partial \lambda_b}{\partial F_a} + \frac{\partial \lambda_c}{\partial F_a} \right] \\
0 &= \frac{1}{p_b} \cdot \frac{\partial \lambda_b}{\partial F_a} + \frac{1}{p_0} \cdot \left[\frac{\partial \lambda_a}{\partial F_a} + \frac{\partial \lambda_b}{\partial F_a} + \frac{\partial \lambda_c}{\partial F_a} \right] \\
0 &= \frac{1}{p_c} \cdot \frac{\partial \lambda_c}{\partial F_a} + \frac{1}{p_0} \cdot \left[\frac{\partial \lambda_a}{\partial F_a} + \frac{\partial \lambda_b}{\partial F_a} + \frac{\partial \lambda_c}{\partial F_a} \right] \\
&\dots \\
0 &= \frac{1}{p_a} \cdot \frac{\partial \lambda_a}{\partial F_b} + \frac{1}{p_0} \cdot \left[\frac{\partial \lambda_a}{\partial F_b} + \frac{\partial \lambda_b}{\partial F_b} + \frac{\partial \lambda_c}{\partial F_b} \right] \\
1 &= \frac{1}{p_b} \cdot \frac{\partial \lambda_b}{\partial F_b} + \frac{1}{p_0} \cdot \left[\frac{\partial \lambda_a}{\partial F_b} + \frac{\partial \lambda_b}{\partial F_b} + \frac{\partial \lambda_c}{\partial F_b} \right] \\
0 &= \frac{1}{p_c} \cdot \frac{\partial \lambda_c}{\partial F_b} + \frac{1}{p_0} \cdot \left[\frac{\partial \lambda_a}{\partial F_b} + \frac{\partial \lambda_b}{\partial F_b} + \frac{\partial \lambda_c}{\partial F_b} \right] \\
&\dots \\
0 &= \frac{1}{p_a} \cdot \frac{\partial \lambda_a}{\partial F_c} + \frac{1}{p_0} \cdot \left[\frac{\partial \lambda_a}{\partial F_c} + \frac{\partial \lambda_b}{\partial F_c} + \frac{\partial \lambda_c}{\partial F_c} \right] \\
0 &= \frac{1}{p_b} \cdot \frac{\partial \lambda_b}{\partial F_c} + \frac{1}{p_0} \cdot \left[\frac{\partial \lambda_a}{\partial F_c} + \frac{\partial \lambda_b}{\partial F_c} + \frac{\partial \lambda_c}{\partial F_c} \right] \\
1 &= \frac{1}{p_c} \cdot \frac{\partial \lambda_c}{\partial F_c} + \frac{1}{p_0} \cdot \left[\frac{\partial \lambda_a}{\partial F_c} + \frac{\partial \lambda_b}{\partial F_c} + \frac{\partial \lambda_c}{\partial F_c} \right]
\end{aligned} \tag{A.3}$$

This again can be simplified as following.

$$\begin{aligned}
\left(1 + \frac{p_0}{p_a}\right) \cdot \frac{\partial \lambda_a}{\partial F_a} + \frac{\partial \lambda_b}{\partial F_a} + \frac{\partial \lambda_c}{\partial F_a} &= p_0 \\
\frac{\partial \lambda_a}{\partial F_a} + \left(1 + \frac{p_0}{p_a}\right) \cdot \frac{\partial \lambda_b}{\partial F_a} + \frac{\partial \lambda_c}{\partial F_a} &= 0 \\
\frac{\partial \lambda_a}{\partial F_a} + \frac{\partial \lambda_b}{\partial F_a} + \left(1 + \frac{p_0}{p_a}\right) \cdot \frac{\partial \lambda_c}{\partial F_a} &= 0 \\
&\dots \\
\left(1 + \frac{p_0}{p_a}\right) \cdot \frac{\partial \lambda_a}{\partial F_b} + \frac{\partial \lambda_b}{\partial F_b} + \frac{\partial \lambda_c}{\partial F_b} &= 0 \\
\frac{\partial \lambda_a}{\partial F_b} + \left(1 + \frac{p_0}{p_a}\right) \cdot \frac{\partial \lambda_b}{\partial F_b} + \frac{\partial \lambda_c}{\partial F_b} &= p_0 \\
\frac{\partial \lambda_a}{\partial F_b} + \frac{\partial \lambda_b}{\partial F_b} + \left(1 + \frac{p_0}{p_a}\right) \cdot \frac{\partial \lambda_c}{\partial F_b} &= 0 \\
&\dots \\
\left(1 + \frac{p_0}{p_a}\right) \cdot \frac{\partial \lambda_a}{\partial F_c} + \frac{\partial \lambda_b}{\partial F_c} + \frac{\partial \lambda_c}{\partial F_c} &= 0 \\
\frac{\partial \lambda_a}{\partial F_c} + \left(1 + \frac{p_0}{p_a}\right) \cdot \frac{\partial \lambda_b}{\partial F_c} + \frac{\partial \lambda_c}{\partial F_c} &= 0 \\
\frac{\partial \lambda_a}{\partial F_c} + \frac{\partial \lambda_b}{\partial F_c} + \left(1 + \frac{p_0}{p_a}\right) \cdot \frac{\partial \lambda_c}{\partial F_c} &= p_0
\end{aligned} \tag{A.4}$$

These three sets of equations can be written in matrix form.

$$\begin{aligned}
 & \begin{bmatrix} \left(1 + \frac{p_0}{pa}\right) & 1 & 1 \\ 1 & \left(1 + \frac{p_0}{pa}\right) & 1 \\ 1 & 1 & \left(1 + \frac{p_0}{pa}\right) \end{bmatrix} \cdot \begin{bmatrix} \frac{\partial \lambda_a}{\partial F_a} \\ \frac{\partial \lambda_b}{\partial F_a} \\ \frac{\partial \lambda_c}{\partial F_a} \end{bmatrix} = \begin{bmatrix} p_0 \\ 0 \\ 0 \end{bmatrix} \\
 & \dots \\
 & \begin{bmatrix} \left(1 + \frac{p_0}{pa}\right) & 1 & 1 \\ 1 & \left(1 + \frac{p_0}{pa}\right) & 1 \\ 1 & 1 & \left(1 + \frac{p_0}{pa}\right) \end{bmatrix} \cdot \begin{bmatrix} \frac{\partial \lambda_a}{\partial F_b} \\ \frac{\partial \lambda_b}{\partial F_b} \\ \frac{\partial \lambda_c}{\partial F_b} \end{bmatrix} = \begin{bmatrix} 0 \\ p_0 \\ 0 \end{bmatrix} \quad (A.5) \\
 & \dots \\
 & \begin{bmatrix} \left(1 + \frac{p_0}{pa}\right) & 1 & 1 \\ 1 & \left(1 + \frac{p_0}{pa}\right) & 1 \\ 1 & 1 & \left(1 + \frac{p_0}{pa}\right) \end{bmatrix} \cdot \begin{bmatrix} \frac{\partial \lambda_a}{\partial F_c} \\ \frac{\partial \lambda_b}{\partial F_c} \\ \frac{\partial \lambda_c}{\partial F_c} \end{bmatrix} = \begin{bmatrix} 0 \\ 0 \\ p_0 \end{bmatrix}
 \end{aligned}$$

Solving for partial derivative vectors:

$$\begin{aligned}
 \begin{bmatrix} \frac{\partial \lambda_a}{\partial F_a} \\ \frac{\partial \lambda_b}{\partial F_a} \\ \frac{\partial \lambda_c}{\partial F_a} \end{bmatrix} &= \begin{bmatrix} \left(1 + \frac{p_0}{pa}\right) & 1 & 1 \\ 1 & \left(1 + \frac{p_0}{pa}\right) & 1 \\ 1 & 1 & \left(1 + \frac{p_0}{pa}\right) \end{bmatrix}^{-1} \cdot \begin{bmatrix} p_0 \\ 0 \\ 0 \end{bmatrix} \\
 &\dots \\
 \begin{bmatrix} \frac{\partial \lambda_a}{\partial F_b} \\ \frac{\partial \lambda_b}{\partial F_b} \\ \frac{\partial \lambda_c}{\partial F_b} \end{bmatrix} &= \begin{bmatrix} \left(1 + \frac{p_0}{pa}\right) & 1 & 1 \\ 1 & \left(1 + \frac{p_0}{pa}\right) & 1 \\ 1 & 1 & \left(1 + \frac{p_0}{pa}\right) \end{bmatrix}^{-1} \cdot \begin{bmatrix} 0 \\ p_0 \\ 0 \end{bmatrix} \quad (\text{A.6}) \\
 &\dots \\
 \begin{bmatrix} \frac{\partial \lambda_a}{\partial F_c} \\ \frac{\partial \lambda_b}{\partial F_c} \\ \frac{\partial \lambda_c}{\partial F_c} \end{bmatrix} &= \begin{bmatrix} \left(1 + \frac{p_0}{pa}\right) & 1 & 1 \\ 1 & \left(1 + \frac{p_0}{pa}\right) & 1 \\ 1 & 1 & \left(1 + \frac{p_0}{pa}\right) \end{bmatrix}^{-1} \cdot \begin{bmatrix} 0 \\ 0 \\ p_0 \end{bmatrix}
 \end{aligned}$$

Fortunately all these sets of matrix equations have the same inverse matrix. Let's denote the coefficient matrix as \mathbf{K} , then the above can be re-written as:

$$\begin{bmatrix} \frac{\partial \lambda_a}{\partial F_a} \\ \frac{\partial \lambda_b}{\partial F_a} \\ \frac{\partial \lambda_c}{\partial F_a} \end{bmatrix} = K^{-1} \cdot \begin{bmatrix} p_0 \\ 0 \\ 0 \end{bmatrix}$$

...

$$\begin{bmatrix} \frac{\partial \lambda_a}{\partial F_b} \\ \frac{\partial \lambda_b}{\partial F_b} \\ \frac{\partial \lambda_c}{\partial F_b} \end{bmatrix} = K^{-1} \cdot \begin{bmatrix} 0 \\ p_0 \\ 0 \end{bmatrix}$$

(A.7)

...

$$\begin{bmatrix} \frac{\partial \lambda_a}{\partial F_c} \\ \frac{\partial \lambda_b}{\partial F_c} \\ \frac{\partial \lambda_c}{\partial F_c} \end{bmatrix} = K^{-1} \cdot \begin{bmatrix} 0 \\ 0 \\ p_0 \end{bmatrix}$$

$$\mathbf{K} = \begin{bmatrix} \left(1 + \frac{p_0}{pa}\right) & 1 & 1 \\ 1 & \left(1 + \frac{p_0}{pa}\right) & 1 \\ 1 & 1 & \left(1 + \frac{p_0}{pa}\right) \end{bmatrix} \quad (\text{A.8})$$

The inverse of this matrix is found as follows.

$$\mathbf{K}^{-1} = \frac{1}{|\mathbf{K}|} \cdot (\mathbf{C}_{ij})^T \quad (\text{A.9})$$

Where $|\mathbf{K}|$ is the *determinant* and \mathbf{C}_{ij} are the *cofactors* of the matrix \mathbf{K} . These

cofactors are found as:

$$\begin{aligned} C_{11} &= \frac{p_0(p_b + p_c + p_0)}{p_b \cdot p_c} & C_{12} &= -\left(\frac{p_0}{p_c}\right) & C_{13} &= -\left(\frac{p_0}{p_b}\right) \\ C_{21} &= -\left(\frac{p_0}{p_c}\right) & C_{22} &= \frac{p_0(p_c + p_a + p_0)}{p_c \cdot p_a} & C_{23} &= -\left(\frac{p_0}{p_a}\right) \\ C_{31} &= -\left(\frac{p_0}{p_b}\right) & C_{32} &= -\left(\frac{p_0}{p_a}\right) & C_{33} &= \frac{p_0(p_a + p_b + p_0)}{p_a \cdot p_b} \end{aligned} \quad (\text{A.10})$$

The determinant of this matrix is equal to:

$$|\mathbf{K}| = \frac{(p_0)^2 \cdot (p_a + p_b + p_c + p_0)}{p_a \cdot p_b \cdot p_c} \quad (\text{A.11})$$

Based on Eqn. A.10, the $(\mathbf{C}_{ij})^T$ is equal to:

$$(C_{ij})^T = \begin{bmatrix} \frac{p_0(p_b + p_c + p_0)}{p_b \cdot p_c} & -\left(\frac{p_0}{p_c}\right) & -\left(\frac{p_0}{p_b}\right) \\ -\left(\frac{p_0}{p_c}\right) & \frac{p_0(p_c + p_a + p_0)}{p_c \cdot p_a} & -\left(\frac{p_0}{p_a}\right) \\ -\left(\frac{p_0}{p_b}\right) & -\left(\frac{p_0}{p_a}\right) & \frac{p_0(p_a + p_b + p_0)}{p_a \cdot p_b} \end{bmatrix}$$

Therefore the inverse of \mathbf{K} is the following:

$$\mathbf{K}^{-1} = \frac{\begin{bmatrix} \frac{p_0(p_b + p_c + p_0)}{p_b \cdot p_c} & -\left(\frac{p_0}{p_c}\right) & -\left(\frac{p_0}{p_b}\right) \\ -\left(\frac{p_0}{p_c}\right) & \frac{p_0(p_c + p_a + p_0)}{p_c \cdot p_a} & -\left(\frac{p_0}{p_a}\right) \\ -\left(\frac{p_0}{p_b}\right) & -\left(\frac{p_0}{p_a}\right) & \frac{p_0(p_a + p_b + p_0)}{p_a \cdot p_b} \end{bmatrix}}{l} \quad (\text{A.12})$$

$$l = \left(\frac{(p_0)^2 \cdot (p_a + p_b + p_c + p_0)}{p_a \cdot p_b \cdot p_c} \right)$$

And finally back substitution of Eqn. A.12 into Eqn. A.7 yields the elements of *P-matrix*.

$$\begin{aligned}
 & \left[\begin{array}{c} \frac{\partial \lambda_a}{\partial F_a} \\ \frac{\partial \lambda_b}{\partial F_a} \\ \frac{\partial \lambda_c}{\partial F_a} \end{array} \right] = \left[\begin{array}{c} \frac{p_a(p_b + p_c + p_0)}{p_a + p_b + p_c + p_0} \\ \frac{-(p_a \cdot p_b)}{p_a + p_b + p_c + p_0} \\ \frac{-(p_a \cdot p_c)}{p_a + p_b + p_c + p_0} \end{array} \right] \\
 & \dots \\
 & \left[\begin{array}{c} \frac{\partial \lambda_a}{\partial F_b} \\ \frac{\partial \lambda_b}{\partial F_b} \\ \frac{\partial \lambda_c}{\partial F_b} \end{array} \right] = \left[\begin{array}{c} \frac{-(p_a \cdot p_b)}{p_a + p_b + p_c + p_0} \\ \frac{p_b(p_c + p_a + p_0)}{p_a + p_b + p_c + p_0} \\ \frac{-(p_b \cdot p_c)}{p_a + p_b + p_c + p_0} \end{array} \right] \quad (A.13) \\
 & \dots \\
 & \left[\begin{array}{c} \frac{\partial \lambda_a}{\partial F_c} \\ \frac{\partial \lambda_b}{\partial F_c} \\ \frac{\partial \lambda_c}{\partial F_c} \end{array} \right] = \left[\begin{array}{c} \frac{-(p_a \cdot p_c)}{p_a + p_b + p_c + p_0} \\ \frac{-(p_b \cdot p_c)}{p_a + p_b + p_c + p_0} \\ \frac{p_c(p_a + p_b + p_0)}{p_a + p_b + p_c + p_0} \end{array} \right]
 \end{aligned}$$

The three vectors on the left-hand side are the three column of the P-matrix i.e.

$$\mathbf{P} = \begin{bmatrix} \frac{\partial \lambda_a}{\partial F_a} & \frac{\partial \lambda_a}{\partial F_b} & \frac{\partial \lambda_a}{\partial F_c} \\ \frac{\partial \lambda_b}{\partial F_a} & \frac{\partial \lambda_b}{\partial F_b} & \frac{\partial \lambda_b}{\partial F_c} \\ \frac{\partial \lambda_c}{\partial F_a} & \frac{\partial \lambda_c}{\partial F_b} & \frac{\partial \lambda_c}{\partial F_c} \end{bmatrix}$$

or

$$\mathbf{P} = \frac{\begin{bmatrix} p_a(p_b + p_c + p_0) & -(p_a \cdot p_b) & -(p_a \cdot p_c) \\ -(p_a \cdot p_b) & p_b(p_c + p_a + p_0) & -(p_b \cdot p_c) \\ -(p_a \cdot p_c) & -(p_b \cdot p_c) & p_c(p_a + p_b + p_0) \end{bmatrix}}{(p_a + p_b + p_c + p_0)} \quad (\text{A.14})$$

Where p_i is the permeance of limb " i " ($i = a, b, c$) and p_0 is that of zero-sequence path. The diagonal elements of the P -matrix indicate the *self-inductances* of primaries (incremental) while the off-diagonal elements represent the *mutual-inductances* (incremental) between those windings. It would not be surprising if we see a pattern in the matrix. In fact the only element which introduces asymmetry is the center limb. If the permeance of the three limbs were equal, the P -matrix would have been completely symmetrical (like the case of bank of three transformers.)

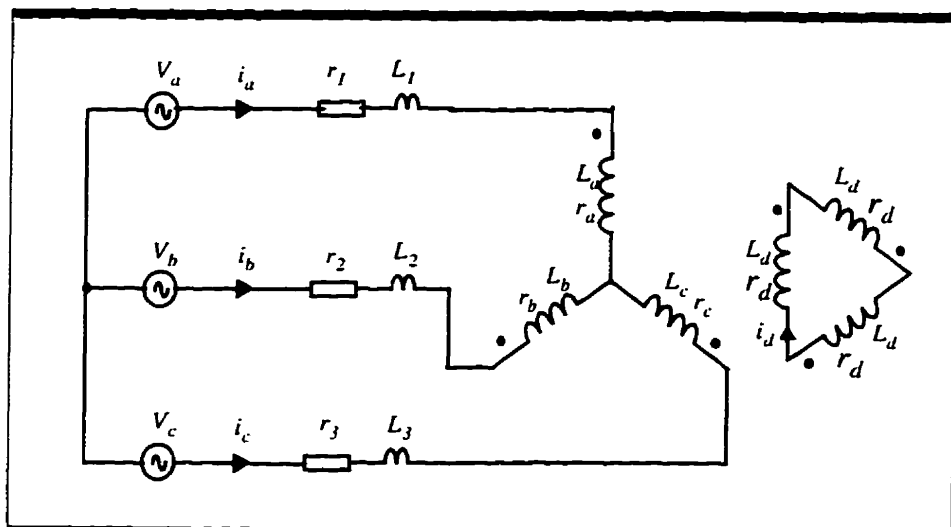
Appendix-B***Star/Delta Electric Equivalent Circuit***

Fig. B.1: Electric equivalent circuit of star/delta connection

$$r_1, r_2, r_3 = \text{line} + \text{source resistance}$$

$$L_1, L_2, L_3 = \text{line} + \text{source inductance}$$

r_a, r_b, r_c = primaries winding resistance

L_a, L_b, L_c = primaries leakage resistance

r_d = secondaries winding resistance

L_d = secondaries leakage inductance

Applying the *KVL* to the primary and secondary circuit yields three differential equations:

$$\begin{aligned} V_a - V_b &= (r_1 + r_a) \cdot i_a - (r_2 + r_b) \cdot i_b + (L_1 + L_a) \cdot \frac{di_a}{dt} - (L_2 + L_b) \cdot \frac{di_b}{dt} + \frac{d\lambda_a}{dt} - \frac{d\lambda_b}{dt} \\ V_b - V_c &= (r_1 + r_a) \cdot i_b - (r_2 + r_b) \cdot i_c + (L_1 + L_a) \cdot \frac{di_b}{dt} - (L_2 + L_b) \cdot \frac{di_c}{dt} + \frac{d\lambda_b}{dt} - \frac{d\lambda_c}{dt} \\ 0 &= (r_d + r_d + r_d) \cdot i_d + (L_d + L_d + L_d) \cdot \frac{di_d}{dt} + n \cdot \frac{d\lambda_a}{dt} + n \cdot \frac{d\lambda_b}{dt} + n \cdot \frac{d\lambda_c}{dt} \end{aligned} \quad (\text{B.1})$$

Applying *KCL* to primaries:

$$i_a + i_b + i_c = 0 \quad (\text{B.2})$$

Combining eqn. B.2 and eqn. B.1 results in the following.

$$\begin{aligned} V_a - V_b &= (r_1 + r_a) \cdot i_a - (r_2 + r_b) \cdot i_b + (L_1 + L_a) \cdot \frac{di_a}{dt} - (L_2 + L_b) \cdot \frac{di_b}{dt} + \frac{d\lambda_a}{dt} - \frac{d\lambda_b}{dt} \\ V_b - V_c &= (r_3 + r_c) \cdot i_a + (r_2 + r_3 + r_b + r_c) \cdot i_b + (L_3 + L_c) \cdot \frac{di_a}{dt} - (L_2 + L_b + L_3 + L_c) \cdot \frac{di_b}{dt} + \frac{d\lambda_b}{dt} - \frac{d\lambda_c}{dt} \\ 0 &= (r_d + r_d + r_d) \cdot i_d + (L_d + L_d + L_d) \cdot \frac{di_d}{dt} + n \cdot \frac{d\lambda_a}{dt} + n \cdot \frac{d\lambda_b}{dt} + n \cdot \frac{d\lambda_c}{dt} \end{aligned}$$

The above equations can be written in matrix notation.

$$\mathbf{V} = \mathbf{R} \cdot \mathbf{i} + \mathbf{L} \cdot \frac{d\mathbf{i}}{dt} + \mathbf{C} \cdot \frac{d\boldsymbol{\lambda}}{dt} \quad (\text{B.3})$$

where:

$$\begin{aligned}
 \mathbf{R} &= \begin{bmatrix} (r_1+r_d) & -(r_2+r_b) & 0 \\ (r_3+r_c) & (r_2+r_3+r_b+r_c) & 0 \\ 0 & 0 & (r_d+r_d+r_d) \end{bmatrix} & \mathbf{V} &= \begin{bmatrix} V_a - V_b \\ V_b - V_c \\ 0 \end{bmatrix} \\
 \mathbf{L} &= \begin{bmatrix} (L_1+L_d) & -(L_2+L_b) & 0 \\ (L_3+L_c) & (L_2+L_3+L_b+L_c) & 0 \\ 0 & 0 & (L_d+L_d+L_d) \end{bmatrix} & \mathbf{i} &= \begin{bmatrix} i_a \\ i_b \\ i_{cb} \end{bmatrix} \\
 \mathbf{C} &= \begin{bmatrix} 1 & -1 & 0 \\ 0 & 1 & -1 \\ n & n & n \end{bmatrix} & \boldsymbol{\lambda} &= \begin{bmatrix} \lambda_a \\ \lambda_b \\ \lambda_c \end{bmatrix}
 \end{aligned} \tag{B.4}$$

In chapter 3 it was discussed that the vector $\frac{d\boldsymbol{\lambda}}{dt} = \left(\frac{d\lambda_a}{dt} \quad \frac{d\lambda_b}{dt} \quad \frac{d\lambda_c}{dt} \right)^T$ can be expressed in terms of *P-matrix* and the applied *mmfs*.

$$\frac{d\boldsymbol{\lambda}}{dt} = \mathbf{P} \cdot \frac{d\mathbf{F}}{dt} \tag{B.5}$$

In this case the applied mmfs are expressed in terms of currents as follows.

$$\begin{aligned}
 F_a &= N \cdot (i_a + n \cdot i_d) \\
 F_b &= N \cdot (i_b + n \cdot i_d) \\
 F_c &= N \cdot (i_c + n \cdot i_d)
 \end{aligned}$$

Substituting for i_c from eqn. B.2:

$$\begin{aligned}
 F_a &= N \cdot (i_a + n \cdot i_d) \\
 F_b &= N \cdot (i_b + n \cdot i_d) \\
 F_c &= N \cdot (-i_a - i_b + n \cdot i_d)
 \end{aligned}$$

This can be written in matrix form as:

$$\mathbf{F} = \mathbf{N} \cdot \begin{bmatrix} 1 & 0 & n \\ 0 & 1 & n \\ -1 & -1 & n \end{bmatrix} \cdot \begin{bmatrix} i_a \\ i_b \\ i_d \end{bmatrix}$$

In matrix notation:

$$\mathbf{F} = \mathbf{M} \cdot \mathbf{i} \quad (B.6)$$

$$\mathbf{M} = \mathbf{N} \cdot \begin{bmatrix} 1 & 0 & n \\ 0 & 1 & n \\ -1 & -1 & n \end{bmatrix} \quad \mathbf{i} = \begin{bmatrix} i_a \\ i_b \\ i_d \end{bmatrix}$$

Combining eqn. B.3, eqn. B.5 and eqn. B.6 will yield the following.

$$\mathbf{V} = \mathbf{R} \cdot \mathbf{i} + \mathbf{L} \cdot \frac{d\mathbf{i}}{dt} + \mathbf{C} \cdot \mathbf{P} \cdot \mathbf{M} \cdot \frac{d\mathbf{i}}{dt}$$

This can be rearranged as:

$$\frac{d\mathbf{i}}{dt} = (\mathbf{L} + \mathbf{C} \cdot \mathbf{P} \cdot \mathbf{M})^{-1} \cdot (\mathbf{V} - \mathbf{R} \cdot \mathbf{i}) \quad (B.7)$$

This equation is in standard form for numerical integration.

Appendix-C

Delta/Delta Electric Equivalent Circuit

The following delta/delta connected transformer can be easily converted to an equivalent Star/Delta connected one by using the conventional transform. Fig. C.2 shows the transformer circuit after the transformation.

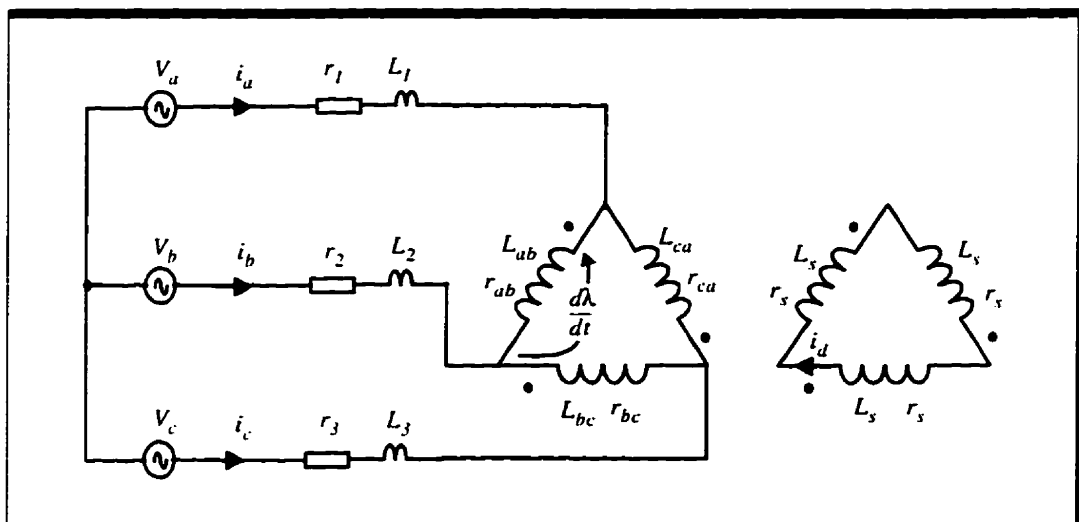


Fig. C.1 Delta/Delta connected transformer

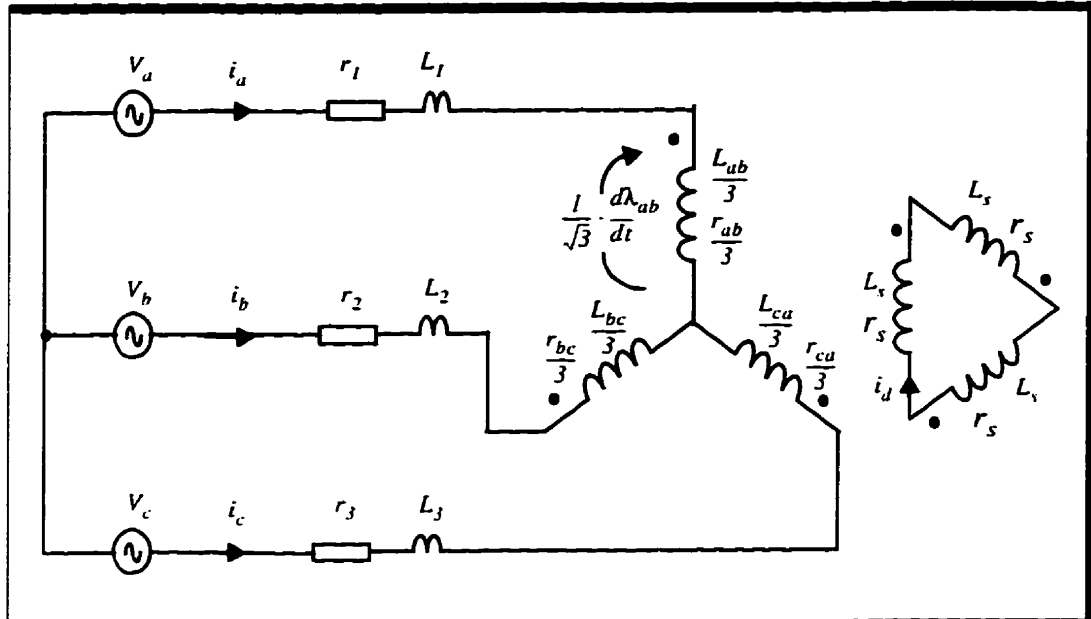


Fig. C.2 The Star/Delta equivalent circuit, after delta to star transform

Once the equivalent Star/Delta transformer is found, it can be solved by the routine which has already been developed for this configuration. The C matrix for this case is found as:

$$C = \begin{bmatrix} \frac{1}{\sqrt{3}} & -\frac{1}{\sqrt{3}} & 0 \\ 0 & \frac{1}{\sqrt{3}} & -\frac{1}{\sqrt{3}} \\ n & n & n \end{bmatrix}$$

Appendix-D

***Schematic Diagram of the
3-Phase Thyristor Switch***

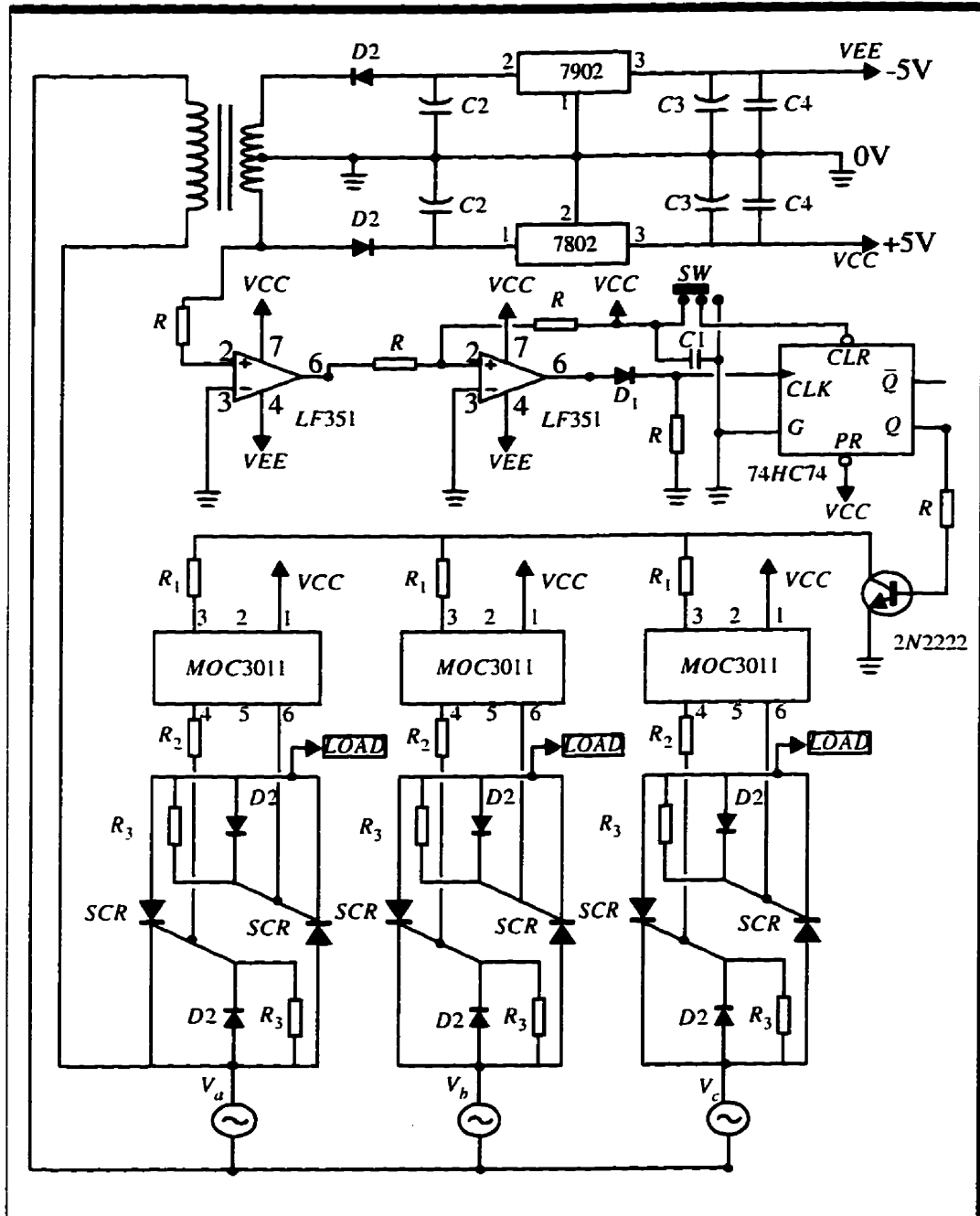


Fig. D.1: Schematic diagram of the three-phase thyristor-controlled switch

D.1 List of components:

- (1) LF351 = BIFET OPERATIONAL AMPLIFIER
- (2) MOC3011 = OPTO COUPLER AND TRIAC DRIVER
- (3) 74HC74 = POSITIVE-EDGE TRIGGERED FLIP-FLOP WITH PRESET AND CLEAR
- (4) LM7802 = POSITIVE VOLTAGE REGULATOR
- (5) LM7902 = NEGATIVE VOLTAGE REGULATOR
- (6) 2N2222 = NPN TRANSISTOR
- (7) SCR = SKK
- (8) D1 = 1N900
- (9) D2 = 1N4002
- (10) C1 = 100 nF
- (11) C2 = 1000 μ F/16V
- (12) C3 = 10 μ F/16V
- (13) C4 = 10 nF
- (14) R = 10 K Ω
- (15) R1 = 270 Ω
- (16) R2 = 56 Ω
- (17) R3 = 1.2 K Ω

Appendix-E

MatLab files

In this section the program codes which are written in MatLab will be presented. The whole program is broken into smaller sections and each section utilizes both the built-in and the developed functions in terms of MatLab *M-files*. The routine which integrates the system of differential equations constitutes the body of the program. This system of equation describes the electrical equivalent circuit of the transformer. Within this main program the necessary functions are called. These functions include both the magnetic circuit solver routine and functions which contain the input electrical and magnetic parameters.

E.1 Null Grounded Star/Delta Connection Functions**E.1.1 Main Routine**

```
function [tout,Iout,xout]=solveYND(yp,tratio)
%-----
%This function Solves the differential equations for 4-wire
%star/delta three-phase transformer. This function is the modified
%version of the built in function "diff45" in matlab M-files.
%diff integrates a system of ordinary differential equations using
%4th and 5th order Runge-Kutta formulas.
%-----
%INPUT:
%yp - the matrix of the system of differential equations
% which describes the electrical circuit of the 4-wire
% star/delta transformer.
%
%tratio - this is the transformer secondary to primary "turn ratio"
% when the secondary is closed tratio=5.
% when the secondary is open tratio=0.
%
%OUTPUT:
%tout - Returned integration time points (column-vector).
%Iout - Returned solution for currents, one solution
%column-vector per tout-value.
%The result can be displayed by: snapshot(tout, Iout).
%xout - Returned solution for fluxes, one solution
```

```

%column-vector per tout-value.
%The result is displayed by: snapshot(tout, xout).
%----- The Fehlberg coefficients: -----
clc
alpha = [1/4 3/8 12/13 1 1/2]';
beta = [ [ 1 0 0 0 0 0 0]/4
         [ 3 9 0 0 0 0 0]/32
         [1932 -7200 7296 0 0 0 0]/2197
         [ 8341 -32832 29440 -845 0 0]/4104
         [-6080 41040 -28352 9295 -5643 0]/20520 ]';
gamma = [ [902880 0 3953664 3855735 -1371249 277020]/7618050
          [-2090 0 22528 21970 -15048 -27360]/752400 ]';
pow = 1/5;
%----- initialization -----
cycle=1/60;
tfinal=0.093;
h = cycle/1000: % time step=(1/500)th of a 60_hertz cycle.
t =0;
[M,C]=matrixY4(tratio);
[phase.x0]=initial; % Imports the Initial values.
x = x0(:)
fa0=feval('fa1',x0(1));
fb0=feval('fb1',x0(2));
fc0=feval('fc1',x0(3));
F=[fa0 fb0 fc0];
I0=[fa0 fb0 fc0 0]/75;

```

```
I=I0(:);
u=x0;
%-----
f = zeros(length(I),6);
k = 1;
tout(k) = t;
xout(k,:) = x0;
Iout(k,:) =I0;
jam(k)=sum(x0);
%----- The main loop -----
tol = 1e-8;% tol - The desired accuracy.

p2=6e-5;

while (t < tfinal) & (t + h > t)
if t + h > tfinal, h = tfinal - t; end

[x.n]=nonl2(F,u,p2);
P=Pmatrix(x.p2);
u=x;

%----- Compute the slopes. -----
temp=feval(yp,t,I,P,ratio);
f(:,1) = temp(:);
for j = 1:5
temp = feval(yp, t+h*alpha(j), I+h*f*beta(:,j), P,ratio);
```

```
f(:,j+1) = temp(:);
end
%-----Estimate the error and the acceptable error.-----
delta = norm(h*f*gamma(:,2),'inf');
tau = tol*max(norm(I,'inf'),1.0);

%-----Update the solution only if the error is acceptable-----
if delta <= tau

    t = t + h;
    dI =h*f*gamma(:,1);
    I =I +dI;    % new I

    k = k+1;
    tout(k) = t;
    xout(k,:) = x;
    F=M*I;
    Iout(k,:) = (I. ');

end

%-----
fluxes=x.';
currents=I;
elapsed_time=t;
time_step=h;
    home, elapsed_time, time_step,currents,fluxes,n
```

~~%----- Update the step size.-----~~

```
if delta ~= 0.0
    h = min(5*h, 0.8*h*(tau/delta)^pow);
end

end                                     %(end of while)

if (t < tfinal)
    disp('Singularity likely.')
    t
end
tout = tout(1:k);
Iout = Iout(1:k,:);
xout = xout(1:k,:);
snapshot(tout,Iout);
```

E.1.2 Electric Circuit and Parameters

```

function yp=IPYND(t,I,P,ratio)
%-----
%This function is a matrix which describes the electrical
%circuit of the 4-wire star/delta three-phase transformer.
%-----
%INPUT:
%t- Time
%I- Current vector.
%P- p-matrix.
%ratio - Secondary to primary turns ratio
% for closed delta set "ratio" to 5
% for open delta set "ratio" to zero.
%-----L-Matrix-----
l1=0; l2=l1; l3=l1; %source inductance.
le=0; %line inductance for null connection.
la=1.295e-4;lb=la;lc=la; %primary leakage inductance.
la2=3.24e-3;lb2=la2;lc2=la2; %secondary leakage inductance.
l11=l1+le+la; l12=le; l13=le; l14=0;
l21=le; l22=l2+lb+le; l23=le; l24=0;
l31=le; l32=le; l33=l3+lc+le; l34=0;
l41=0; l42=0; l43=0; l44=la2+lb2+lc2;

```

```

L=[ [111 112 113 114]
    [121 122 123 124]
    [131 132 133 134]
    [141 142 143 144] ];

%-----R-Matrix-----
r1=0.87+0.1;r2=r1;r3=r1; %source + cable resistance
ra=0.106;rb=ra;rc=ra; %copper resistance of primaries.
ra2=2.73;rb2=ra2;rc2=ra2; %copper resistance of secondaries.
re=0; %resistance of the null connector wire.
r11= r1+re+ra;r12= re; r13= re; r14= 0;
r21= re; r22= r2+rb+re; r23= re; r24= 0;
r31= re; r32= re; r33= r3+rc+re; r34= 0;
r41= 0; r42= 0; r43=0; r44=ra2+rb2+rc2;
R=[ [r11 r12 r13 r14]
    [r21 r22 r23 r24]
    [r31 r32 r33 r34]
    [r41 r42 r43 r44] ];

%-----
[M,C]=matrixY4(tratio); % coefficient matrices.
V=Vynd(t); % the vector of the three-phase voltages.
A=L+C*P*T;
B=V-R*I;
yp=A\B;

```

E.1.3 Supply Voltage Vector

```
function V=Vynd(t)
%-----
%This function is the source voltage vector for 4-wire
  star/delta configuration.
%-----
%INPUT:
%   -initial phase angle for phase "a" in degree,
%   t -time in seconds.
%OUTPUT:
%V -voltage vector for YN/D configuration
.
[phase,x0]=initial;
ph=phase*(pi/180);%(degree to radian conversion.)
vm=120*sqrt(2);%(maximum voltage in VOLTS.)
w=2*pi*60;      %(angular speed for 60 Hz. in Rad./sec.)
va=vm*sin((w*t)+ph)    ;
vb=vm*sin((w*t)+ph-2*pi/3) ;
vc=vm*sin((w*t)+ph-4*pi/3) ;
      V=[ [ va ]
          [ vb ]
          [ vc ]
          [ 0*t ] ];
end
```

E.1.4 Coefficient Matrices

```
function [M,C]=matrixY4(n)
%-----
%This function is just the matrix of coefficients used in
%the electrical circuit description (in chapter 3) for the
%null grounded star/delta transformer.
%-----
% INPUT:
% n   -turns ratio
%     for open delta set n to 0
%     for closed delta set n to 5

N=75;
k=n;

C=[ [ 1   0   0 ]
    [ 0   1   0 ]
    [ 0   0   1 ]
    [ k   k   k ] ];

M=[ [ 1   0   0   k]
    [ 0   1   0   k]
    [ 0   0   1   k] ]*N;
```

E.2 Magnetic Circuit Solver Routine

```
function [X,n]=nonl2(F,u,p2)
%-----
%This function solves a nonlinear system of equations which
%describes the magnetic circuits of the 3-phase transformer.
%the Newton-Raphson method is employed.
%-----
%INPUT:
%F- Applied mmfs vector to the three limbs of the
% transformer.
%u- Initial guess for flux linkages.
%p2- Permeance of the zero-sequence path.
%
%OUTPUT:
%X- the linkage flux vector.
%n- Number of iterations needed to converge to the solution
% useful for checking the stability of the calculations.
%-----

x=l*u; % Initial guess for flux linkage.
Dx=[1 2 3];
h0=[0 0 0];
n=0;
k=1.0e-8;% the desired tolerance.
while norm(Dx)>=k
```

```
ya=der('fa1',x(1)); % derivatives of the saturation curves.
yb=der('fb1',x(2));
yc=der('fc1',x(3));

J=[ [(1/p2)+ya    1/p2    1/p2 ]
     [ 1/p2    (1/p2)+yb    1/p2 ]
     [ 1/p2    1/p2    (1/p2)+yc ] ]; % the Jakobian

s=(1/p2)*( x(1) +x(2) +x(3));
h1= fa1(x(1))+s -F(1); % the system of three equations
h2= fb1(x(2))+s -F(2); % which describe the magnetic circuit
h3= fc1(x(3))+s -F(3); % of the three phase transformer.
h=[h1 h2 h3];
dh=h0-h;
Dh=(dh)';
dx=J\Dh;
Dx=(dx)';
x=x+Dx;
n=n+1;
end
X=x;
```

E.3 Star/Delta Connection Functions

E.3.1 Main Routine

```
function [tout, iout,xout] = solveYD(yp,tratio)
%-----
%This function Solves the differential equations for
%star/delta three-phase transformer. This function is the modified
%version of the built in function "diff45" in matLab M-files.
%"diff" integrates a system of ordinary differential equations using
%4th and 5th order Runge-Kutta formulas.
%-----
%INPUT:
%yp - the matrix of the system of differential equations
% which describes the electrical circuit of the
% star/delta transformer.
%
%tratio - this is the transformer secondary to primary "turn ratio"
% when the secondary is closed tratio=5.
% when the secondary is open tratio=0.
%
%OUTPUT:
%tout - Returned integration time points (column-vector).
%Iout - Returned solution for currents, one solution
%column-vector per tout-value.
%The result can be displayed by: snapshot(tout, Iout).
%xout - Returned solution for fluxes, one solution
```

```
%column-vector per tout-value.
%The result is displayed by: snapshot(tout, xout).
%-----The Fehlberg coefficients-----
clc
alpha = [1/4 3/8 12/13 1 1/2]';
beta = [ [ 1 0 0 0 0 0 ]/4
         [ 3 9 0 0 0 0 ]/32
         [ 1932 -7200 7296 0 0 0 ]/2197
         [ 8341 -32832 29440 -845 0 0 ]/4104
         [-6080 41040 -28352 9295 -5643 0 ]/20520 ]';
gamma = [ [902880 0 3953664 3855735 -1371249 277020 ]/7618050
          [-2090 0 22528 21970 -15048 -27360 ]/752400 ]';
pow = 1/5;
%-----initialization-----
cycle=1/60;
tfinal=0.093;
h = cycle/500; % time step=(1/500)th of a 60_hertz cycle.
t =0;
[M.C]=matrixY3(tratio);
[phase,x0]=initial; % Imports the Initial values.
x = x0(:)
fa0=feval('fa1',x0(1));
fb0=feval('fb1',x0(2));
fc0=feval('fc1',x0(3));
F=[fa0 fb0 fc0];
I0=[fa0 fb0 0]/75;
```

```
I=I0(:);
u=x0;
%-----
f = zeros(length(I),6);
k = 1;
tout(k) = t;
xout(k,:) = x0;
Iout(k,:) = I0;
jam(k)=sum(x0);
Ic(k.)=-Iout(k,1)-Iout(k,2);
%----- The main loop -----
tol = 1e-8;% tol - The desired accuracy.
p2=6e-5;

while (t < tfinal) & (t + h > t)
if t + h > tfinal, h = tfinal - t; end

    [x,n]=nonl2(F,u,p2);
    P=Pmatrix(x,p2);
    u=x;

%----- Compute the slopes. -----
temp=feval(yp,t,I,P,ratio);
f(:,1) = temp(:);
for j = 1:5
```

```
temp = feval(yp, t+h*alpha(j), I+h*f*beta(:,j), P, tratio);
f(:,j+1) = temp(:);
end
%-----Estimate the error and the acceptable error.-----

delta = norm(h*f*gamma(:,2), 'inf');
tau = tol*max(norm(I, 'inf'), 1.0);

%-----Update the solution only if the error is acceptable-----
if delta <= ta
    t = t + h;
    dI = h*f*gamma(:,1);
    I = I + dI;    % new I
    k = k+1;
    tout(k) = t;
    xout(k,:) = x;

    F=M*I;
    Iout(k,:) = (I. ');
    Ic(k,:) = -Iout(k,1) - Iout(k,2);
end
%-----

fluxes=x. ';
currents=I;
elapsed_time=t;
time_step=h;
```

```
        home, elapsed_time, time_step,currents,fluxes,n
    %pause;

    %-----Update the step size.-----
    if delta ~= 0.0
        h = min(5*h, 0.8*h*(tau/delta)^pow);
    end

end % (end of while)
if (t < tfinal)
    disp('Singularity likely.')
    t
end
tout = tout(1:k);
Iout = Iout(1:k,:);
xout = xout(1:k,:);
iout(1:k,1)=Iout(1:k,1);
iout(1:k,2)=Iout(1:k,2);
iout(1:k,3)=Ic(1:k,:);
iout(1:k,4)=Iout(1:k,3);
snapshot(tout,iout);
```

E.3.2 Electric Circuit and Parameters

```

function Ip=IPYD(t,I,P,ratio)
%-----
%This function is a Matrix which describes the electrical
%  circuit of the star/delta three-phase transformer.
%-----
%INPUT:
%t- Time
%I- Current vector.
%P- p-matrix.
%ratio - Secondary to primary turns ratio
% for closed delta set "ratio" to 5
% for open delta set "ratio" to zero.
%-----L-Matrix-----
l1=0;   l2=l1;   l3=l1;           %source inductance.

la=1.295e-4; lb=la; lc=la;      %primaries leakage inductances.
la2=3.24e-3;lb2=la2; lc2=la2;   %secondries leakage inductances.
l11=l1+la;  l12=-(l2+lb); l13=0;
l21=l3+lc;  l22=l2+l3+lb+lc; l23=0;
l31=0;     l32=0;     l33=(la2+lb2+lc2);

L=[ [l11 l12 l13 ]
    [l21 l22 l23 ]
    [l31 l32 l33 ] ];

```

```
%-----R-Matrix-----  
rs=0+0.1;  
r1=rs; r2=rs; r3=rs; %source + cable resistance  
ra=0.106; rb=ra; rc=ra %copper resistance of primaries.  
ra2=2.73; rb2=2.73; rc2=2.73; %copper resistance of secondaries.  
r11=r1+ra; r12=-(r2+rb); r13=0;  
r21=r3+rc; r22=r2+r3+rb+rc; r23=0;  
r31=0; r32=0; r33=(ra2+rb2+rc2);  
R=[ [r11 r12 r13 ]  
    [r21 r22 r23 ]  
    [r31 r32 r33 ] ];  
  
%-----  
[M.C]=matrixY3(tratio);  
V=Vyd(t);  
%-----  
A=L+C*P*T;  
B=V-R*I;  
Ip=A\B;
```

E.3.3 Supply Voltage Vector

```
function V=Vyd(t)
%-----
%This function is the source voltage vector for 4-wire star/delta
%configuration.
%-----
%INPUT:
%   -initial phase angle for phase "a" in degree.
%   t   -time in seconds.
%OUTPUT:
%V   -voltage vector for YN/D configuration.

[phase,x0]=initial;
ph=phase*(pi/180);%(degree to radian conversion.)
vm=120*sqrt(2);%(maximum voltage in VOLTS.)
w=2*pi*60;      %(angular speed for 60 Hz. in Rad./sec.)
va=vm*sin((w*t)+ph)    ;
vb=vm*sin((w*t)+ph-2*pi/3) ;
vc=vm*sin((w*t)+ph-4*pi/3) ;
V=[ [(va-vb)]
     [(vb-vc)]
     [ 0 ] ];

end
```

E.3.4 Coefficient Matrices

```
function [M,C]=matrixY3(n)
%-----
% This function is just the matrix of coefficients used in
% the electrical circuit description for the star/delta transformer.
%-----
% INPUT:
% n -turns ratio
%   for open delta set n to 0
%   for closed delta set n to 5

N=75;
k=n;
C=[ [ 1   -1   0 ]
    [ 0    1  -1 ]
    [ k    k   k ] ];

M=[ [ 1  0  k ]
    [ 0  1  k ]
    [-1 -1  k ] ]*N;
```

E.4 P-matrix

```
function P=Pmatrix(x,p2)
%-----
%this function calculates the p matrix.
%-----
%INPUT:
%x-flux linkage vector.
%p2-permeance of the zero-sequence permeance.
%OUTPUT:
%P-the p-matrix
%-----

ya=der('fal',x(1));
yb=der('fbl',x(2));
yc=der('fcl',x(3));
pa=1/ya;
pb=1/yb;
pc=1/yc;
ps=pa+pb+pc+p2;

P=[ [+pa*(pb+pc+p2) -pa*pb    -pa*pc ]
    [-pa*pb    +pb*(pa+pc+p2) -pb*pc ]
    [-pa*pc    -pb*pc    +pc*(pa+pb+p2) ] ]/ps;
```

E.5 Plot Routine

```
function snapshot(t,y,k1,k2)
%-----
%This function plots a snapshot of the calculated flux
%and current vector versus time by specifying the beginning
% and ending of the time interval.
%-----
%INPUT:
%t-Time
%y-the quantity to be plotted (i.e. flux or current vector.)
%k1-start of the time interval.
%k2-end of the time interval.

l=length(t);
if nargin<3 k1=1; k2=l; end
if k1<=l & k2<=l
Y=y(k1:k2,:);
T=t(k1:k2)-0.025;
plot(T, Y(:,1)-100,'r-')
hold on
plot(T, Y(:,2)+100,'g-')
hold on
plot(T, Y(:,3)+300,'c-')

elseerror("'k" or "l" out of the computed range')
```


end

xlabel('Time (second)')

ylabel ('Inrush currents (Ampere)')

E.6 Core Characteristics

E.6.1 Core Characteristics for Limb “a”

```
function u=fal(x)
%-----
%   This function fits an 8-piece curve into the magnetic data
%   which was experimentally obtained for limb “a”
%-----
k=14;
y1= 52*x;
y2= 5.2+(52*(x-0.1)).*(exp(10.3*(x-.1)));
y3= 674.6266+(8.8080e+003*(x-0.45)).*(exp(6.123*(x-.45)));
y4= 1.8246e+003+(2.1417e+004*(x-0.53)).*(exp(k*(x-.53)));
y5= 52*x;
y6= -5.2+(52*(x+0.1)).*(exp(-10.3*(x+.1)));
y7= -674.6266+(8.8080e+003*(x+0.45)).*(exp(-6.123*(x+.45)));
y8= -1.8246e+003+(2.1417e+004*(x+0.53)).*(exp(-k*(x+.53)));
if      x>=0 & x<+0.1      y=y1
elseif  x>=.1 & x<0.45    y=y2
elseif  x>=.45 & x<0.53  y=y3
elseif  x>=0.53          y=y4
elseif  x>=-0.1 & x<0    y=y5
elseif  x>=-0.45 & x<-0.1 y=y6
elseif  x>=-0.53 & x<-0.45 y=y7
elseif  x<-0.53          y=y8
end
```

```
u=l*y;
```

E.6.2 Core Characteristics for Limb “b”

```
function u=fb1(x)
%-----
%   This function fits an 8-piece curve into the magnetic data
%   which was experimentally obtained for limb “b”
%-----
k=14;
y1= 52*x;
y2= 5.2+(52*(x-0.1)).*(exp(10.3*(x-.1)));
y3= 674.6266+(8.8080e+003*(x-0.45)).*(exp(6.123*(x-.45)));
y4= 1.8246e+003+(2.1417e+004*(x-0.53)).*(exp(k*(x-.53)));
y5= 52*x;
y6= -5.2+(52*(x+0.1)).*(exp(-10.3*(x+.1)));
y7= -674.6266+(8.8080e+003*(x+0.45)).*(exp(-6.123*(x+.45)));
y8= -1.8246e+003+(2.1417e+004*(x+0.53)).*(exp(-k*(x+.53)));
if      x>=0 & x<+0.1      y=y1
elseif  x>=.1 & x<0.45    y=y2
elseif  x>=.45 & x<0.53  y=y3
elseif  x>=0.53          y=y4
elseif  x>=-0.1 & x<0    y=y5
elseif  x>=-0.45 & x<-0.1 y=y6
elseif  x>=-0.53 & x<-0.45 y=y7
elseif  x<-0.53          y=y8
end
```

```
u=0.35*y;
```

E.6.3 Core Characteristics for Limb “c”

```
function u=fcl(x)
%-----
%   This function fits an 8-piece curve into the magnetic data
%   which was experimentally obtained for limb “c”
%-----
k=14;
y1= 52*x;
y2= 5.2+(52*(x-0.1)).*(exp(10.3*(x-1)));
y3= 674.6266+(8.8080e+003*(x-0.45)).*(exp(6.123*(x-.45)));
y4= 1.8246e+003+(2.1417e+004*(x-0.53)).*(exp(k*(x-.53)));
y5= 52*x;
y6= -5.2+(52*(x+0.1)).*(exp(-10.3*(x+1)));
y7= -674.6266+(8.8080e+003*(x+0.45)).*(exp(-6.123*(x+.45)));
y8= -1.8246e+003+(2.1417e+004*(x+0.53)).*(exp(-k*(x+.53)));
if      x>=0 & x<+0.1      y=y1
elseif  x>=.1 & x<0.45    y=y2
elseif  x>=.45 & x<0.53  y=y3
elseif  x>=0.53          y=y4
elseif  x>=-0.1 & x<0    y=y5
elseif  x>=-0.45 & x<-0.1 y=y6
elseif  x>=-0.53 & x<-0.45 y=y7
elseif  x<-0.53          y=y8
end
```

```
u=l*y;
```

E.7 Integrator

```
function [tout,flux]=integ(V)
%-----
%This function was used to determine the flux by
%integrating the voltage across the search coil.
%since the time interval between voltage samples
%very small the Trapezoidal rule was used.
%INPUT:
%V - The developed voltage across the search coil.
%OUTPUT: flux.
%-----
name=[yp '.txt'];
eval(['load ' name] );
a=eval([yp]);
t0=a(1,1);
t=a(:,1)-t0;
volt=(1/5)*a(:,2);
fx=0;
for k=1:length(t)-1;
u=(volt(k)+volt(k+1))/2;
dt=t(k+1)-t(k);
fx=fx+u*dt;
flux(k)=fx;
tout(k)=t(k);
```

```
end  
plot(tout,flux,'w')
```